Title
Identification and Analysis of Negative Heterochromatin Regulators in Saccharomyces cerevisiae

Author
Raisner, Ryan

Publication Date
2008-01-10

Peer reviewed|Thesis/dissertation

Identification and Analysis of Negative Heterochromatin Regulators in Saccharomyces cerevisiae

by

Ryan M. Raisner

DISSERTATION

Submitted in partial satisfaction of the requirements for the degree of

DOCTOR OF PHILOSOPHY

in

Biochemistry and Genetics

in the

GRADUATE DIVISION

of the

UNIVERSITY OF CALIFORNIA, SAN FRANCISCO

Acknowledgements

The time has finally arrived to close a large chapter of my life. I have mixed feelings about my experiences in graduate school, but when I look back many years down the road, I feel like it will be mostly positive. Now, I obviously could not have made it as far as I have to this point if not for the contributions and support of a large number of people throughout the years.

The biggest, and thus most important influence on me in direct relation to my thesis research has been my advisor Hiten Madhani. I think my lasting impression from Hiten is that he is the one person that forced me to think very deeply and critically about every problem I approached. At times, it felt like this would just give me a headache, but more often than not this has proven to be an invaluable methodology that I hope has imprinted upon me. Also he has taught me the importance of taking a scientific concept or result, and to be able to communicate it in a clear and concise manner. Lastly, one of the qualities I admire most in Hiten is his willingness to allow his students explore things scientifically and take some big, albeit tempered risks. For one thing, this is what makes science worth doing to me, purely for the sense of adventure, but also because I really feel like it fosters the types of projects that lead to the most interesting results.

My Thesis committee members were Joe Derisi and Sandy Johnson. Joe can be downright intimidating with the level of intensity he attacks a problem, and more than once I found him thinking harder about my project than I probably was, which served as a valuable reality check to me. Joe's input was always very insightful and helpful, in

addition to him being a constant source of information on the latest and greatest cutting edge technologies. Despite his busy schedule, he was always very accommodating of me whenever I dropped by with a question. My only regret is that I did not take the initiative to utilize Joe's input and advice more often.

Sandy is the one person who is probably the most responsible for where I am today. Out of college, Sandy hired me to work as a technician in his lab, despite a relative lack of lab experience and a less than stellar academic record. Within months of starting in his lab, I was working on my own projects, some of which turned out to be fruitful and pretty much resulted in my coming to UCSF as a grad student. I could go on for pages and pages writing funny anecdotes about Sandy, but it would be hard to know where to stop. I think my favorite thing about Sandy is his competitive but playful nature. This was exemplified over and over whenever I would go for a jog with a coworker, or play some ball, or pool, or squash – his question would never be "why were you goofing off and not working?", but instead "well, who won?!". Sandy is the epitome of a scientist to me: he is a fantastic writer, incredibly well read, a deep thinker, and he balances it all with a fairly normal life.

Rather than taking up the innumerous pages that would be required to thank everyone that has positively affected me, I would just like to acknowledge a select few. First, as a whole I would like to thank the Madhani lab members, past and present. As with any family, there were many ups and downs, but in the end I have a number of fond memories from people in the lab. Thinking back on our annual ski and rafting trips, as well as some of our random outings (usually involving somebody having too much to drink) always brings a smile to my face. I would like to specifically thank Paul Hartley, a

student in the lab who was an indispensable contributor to my project, in addition to being a pretty fun guy to hang out with. Not only that, but I don't know if I've ever worked with somebody that works as hard as Paul does. I wish him the very best in his future endeavors.

My former coworkers from the Johnson lab were a constant source of support, advice, and friendship. Matt Miller was my former bay-mate in Sandy's lab, and I will just sum him up by saying the guy is a lot of fun, in so many ways. Been a pleasure Matt! Annie Tsong has been an incredibly good friend for just about my entire time at UCSF, from camping trips to hockey games to going to concerts. I want to thank her for all her support and friendship over the last decade.

Mark McCleland, Paul Temkin, and Manisha Ray must all be mentioned here, because of the obscene amount of time I spend hanging out with them. Mostly because of our mutual love of playing soccer or other outdoor activities. Thanks for the (continued) good times! Brad Zuchero and Chris Campbell are two people very responsible for me keeping my sanity during the grueling process of grad school. In addition to providing me with really awesome new music all the time, they are a ton of fun to hang out with, talk about science with…rant about science or lab stuff with, or just to shoot the breeze while we're bobbing in the ocean on surfboards.

To Nate Gosse and Julie Pinkston-Gosse, my two closest friends during my time at UCSF: Not much for me to say here that I haven't already told them, suffice it to say thanks for being everything friends should be. It would be impossible to get through the ordeal of grad school without people like them in my life.

Last but of course not least, I want to thank my parents Bob and Cornelia, without whom none of this would have been possible. Their continued support from when I was a young truant that wouldn't even go to his classes in 7th grade, to someone who has seemingly been unable to get out of school finally until now, has been all I could ask for. I will always be grateful.

The text of Chapter 2 is a reprint of the material as it appears in “Histone variant H2A.Z marks the 5' ends of both active and inactive genes in euchromatin.” In Cell. 2005 Oct 21;123(2):233-48, with permission from Elsevier Publishing. The coauthor listed in this publication directed and supervised the research that forms the basis for the dissertation/thesis.

The text of Chapter 3 is a reprint of the material as it appears in “Patterning chromatin: form and function for H2A.Z variant nucleosomes.” In Curr Opin Genet Dev. 2006 Apr;16(2):119-24. Epub 2006 Feb 28., with permission from Elsevier Publishing. The coauthor listed in this publication directed and supervised the research that forms the basis for the dissertation/thesis.

.

Identification and Analysis of Negative Heterochromatin Regulators in *Saccharomyces cerevisiae*

By

Ryan M. Raisner

Abstract

Chromatin architecture has an incredible influence on the transcription state of genes in a cell. Chromatin occurs primarily in two generalized states: transcriptionally active euchromatin, and transcriptionally silent heterochromatin. This distinction of chromatin states can be accomplished by a number of regulatory processes, including post-translational modification by a variety of enzymes, and by the incorporation of histone variants. In the budding yeast *Saccharomyces cerevisiae,* transcriptional silencing by heterochromatin is dependent on the silent information regulators, or Sir proteins. Here we describe the results of a genome-wide screen designed to identify novel factors that are able to antagonize the encroachment of heterochromatin into actively transcribed regions. This screen identified a number of both known and novel factors that can to antagonize silencing. Among the proteins identified by the screen were several histone acetyl transferases, the histone tail binding proteins Bdf1 and Bdf1, and components of the Swr1 complex, which is responsible for the deposition of histone variant H2A.Z, a known anti-silencer. This was suggestive of a potential mechanism involving histone tail acetylation to specifically target H2A.Z to regions of chromatin to protect from the encroachment of silencing. Indeed, we were able to successful demonstrate that this is a mode of H2A.Z deposition. However, to our surprise, we found H2A.Z has a wide spread deposition throughout the yeast genome. More specifically, H2A.Z is precisely targeted to single nucleosomes on one, or both sides of a nucleosome-free region, which flanks the transcription initiation site for the vast majority of genes. Additionally, we have shown that this deposition can occur in the absence of active, demonstrating that

eukaryotic cells possess a mechanism for marking the 5’ ends of genes independent of transcription.

Table of contents

List of Tables

List of figures

Chapter One

Genome-wide screen for negative regulators of sirtuin activity reveals 40 loci and links to metabolism

Genome-wide screen for negative regulators of sirtuin activity reveals 40 loci and links to metabolism

Ryan M. Raisner and Hiten D. Madhani[1]

Dept. of Biochemistry and Biophysics

University of California

600 16th St.

San Francisco, CA 94143

[1]Corresponding author

hiten@biochem.ucsf.edu

tel: 415-514-0594

fax: 415-502-4315

ABSTRACT

Sirtuins are conserved proteins implicated in myriad key processes including gene control, aging, cell survival, metabolism, and DNA repair. In *Saccharomyces cerevisiae*, the sirtuin Sir2 promotes silent chromatin formation, suppresses recombination between repeats, and inhibits senescence. We performed a genome-wide screen for factors that negatively regulate Sir activity at a reporter gene placed immediately outside a silenced region. After linkage analysis, assessment of Sir-dependency, and knockout tag verification, 38 loci were identified, including 20 of which have not been previously described to regulate Sir. In addition to chromatin-associated factors known to prevent ectopic silencing (Bdf1, SAS-I complex, Rpd3L complex, Ku), we identified the Rtt109 DNA repair-associated histone H3 lysine 56 acetyltransferase as an anti-silencing factor, showed that it functions independently of its proposed effectors, the Rtt101 cullin, Mms1 and Mms22, and demonstrated unexpected interplay between H3-K56 and H4-K16 acetylation. The screen also identified subunits of mediator (Soh1, Srb2, and Srb5) and mRNA metabolism factors (Kem1, Ssd1), thus raising the possibility that weak silencing affects some aspect of mRNA structure. Finally, several factors connected to metabolism were identified. These include the PAS-domain metabolic sensor kinase Psk2, the mitochondrial homocysteine detoxification enzyme Lap3, and the Fe-S cluster protein maturase Isa2. We speculate that PAS kinase may integrate metabolic signals to control sirtuin activity.

INTRODUCTION

Sirtuins are a conserved family of proteins found in all domains of life. In eukaryotic cells, they have been characterized as deacetylases, ADP-ribosylases, or both (IMAI *et al.* 2000; LANDRY *et al.* 2000; TANNY *et al.* 1999). Work in a variety of systems has shown that they play roles in many key cellular processes including gene regulation, aging, cell survival, metabolic control, and DNA repair (BRACHMANN *et al.* 1995; KAEBERLEIN *et al.* 1999; LANGLEY *et al.* 2002; LIN *et al.* 2000). Small molecule inhibitors and activators of sirtuin activity have received considerable attention recently as potential therapeutic agents for aging-associated diseases including Parkinson's disease and type II diabetes (Smith and Denu 2007). Thus, there is considerable general interest in understanding how this family of enzymes is regulated.

The founding member of the sirtuin family is the budding yeast *Saccharomyces cerevisiae* gene silencing factor Sir2 (Silent information regulator 2), which is required for the formation of virtually all silent chromatin in budding yeast (FRITZE *et al.* 1997; RINE and HERSKOWITZ 1987; STRAHL-BOLSINGER *et al.* 1997). Sir2 acts in conjunction with the other Sir proteins to promote silencing. It forms a NAD-dependent histone deacetylase complex with Sir3 and Sir4 and is recruited to the silent mating type cassettes through interactions with Sir1. Additionally, silencing at telomeres is mediated by the recruitment of the Sir proteins by Rap1 protein. Furthermore, Sir2 acts at the rDNA to promote silencing and to suppress recombination between rDNA repeats (Smith and Boeke 1997). Sir2 also inhibits the senescence of mother cells; it has been suggested that this is related to its anti-recombination activity at the rDNA(KAEBERLEIN *et al.* 1999) .

The Sir complex appears to spread laterally from its nucleation points[reference]. This is thought to be accomplished through a cycle of histone tail deacetylation by Sir2 which enables binding of additional copies of the Sir complex through the histone-tail binding sites in Sir3 and Sir4, whose binding to nucleosomes is inhibited by histone-tail acetylation. This mechanism of Sir protein spreading presents a potential problem in that ectopic spread of silencing activity to regions designated to be transcriptionally active would presumably be deleterious. Recent work has identified several mechanisms that prevent the local ecoptic spread of silent chromatin in budding yeast. A tRNA gene at right (telomere-proximal) border of the *HMR***a** acts as a boundary element that blocks the lateral spread of silent chromatin(DONZE *et al.* 1999) . Subsequent work has identified similar boundary elements in other species(BELL and FELSENFELD 2000; BELL *et al.* 2001; LITT *et al.* 2001). Substitution of histone H2A with the H2A.Z variant in euchromatin also antagonizes silencing, as do three distinct methylations in histone H3 (MENEGHINI *et al.* 2003; TOMPA and MADHANI 2007; VENKATASUBRAHMANYAM *et al.* 2007), and acetylation on lysine 16 on the H4 tail (SUKA *et al.* 2002). In at least one case, these factors act redundantly to block the global spread of silencing: we recently reported that H2A.Z substitution and the Set1 complex act together to prevent the global spread of silencing (VENKATASUBRAHMANYAM *et al.* 2007).

A forward insertional mutagenesis screen aimed at identifying factors that prevent the spread of silencing from the *HMR***a** locus has been reported (JAMBUNATHAN *et al.* 2005). This work utilized a rearranged *HMR***a** locus containing a partial duplication in which the previously mentioned tRNA boundary element at *HMR***a** was moved to delete a segment of the *HMR***a**1-**a**2 region, and an intact copy of the *HMR***a**1 gene placed to the

right of this element deleting the *HMR*-I silencer. Using mating as an assay for the repression of the **a**1 gene, this screen identified the known anti-silencing factors *SAS4*, *SAS5*, and *RPD3*, as well as one protein not previously linked to silencing, the bromodomain protein *YTA7*.

To identify novel negative regulators of sirtuin activity in this context, we sought to extend this analysis to the whole-genome level using the yeast nonessential deletion collection. We crossed the collection to a strain containing a simple insertion of a sensitized *URA3* reporter gene just to the right of the tRNA boundary element that flanks the *HMR***a** locus.

RESULTS

Genome-wide screen to identify anti-silencing factors

To identify factors responsible for antagonizing the spread of Sir activity to proximal regions, we devised the following strategy to screen the entire yeast non-essential gene deletion library using a reporter-based assay. The reporter strain contains a promoter-truncated allele of the *Candida albicans URA3* homolog, which is able to complement *S. cerevisiae ura3* mutants (Figure 1A). Several promoter-truncation alleles of varying length were integrated outside of *HMR*, 200 bp to the telomere-proximal side of its characterized boundary element, and tested for activity. The goal of performing these integrations was to obtain a low-expressing allele of *URA3* that was sensitized to spread of silencing events in mutants such as the *htz1*Δ mutant (MENEGHINI *et al.* 2003). Our criteria for selecting the reporter strain were three-fold: 1) a reproducible 5-fluoroorotic acid resistance (FOA^R) phenotype in the *htz1*Δ mutant but not in wild-type cells to demonstrate sensitivity to the spread of silencing, 2) the smallest possible promoter fragment, and 3) a Ura+ phenotype when plated on –Ura media indicating that the reporter has sufficient expression of *C.a. URA3* that allows for assaying on this media. The strain containing the allele with 70 bp of its endogenous promoter (Fig. 1B) best fit these criteria and was chosen as the bait strain in our screen.

We adapted the SGA method developed by others (TONG *et al.* 2001) to cross our reporter strain with the available gene deletion library to generate a library of yeast colonies that were *MAT***a** haploids, bearing the reporter gene along with a single gene deletion. In addition, the parent strain contained dominant drug selection markers to

track the segregation of the reporter allele, independent of potential silencing effects. These strains were arrayed on plates in 768-colony format in which each of 384 strains were arrayed in duplicate. They were then transferred to 5-FOA containing plates for phenotypic testing. Because this automated method transfers a relatively large percentage of the colony to the new plate, and also because 5-FOA will select for spontaneous *C.a. ura3* mutants that produce colony papillations, we were selective about scoring positives: specifically, only colonies that were symmetric and lacked obvious papillations, and were present as pairs (meaning that they had to arise from independent meioses) were chosen. These putative positive colonies were tested for *URA3* expression, by testing their ability to grow on synthetic media lacking uracil (SD-Ura) to screen for undesired Ura- mutants. Our original reporter strain contained a single dominant selectable drug marker, *NatMX4*, integrated 3,800 bp telomere-proximal to the reporter at coordinate 299,553 of chromosome III (Figure 1A). Because of the large number of meioses that are potentially screened by this method, 5-FOA resistant colonies arose. Upon further investigation, these were determined to be Ura- strains that likely arose from recombination events between the reporter and drug marker. The first pass of the screen with this strain had a 5-FOA^R rate of ~5% (~220/4600). However, the majority of these strains were found to have undergone recombination between the reporter and the positive drug selection marker, and were therefore Ura-. To avoid this problem, a second reporter strain was generated with an additional drug marker (*HphMX4*) integrated 5,300 bp centromere proximal to the reporter at coordinate 290,254 of chromosome III. The probability of a double recombination event leading to a drug resistant strain lacking the reporter allele considerably less likely than the single

crossover event; reducing the likelihood of recovering 5-FOA resistant colonies due to loss of the reporter gene. The screen was repeated accordingly and an additional 100 mutants that fit our criteria were scored as positives.

Secondary screenings for phenotypic linkage

The two passes of the screen yielded 320 total candidates. Because this large-scale screening technique allowed for a variety of events that would lead to false detections, we imposed additional criteria: 1) The colonies needed to grow when streaked as singles on SD –Ura, while retaining the ability to yield FOA^R colonies when replica-plated, a hallmark of anti-silencing factors. 2) The phenotype was tightly linked to the knockout. For this, a minimum of 100 random spores were plated for each mutant and tested for linkage between the knockout and reporter genotypes, and 5-FOA resistance. 3) The identity of the knockout allele was verified by amplification and sequencing of the bar codes present in each deletion allele. This was necessary due to potential errors in the knockout collection and possible cross-contamination events arising in the course of the automated strain generation and scoring.

These measures taken reduced the number of non-redundant positively scoring mutants from this screen to 46. The final results of both screens are summarized in Table 1. While we have confirmed in the identity of the knockouts in all the strains, as well as the linkage of the knockout alleles with the FOA^R phenotype, we cannot of course rule out the possibility that a spontaneous mutation in a gene tightly linked to the marked gene deletion is responsible for a given phenotype.

Phenotypic characterization of anti-silencing mutants

To quantitatively assess the anti-silencing phenotypes of the mutants, we plated serial dilutions of each mutant on 5-FOA media (Fig. 2). Each plate contains the controls of the parental strain (wild-type containing reporter construct), a *ura3*Δ strain, and an *htz1Δ* harboring the reporter, as well as a number of mutants. Mutants in known pathways or complexes, such as the SAS-I histone acetyl transferase components *SAS2*, *SAS4*, and *SAS5*, were plated side by side (Fig. 2A). Other mutants were placed together using available Gene Ontology (GO) assignments curated at the *Saccharomyces* Genome Database (www.yeastgenome.org). Additionally, we also plated the strains on synthetic complete media (SC) and media lacking uracil (SC –Ura) to control for plating efficiency, and *URA3* expression. As evidenced by these platings, genes belonging to common functional categories tended to display similar phenotypic strength: mutants in the Rpd3-L complex provide one example (Figure 2B). Phenotypic strength varied from a strong anti-silencing defect such as that of the *sas2Δ* mutant, in which nearly 10% of the colonies plate 5-FOA (compared to SC media), to weak ones such as the *nap1Δ* mutant (Fig. 2E), which had an approximate relative plating efficiency of $1/5^5$. As a reference, the wild-type reporter strain was generally observed to have less than $1/5^8$ relative plating efficiency, while the *ura3Δ* control strain displayed ~100% efficiency. The quantitative relative plating efficiencies for the mutants are listed in Table 1.

Sir-dependence of increased repression of *C.a. URA3* reporter in FOA+ mutants

The screen was designed to identify any mutant strain for which there was a large enough decrease in *URA3* expression to allow for an increased growth on 5-FOA.

Mutants were predicted to fall into two categories: genes that are essential for full *URA3* expression independently of silencing, and genes that normally prevent a spread of silencing activity from *HMR***a**. Because we were only interested in the latter, we sought to identify mutants that have phenotypes dependent on Sir activity. To do this, we deleted *SIR3*, an essential subunit of the Sir complex: a gene with anti-silencing properties should revert to a 5-FOA sensitive phenotype in the absence of *SIR3*. Conversely, genes involved in processes such as the uracil biosynthesis, transcription *per se*, or drug resistance, should not display a *sir3Δ*-suppressible phenotype.

For each mutant isolated in the screen, we deleted *SIR3*, and tested for 5-FOA resistance. Deletion of *SIR3* by itself does not confer any fitness benefit compared to wild-type (Fig. 3A). As in Fig. 2, each plate displayed in Fig. 3 includes wild-type and *ura3Δ* strains as controls. Additionally, each plate assays a 5-FOA resistant deletion strain next to its respective double mutant with *sir3*Δ as a reference. As shown in Fig. 3A-C, a large fraction (35/46) of the genes from the screen have 5-FOA phenotypes that are fully suppressed by deletion of *SIR3*. The genes *PRR1*, *PSK2*, *RAD10*, *BDF1*, and *BDF2* show partial suppression of the phenotype, as evidenced by retention of some 5-FOA resistance (Figure 3B, C, and G). This is suggestive of multiple roles in anti-silencing and transcription. Finally, the genes *RAD54*, *VRP1*, *ECM33 YOR206W*, *YMR007W*, and *YOR305W* (Fig. 3F and G) have phenotypes that are completely unaffected by deletion of *SIR3,* suggesting they affect expression or genetic mutability of the *URA3* reporter gene. Quantitative estimations of the relative 5-FOA plating efficiencies for the double deletions are listed in Table 1.

Rtt109/Asf1 antagonizes silencing of reporter gene

Our screen identified Rtt109 and Asf1, which form a complex that acetylates the lysine 56 core residue of histone H3 (H3K56) (DRISCOLL *et al.* 2007; HAN *et al.* 2007). The complex acetylates non-chromatin-associated H3 during DNA replication. Together with the Hst3 deacetylase that acts outside of S phase, this mechanism restricts H3K56 acetylation to S phase (MAAS *et al.* 2006). For unknown reasons, cells defective in this modificiation are sensitive to DNA damage. Based on genetic interaction maps, it has been suggested that the role of this mechanism in DNA repair is affected by the proteins Mms1, Mms22, and Rtt101(COLLINS *et al.* 2007) . Interestingly however, only *RTT109* and *ASF1* share additional synthetic interactions with the Swr1 complex, which deposits H2A.Z(COLLINS *et al.* 2007). This is consistent with the results of the screen, which only identified anti-silencing phenotypes for *asf1Δ* and *rtt109Δ* mutants (Fig. 2). However, it remained possible mutants in *MMS1*, *MMS22*, and *RTT101* were false-negatives. Therefore, we generated deletions of these genes by homologous recombination in the reporter strain background and tested them for growth on 5-FOA media (Fig. 4). We observed that *mms1Δ*, *mms22Δ*, and *rtt101Δ* did not display resistance to 5-FOA, in contrast to *asf1Δ* and *rtt109Δ* mutants.

Silencing outside of *HMR***a** in the *rtt109*Δ mutant results in decreased H4-K16 acetylation without a detectable increase in Sir3 binding

We investigated the phenotype of the *rtt109*Δ mutant further using chromatin immunoprecipitation (ChIP) using the probes shown in Fig. 5A. Probes A-F span the *HMR***a** silent cassette, probes G-J span the *C.a. URA3* reporter gene, probes K-M

correspond to the promoter regions of the three genes to the right (telomere-proximal) of the reporter gene, and probe N corresponds to the promoter of *HML*α-proximal gene *MRC1*. We also examined the promoter regions of several genes in euchromatic segments of chromosome III (probes O-S) and two probe sets (probes T and U) in the middle of the large ORF of the *BUD3* gene (used for normalization in Fig. 5B). We first performed ChIP using polyclonal antibodies against Sir3 in the wild-type reporter strain, as well as in the mutant strains *rtt109Δ* and the previously characterized anti-silencing mutant *sas2Δ* as a control. Consistent with previous reports, Sir3 is dramatically enriched within *HMR***a**, while regions outside have very little or no observable Sir3 (Fig. 5B). The data in all of our ChIP experiments were normalized to values obtained using ChIP performed with antibodies histone H3 to control for nucleosome density. Additionally, for the Sir3 ChIP data, we normalized the data to the *BUD3* ORF region, which shows no detectable Sir3 binding in wild-type cells. Notably, the promoter regions of the reporter construct (probe G) displayed less Sir3 association than the immediately adjacent *HMR***a** region, but more than that observed at control regions. Strikingly, when we examined Sir3 localization in the *rtt109*Δ and *sas2*Δ strains, no increased association of Sir3 within the reporter gene region was apparent, suggesting in this context, Rtt109 and Sas2 act downstream of Sir binding to antagonize silencing. Since a key function of the Sir complex is to deacetylate lysine 16 of histone H4 (H4K16), we examined the acetylation status of this residue (Fig. 5C). We observed decreased acetylation on H4K16 using probes that cover the reporter gene in the *rtt109*Δ mutant (Fig. 5C), which supports the idea that the increased activity of the Sir complex is responsible for the change in reporter gene expression in this mutant. Consistent with previous reports, we observed a dramatic

depletion of this acetylation from *HMR***a** and we observed that its presence was dependent on the H4K16 HAT Sas2 at many, but not all, locations (Fig. 5C). We also examined H3K56 acetylation by ChIP (Fig. 5D). Although its removal has been suggested to be important for silencing (XU *et al.* 2007), we observed only a modest decrease of this modificiation within *HMR***a** compared to euchromatic sites and only a slight decrease at the reporter gene in the *sas2*Δ mutant. Importantly, the signal we observed in this region was entirely dependent on *RTT109*.

DISCUSSION

Systematic screen for negative regulators of sirtuin activity

We present a strategy and results for identification of genes that negatively impact the Sir2-dependent repression of a reporter gene placed just outside a chromatin boundary element in *S. cerevisiae*. Our screen is similar in overall design to that reported by Donze and colleagues, which identified the bromodomain/AAA+ ATPase-encoding gene *YTA7* as a new negative regulator of silencing (JAMBUNATHAN *et al.* 2005). The major differences are that 1) we used a crippled, sensitized *C. albicans URA3* reporter gene and growth on FOA as output instead of a rearranged *HMR***a**1 locus and mating and 2) we used an SGA approach and the yeast deletion collection instead of mTn insertional mutagenesis. Although our screen did not identify *YTA7*, it did identify a number of previously described anti-silencing factors that were identified in the previous screen including *RPD3, SAS4*, and *SAS5*. As discussed above, given the potential for threshold and reporter-specific effects, false-negatives are difficult to avoid in any genome-wide reporter-based screen. Nonetheless, we identified 20 new loci that negatively regulate silencing outside of the tRNA boundary element. These assignments were based on individual mutants passing tests of linkage to the deletion collection marker, verification of the deletion barcodes, and dependency on *SIR2* for the increased-repression FOA phenotype.

Negative regulation of Sir2 by regulators of chromatin and DNA metabolism

In our effort to take an unbiased approach to identify novel negative regulators of silencing, we uncovered a disparate range of protein activities. Figure 6 describes the reported locations, complexes and functions of the 40 proteins identified in our screen that displayed *SIR*-dependent increased repression of the *C.a. URA3* reporter gene based on available annotation curated at the *Saccharomyces* Genome Database (www.yeastgenome.org). The majority of the chromatin modifying factors had been implicated previously in regulation of *SIR* activity. These include Bdf1 (a component of both the Swr1 complex that deposits H2A.Z and TFIID), the SAS-I H4K16 acetyltransferase complex, the Rpd3-L HDAC complex, and a number of factors reported to control telomere length (Yku80, Rif1, Dot1, Pog1, Cac2, Elg1, and Mediator). The latter may act by the producing a longer telomere near *HMR***a**, which lies approximately 35 kb from the right telomere of chromosome III. Increased Sir complex nucleation might then lead to increased Sir-dependent repression of the reporter gene. Alternatively, some members of this group might act by distinct mechanisms as suggested previously for Yku (MAILLET *et al.* 2001). The negative role for Rpd3-L in silencing remains a mystery since this HDAC complex opposed the activity of the Sir HDAC complex. One possibility is that Rpd3-L antagonizes acetylation of the Sir complex. Indeed, N-terminal acetylation of Sir3 has been reported to promote silencing (WANG *et al.* 2004).

A Novel Function for H3K56 acetylation

Another protein complex identified in our screen is the Rtt109 histone H3K56 acetyltransferase complex (Fig. 6). H3K56 acetylation of cell-cycle regulated and peaks in S-phase due to the down-regulation of the Hst3 Sir2-related HDAC which apparently

removes the modification (MAAS *et al.* 2006). Mutations of H3K56 have been shown to disrupt silencing (XU *et al.* 2007). Specifically, mutation of this residue to an identity that mimics either the acetylated (K>Q) or deacetylated (K>R) resulted in decreased silencing of a subtelomeric silencing reporter as did a mutation (K>G) that removed the side-chain altogether. This loss of silencing was not associated with a decrease in silencing protein binding, however there is an apparent increase in chromatin accessibility in that region (XU *et al.* 2007). Mutation of *SIR2* resulted in increased K56 acetylation in silenced regions, and it has been suggested that deacetylation of this residue by Sir2 is necessary for silencing(XU *et al.* 2007) . Curiously, our data indicate a reduction in K56 acetylation *HMR***a** relative to euchromatic sites (Fig. 5D). Since a mutation that mimics the deacetylated state disrupts silencing, it seems difficult to rule out other roles for the Rtt109 complex in silencing. In any case, our data demonstrate that Rtt109 can inhibit the action of the Sir complex outside of the normal boundaries of silent chromatin. As described above, it has been suggested that Rtt101, a cullin homolog cooperates with Mms1 and Mms22 to affect the function of H3-K56 acetylation in genome stability. However, our results indicate that these factors are dispensable for the anti-silencing function of the Rtt109 complex, indicating a branch in the pathway.

In contrast, two other factors implicated in DNA repair affect silencing. These appear not to act by increasing the mutability of the *C.a.URA3* reporter gene since their effects were *SIR2*-dependent. These are Rad10 and Elg1. Elg1, which functions in an alternative RFC-like clamp loader complex, has been implicated previously in both genome stability and silencing (BEN-AROYA *et al.* 2003). Rad10 is a single-stranded DNA endonuclease involved in nucleotide excision repair repair (Prakash 1977).

Precisely how these factors control silencing remains unknown, but they suggest an intriguing link between DNA repair factors and the regulation of sirtuin function. Such links are not without precedent. For example, Sir2 itself suppresses recombination between the rDNA repeats (Gottlieb and Esposito 1989).

Negative regulation of Sir2 by factors linked to metabolism

Given the established role of Sir2 and its orthologs in aging and metabolism in a variety of organisms, there is a great deal of interest in understanding how Sir2 activity is globally regulated. Current thinking focuses mostly on the fact that sirtuins require NAD for their decetylatse and/or ADP-ribosylation activities, but other mechanisms of control have not been ruled out. Three proteins identified in our screen seem notable in this respect. First, we identify the PAS domain kinase Psk2 as a negative regulator of Sir2. This factor has been shown to phosphorylate a number of proteins involved in metabolism (RUTTER *et al.* 2002). It has been suggested to be a sensor kinase, which, perhaps through its PAS domain, senses some aspect of metabolic state and transduces this to control metabolism. However, what the PAS domain binds to or senses and the biologically relevant outputs of this conserved kinase remain poorly understood. It is intriguing to note that one of the factors identified in our screen, Ygl081w, contains a FHA domain. Such domains in other proteins have been shown to be a binding motif for phosphorylated proteins(LI *et al.* 2004) . Likewise, our screen identified Lap3, a protein originally identified as a bleomycin hydrolase, but which his thought to function to limit the levels of the toxic metabolic side-product homocysteine in cells(Xu and Johnston 1994) . It is tempting to speculate that Lap3 and Psk2 are connected in some way.

Another intriguing possibility would be that Lap3 limits silencing by hydrolyzing the o-acetyl-ADP-ribose product of the Sir2 deacetylase reaction, which has been shown *in vitro* to promote the assembly of the Sir complex. If Lap3 and Psk2 function are related, perhaps the PAS domain of Psk2 binds o-acetyl-ADP-ribose. Finally, we note that Isa2, identified in our screen, is required for the maturation of Fe-S cluster proteins, again suggesting a link bewteen Sir2 and metabolism.

Conclusion

Our screen represents the most comprehensive survey to date for negative regulators of sirtuin activity in any system. Our survey identified 40 genes including 20 genes not previously known to be involved in regulating Sir. The precise mechanisms by which they function in this context, and their relationship to each other remain fertile ground for future investigation. Although we have emphasized potential regulation of Sir2 activity, any of the factors we describe could act by affecting steps in the expression of Sir proteins ranging from synthesis to degradation of the corresponding mRNAs and proteins. Likewise, given that there are limited pools of Sir2 in the cell and competition between Sir2 association between the silent cassettes, telomeres, and the rDNA, it is possible that some of the mutations described here affect that competition. We note, however, that rDNA-specific silencing loss mutations described previously (Smith and Boeke 1997) , were not identified in our screen with the exception of *cac1*. Regardless of their mechanism of action of the individual factors, we hope that our results will provide a useful resource for the field for future investigation of sirtuin regulation. In particular, the exploration of links between Sir2 and processes of DNA repair and metabolic control.

Given the central important of this family of regulators in biology, understanding how they are controlled in *S. cerevisiae* may ultimately provide insights onto the regulation of the sirtuins in humans, which have been suggested to play roles in common maladies ranging from aging to diabetes to cancer.

METHODS

SGA screen

Colonies were transferred using a Virtek colony arrayer as described in (TONG *et al.* 2001).. The yeast *MAT***a** knockout library (www.ResGen.com) was grown for 2 days on rich media (YPAD) and pinned onto lawns of the reporter (bait) strain, and then grown for another day at 30°C to cross. Diploid progeny were selected on rich media plus G418 (120 mg/L) and ClonNat (60 mg/L) drugs, and grown for two days. Diploids were transferred to pre-sporulation media (GNA) and grown at 30°C for 1 day, then transferred to sporulation media (NGS) and incubated at 23°C in an open-air humified chamber for 5 days. Colonies were transferred to SGA –His –Arg +canavanine plates and grown for 2 days at 30 degrees to select for *MAT***a** haploid progeny. Colonies were then transferred to SGA –His –Arg +canavanine +G148 plates and grown at 30°C for 1 day to select for recombinant progeny. Colonies were then transferred to SGA –His –Arg +canavanine +G148 +HygromycinB (180 mg/L) plates and grown at 30°C for 2 days, followed by 1 day of growth on SGA –His –Arg +canavanine +G148 +Hygromycin B +clonNat plates to select for *MAT***a** progeny containing a gene knockout allele and the reporter gene. These colonies were transferred to SC +5-FOA(2g/L) plates and grown for 3-5 days prior to phenotypic scoring. Positively-scored colonies were streaked to SC –Ura plates to verify maintenance of the *C.a. URA3* reporter gene, and subsequently replica-plated to 5-FOA media to confirm the resistance.

Strains

All strains used in this study are listed with their genotype in Table S1. The reporter strains used were generated by integrating the *C. albicans URA3* gene at position 295,754 of *S. cerevisiae* chromosome III by homologous recombination. The dominant drug markers *NatMX4* and *HphMX4* (HygromycinB resistance) (GOLDSTEIN and MCCUSKER 1999)were integrated at position 299,553 and 290,254 of chromosome III respectively. Strain genotypes of single knockouts recovered from the screen were confirmed by sequencing. Strains containing deletions of the *SIR3* gene were created by homologous recombination using either *HphMX4* or the *LYS2* gene from *Candida albicans*, and were confirmed by PCR for presence of integrated deletion cassette, and loss of wild-type *SIR3* allele. Primers used for strain construction are listed in Table S2.

Chromatin Immunoprecipitation

All ChIP experiments were performed according to the protocol used in (RAISNER *et al.* 2005b). For each sample, we used 2.5 ul of the H3K56-ac antibody, which was generously donated by the lab of Michael Grunstein. We used 20 ul of the Sir3 antibody, which was used as serum and generated against a GST-tagged C-terminal fragment of the protein. We used 2.5 ul of the H4K16-ac antibody (Upstate #07-329) and 1 ul of the H3 antibody (Abcam #Ab1791) per sample.

Plate assays

For all plate assays, cells were pre-grown on rich (YPAD) media, then resuspended in water, plated in 5-fold dilutions. The same dilutions were plated at the same time to rich media (SC), rich media (SC) containing 5-FOA (1g/L), and media lacking uracil (SC – Ura). Plates were incubated for 3 days at 30°Cprior to photography.

Figure 1. Reporter strain for assaying spread of silencing activity from *HMR*a.

A. Promoter-truncated alleles of the *Candida albicans URA3* gene were integrated adjacent to the right boundary element of the silenced *HMR***a** locus. Reporter alleles were integrated by homologous recombination of PCR amplified genomic *C. albicans URA3* of varying length, containing 50 bp of homology upstream and downstream of the region 200 bp to the right of *HMR***a**. **B**. Five-fold serial dilutions to test growth rate of 70 bp promoter bearing reporter construct on rich media (SC), 5-FOA, and media lacking uracil (SC –ura).

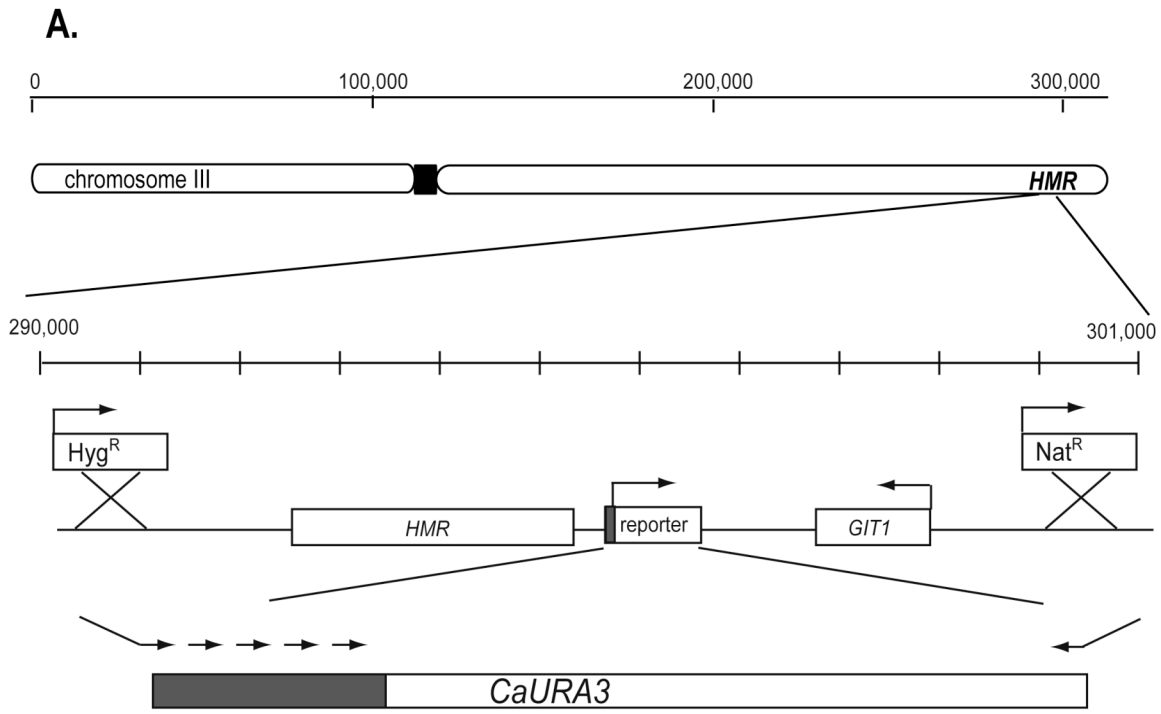
A.
0
100,000
200,000
300,000
chromosome III
HMR
290,000
301,000
Hyg^R
Nat^R
HMR
reporter
GIT1
CaURA3

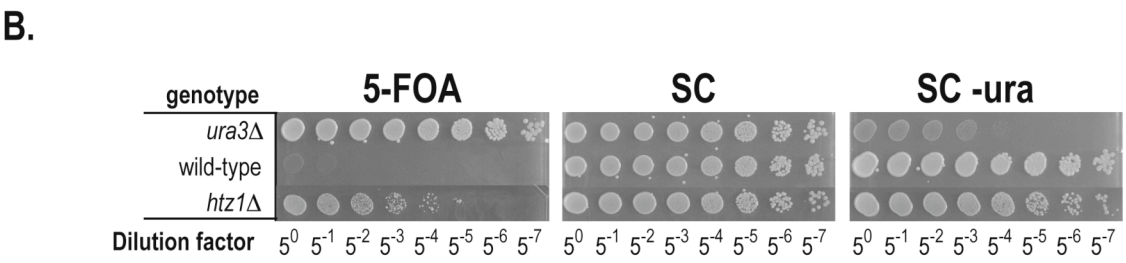
B.
genotype
5-FOA
SC
SC -ura
ura3Δ
wild-type
htz1Δ
Dilution factor
5^0 5^-1 5^-2 5^-3 5^-4 5^-5 5^-6 5^-7

Figure 2. Quantitative reporter plating assay for spread of silencing.

Serial platings of mutant strains show increased growth on 5-FOA media, assembled into sub-categories. Each plate contains a *ura3*Δ strain as a positive control, and a reporter strain bearing no knockouts (wild type) as a negative control, and an *htz1*Δ mutation in the reporter strain as an example of ectopic silencing phenotype. **A.** SAS-I complex and Mediator components. **B.** Rpd3-L complex components. **C**. Telomere maintenance genes. **D.** Genes affecting protein phosphorylation and others. **E.** Swr1 and Rtt109 complex components. **F.** Metabolism-linked genes.

Figure 2

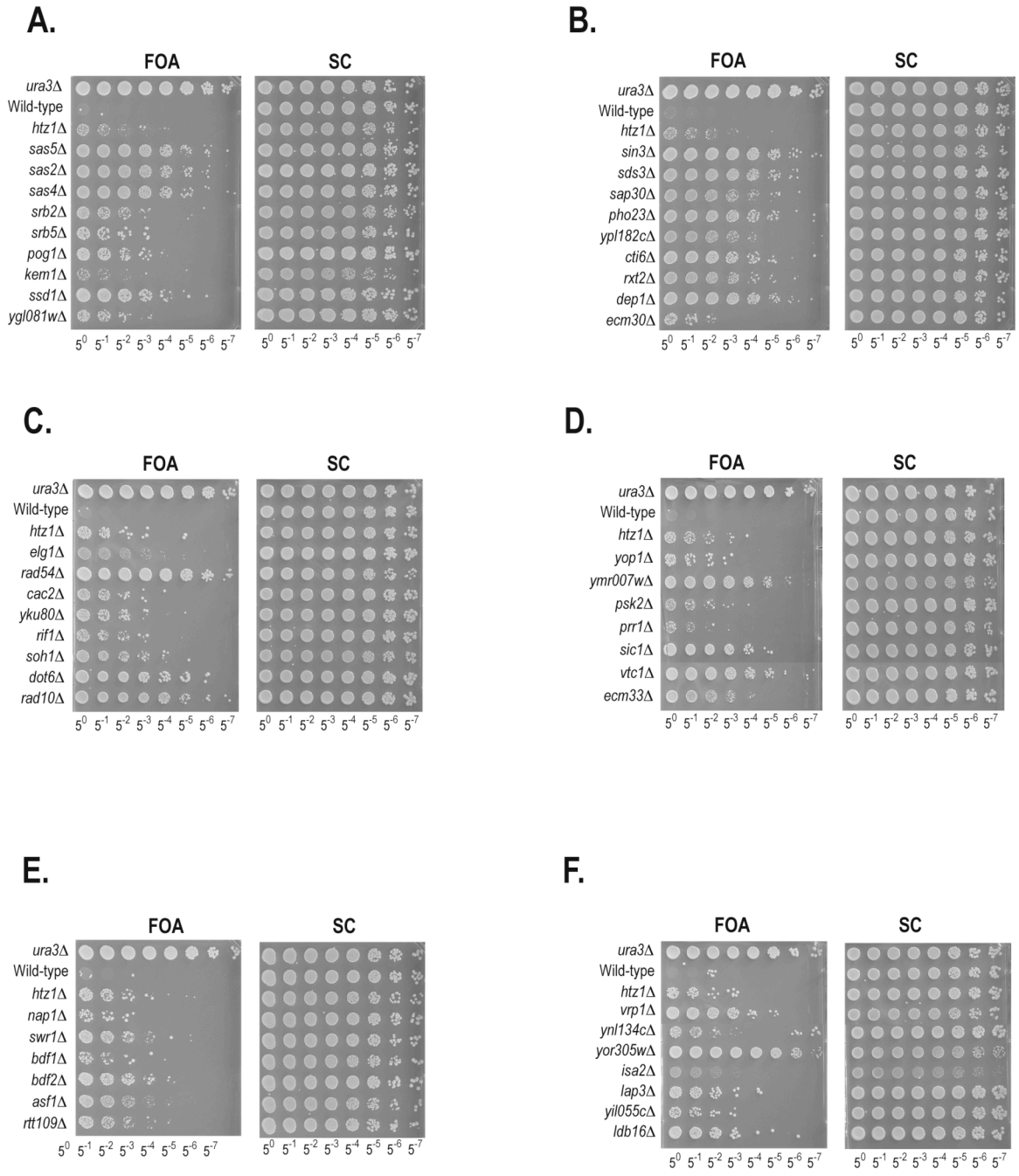
A.
FOA
SC
ura3Δ
Wild-type
htz1Δ
sas5Δ
sas2Δ
sas4Δ
srb2Δ
srb5Δ
pog1Δ
kem1Δ
ssd1Δ
ygl081wΔ
B.
FOA
SC
ura3Δ
Wild-type
htz1Δ
sin3Δ
sds3Δ
sap30Δ
pho23Δ
ypl182cΔ
cti6Δ
rxt2Δ
dep1Δ
ecm30Δ
C.
FOA
SC
ura3Δ
Wild-type
htz1Δ
elg1Δ
rad54Δ
cac2Δ
yku80Δ
rif1Δ
soh1Δ
dot6Δ
rad10Δ
D.
FOA
SC
ura3Δ
Wild-type
htz1Δ
yop1Δ
ymr007wΔ
psk2Δ
prr1Δ
sic1Δ
vtc1Δ
ecm33Δ
E.
FOA
SC
ura3Δ
Wild-type
htz1Δ
nap1Δ
swr1Δ
bdf1Δ
bdf2Δ
asf1Δ
rtt109Δ
F.
FOA
SC
ura3Δ
Wild-type
htz1Δ
vrp1Δ
ynl134cΔ
yor305wΔ
isa2Δ
lap3Δ
yil055cΔ
ldb16Δ
5^0 5^-1 5^-2 5^-3 5^-4 5^-5 5^-6 5^-7

Figure 3. Sir-suppressible and non-suppressible anti-silencing phenotypes of mutant strains.

Serial platings of mutant strains show increased growth on 5-FOA media, assembled into sub-categories. Each plate contains *ura3*Δ as a positive control for 5-FOA resistance, and a reporter strain bearing no knockouts (wild-type) as a control for 5-FOA sensitivity, and a *sir3D* in the reporter strain as a negative control for Sir-independent effects. **A, B, C,** and **D**: Cases of full suppression of 5-FOA phenotypes by *sir3*Δ. **E** and **G**: cases of partial suppression. **F** and **G**: cases of non-suppression.

Figure 3

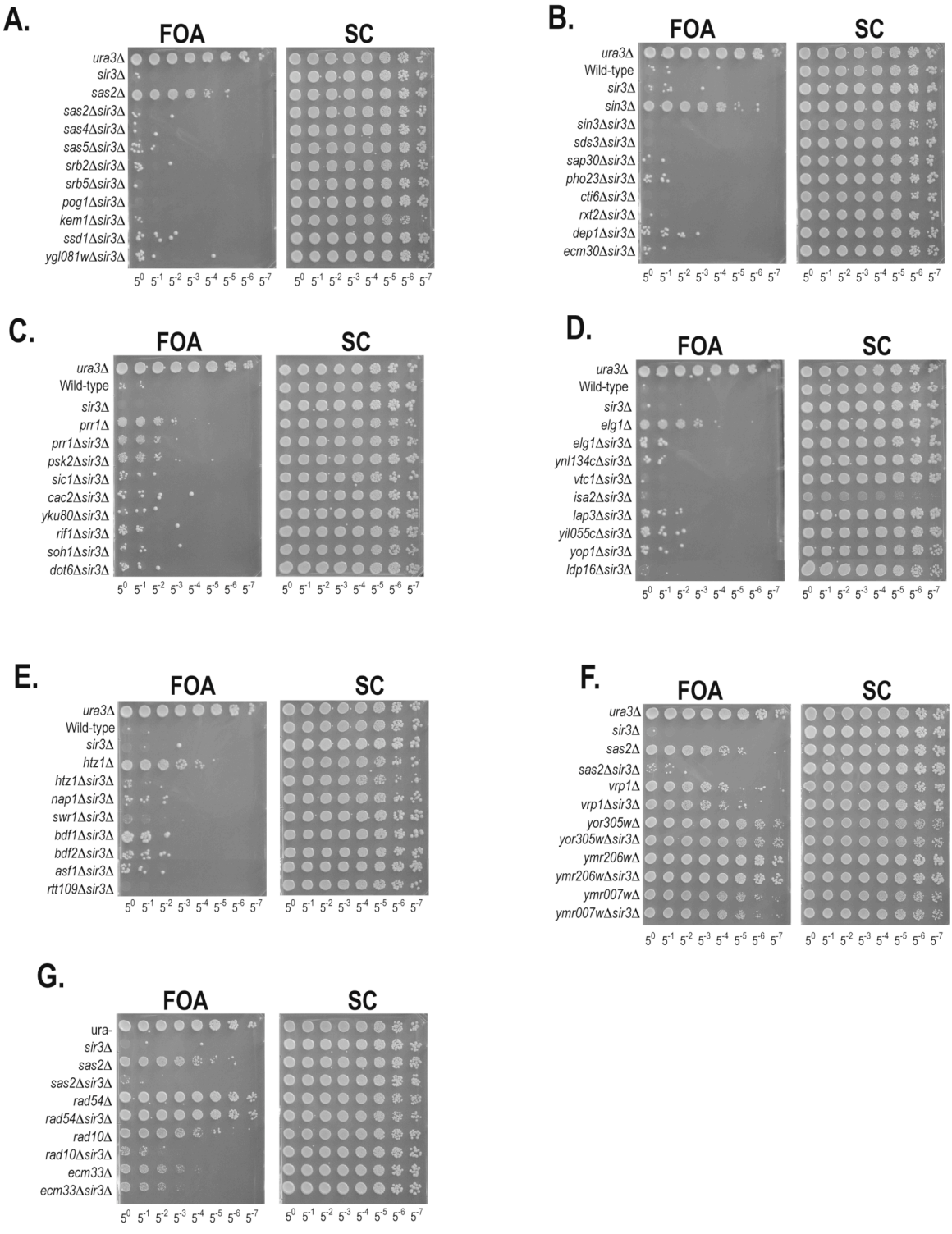
A.
FOA
SC
ura3Δ
sir3Δ
sas2Δ
sas2Δsir3Δ
sas4Δsir3Δ
sas5Δsir3Δ
srb2Δsir3Δ
srb5Δsir3Δ
pog1Δsir3Δ
kem1Δsir3Δ
ssd1Δsir3Δ
ygl081wΔsir3Δ
B.
FOA
SC
ura3Δ
Wild-type
sir3Δ
sin3Δ
sin3Δsir3Δ
sds3Δsir3Δ
sap30Δsir3Δ
pho23Δsir3Δ
cti6Δsir3Δ
rxt2Δsir3Δ
dep1Δsir3Δ
ecm30Δsir3Δ
C.
FOA
SC
ura3Δ
Wild-type
sir3Δ
prr1Δ
prr1Δsir3Δ
psk2Δsir3Δ
sic1Δsir3Δ
cac2Δsir3Δ
yku80Δsir3Δ
rif1Δsir3Δ
soh1Δsir3Δ
dot6Δsir3Δ
D.
FOA
SC
ura3Δ
Wild-type
sir3Δ
elg1Δ
elg1Δsir3Δ
ynl134cΔsir3Δ
vtc1Δsir3Δ
isa2Δsir3Δ
lap3Δsir3Δ
yil055cΔsir3Δ
yop1Δsir3Δ
ldp16Δsir3Δ
E.
FOA
SC
ura3Δ
Wild-type
sir3Δ
htz1Δ
htz1Δsir3Δ
nap1Δsir3Δ
swr1Δsir3Δ
bdf1Δsir3Δ
bdf2Δsir3Δ
asf1Δsir3Δ
rtt109Δsir3Δ
F.
FOA
SC
ura3Δ
sir3Δ
sas2Δ
sas2Δsir3Δ
vrp1Δ
vrp1Δsir3Δ
yor305wΔ
yor305wΔsir3Δ
ymr206wΔ
ymr206wΔsir3Δ
ymr007wΔ
ymr007wΔsir3Δ
G.
FOA
SC
ura-
sir3Δ
sas2Δ
sas2Δsir3Δ
rad54Δ
rad54Δsir3Δ
rad10Δ
rad10Δsir3Δ
ecm33Δ
ecm33Δsir3Δ
5^0 5^-1 5^-2 5^-3 5^-4 5^-5 5^-6 5^-7

Figure 4. Rtt109 and Asf1 have phenotypes distinct from Rtt101 cullin complex.

Indicated genotypes were analyzed for reporter gene expression as described in Figures 2 and 3.

Figure 4

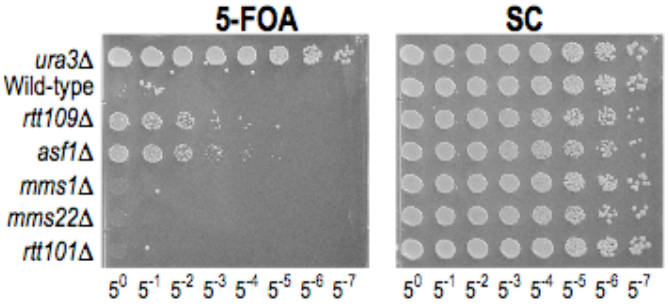
5-FOA
SC
ura3Δ
Wild-type
rtt109Δ
asf1Δ
mms1Δ
mms22Δ
rtt101Δ
5^0 5^-1 5^-2 5^-3 5^-4 5^-5 5^-6 5^-7
5^0 5^-1 5^-2 5^-3 5^-4 5^-5 5^-6 5^-7

Figure 5. ChIP data for Sir3, H3K56 acetylation, and H4K16 acetylation.

A. Schematic of *HMR***a** and surrounding region with locations of PCR amplicons used for quantitation. Primer set N corresponds to the promoter of the *HML*α-proximal gene *MRC1*, primer sets O, P, Q, R, and S correspond to the promoters of the euchromatic genes *CDC10*, *CWH43*, *NFS1, DCC1*, and *RBK1*. Primer sets T and U are to the middle of the ORF region of *BUD3*. All data shown are averages of three independent ChIP experiments with standard error of the mean error bars. T-tests were applied for loci denoted by *. **B.** Sir3 ChIP data for wild-type, *sas2*Δ, and *rtt109*Δ strains. Data are normalized to H3 ChIP values for each locus, and all loci are normalized to the average of primer sets T and U. **C.** H4K16-ac ChIP values for wild-type, *sas2*Δ, and *rtt109*Δ, normalized to H3 enrichment. **D.** H3K56-ac ChIP values for wild-type, *sas2*Δ, and *rtt109*Δ, normalized to H3 enrichment.

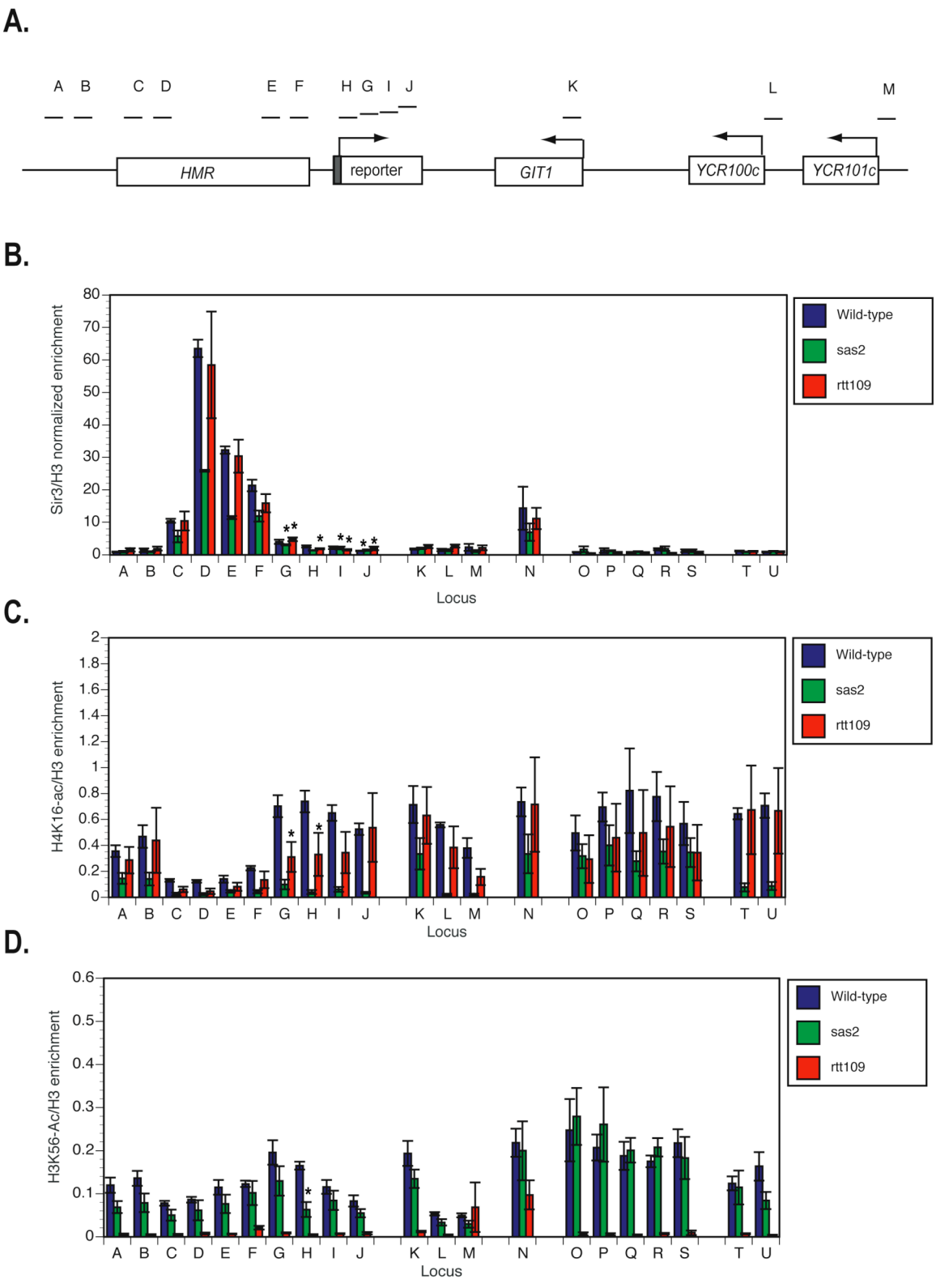
A.
A B C D E F H G I J K L M
HMR
reporter
GIT1
YCR100c
YCR101c
B.
Sir3/H3 normalized enrichment
Wild-type
sas2
rtt109
A B C D E F G H I J K L M N O P Q R S T U
Locus
C.
H4K16-ac/H3 enrichment
Wild-type
sas2
rtt109
A B C D E F G H I J K L M N O P Q R S T U
Locus
D.
H3K56-Ac/H3 enrichment
Wild-type
sas2
rtt109
A B C D E F G H I J K L M N O P Q R S T U
Locus

Figure 6. Chart depicting functional and localization categories of Sir-dependent genes in this study.

Genes are assigned functional categories based on available functional or biochemical annotation (light colored boxes), and those are overlaid on cellular localization annotations.

Figure 6

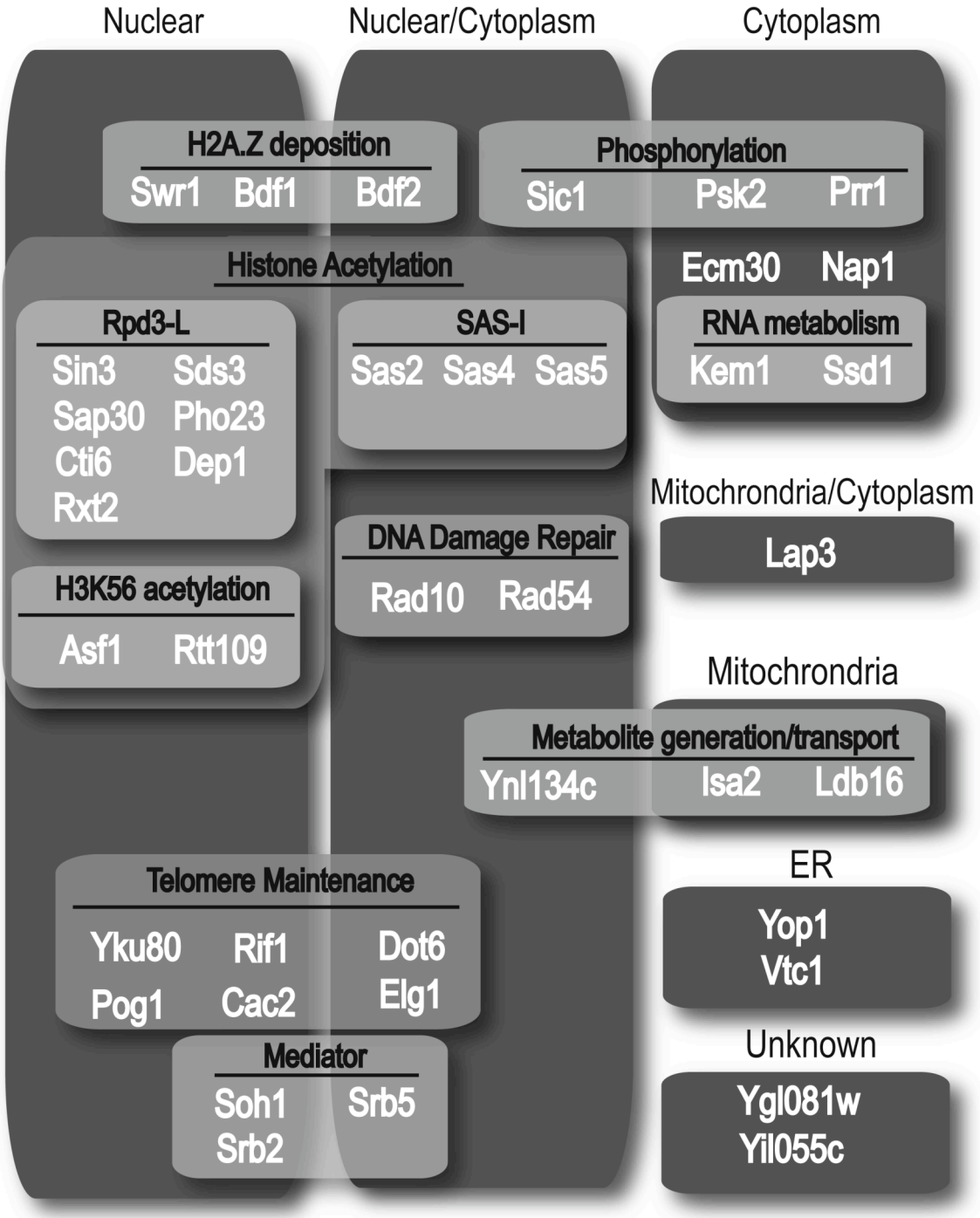
Nuclear
Nuclear/Cytoplasm
Cytoplasm
H2A.Z deposition
Swr1 Bdf1 Bdf2
Phosphorylation
Sic1 Psk2 Prr1
Histone Acetylation
Ecm30 Nap1
Rpd3-L
Sin3 Sds3
Sap30 Pho23
Cti6 Dep1
Rxt2
SAS-I
Sas2 Sas4 Sas5
RNA metabolism
Kem1 Ssd1
Mitochrondria/Cytoplasm
Lap3
DNA Damage Repair
Rad10 Rad54
H3K56 acetylation
Asf1 Rtt109
Mitochrondria
Metabolite generation/transport
Ynl134c Isa2 Ldb16
ER
Yop1
Vtc1
Telomere Maintenance
Yku80 Rif1 Dot6
Pog1 Cac2 Elg1
Mediator
Soh1 Srb5
Srb2
Unknown
Ygl081w
Yil055c

Table 1

Systematic Name	Gene Name	Cellular Localization	GO-terms	FOA Plating efficiency	sir3Δ FOA plating efficiency	*SIR*-dependent?
YNL134C	*YNL134C*	cytoplasm/nucleus	alcohol dehydrogenase (NADP+) activity	6.40E-05	2.56E-06	y
YML102W	*CAC2*	nucleus	chromatin assembly, DNA repair, nucleosome assembly	3.20E-04	2.56E-06	y
YOR144C	*ELG1*	cytoplasm/nucleus	telomere maintenance, DNA replication, DS-break repair	1.60E-03	2.56E-06	y
YMR106C	*YKU80*	nucleus	chromatin assembly, chromatin silencing, telomere maintenance	3.20E-04	2.56E-06	y
YER088C	*DOT6*	cytoplasm/nucleus	chromatin silencing at rDNA, chromatin silencing at telomere	8.00E-03	2.56E-06	y
YBR275C	*RIF1*	nucleus	chromatin silencing, telomere maintenance	3.20E-04	2.56E-06	y
YGL127C	*SOH1*	nucleus	mediator complex, telomere maintenance, DNA repair	1.60E-03	2.56E-06	y
YHR041C	*SRB2*	cytoplasm/nucleus	mediator complex, telomere maintenance	3.20E-04	2.56E-06	y
YGR104C	*SRB5*	nucleus	mediator complex, telomere maintenance	3.20E-04	2.56E-06	y
YDL070W	*BDF2*	cytoplasm/nucleus	bromodomain protein, redundant with Bdf1	1.60E-03	1.28E-05	partial
YLR399C	*BDF1*	nucleus	SWR1 complex, chromatin remodeling	6.40E-05	1.28E-05	partial
YDR334W	*SWR1*	nucleus	SWR1 complex, chromatin remodeling, Swi2/Snf2 related ATPase	3.20E-04	2.56E-06	y
YOR213C	*SAS5*	cytoplasm/nucleus	H3/H4 histone acetyltransferase activity, chromatin silencing at telomere	4.00E-02	2.56E-06	y
YMR127C	*SAS2*	cytoplasm/nucleus	H3/H4 histone acetyltransferase activity, chromatin silencing at telomere	4.00E-02	2.56E-06	y
YDR181C	*SAS4*	cytoplasm/nucleus	H3/H4 histone acetyltransferase activity, chromatin silencing at telomere	4.00E-02	2.56E-06	y
YLL002W	*RTT109*	nucleus	histone acetyltransferase activity, negative regulation of transposition, DNA damage reponse	3.20E-04	2.56E-06	y
YJL115W	*ASF1*	nucleus	chromatin assembly, chromatin silencing, histone exchange, histone acetylation	3.20E-04	2.56E-06	y
YKR048C	*NAP1*	cytoplasm	Histone binding, nucleosome assembly	6.40E-05	2.56E-06	y
YOL004W	*SIN3*	mitochondrion	RPD3s, RPD3L, Histone deacetylase	4.00E-02	2.56E-06	y
YIL084C	*SDS3*	nucleus	histone deacetylation, Rpd3L complex	4.00E-02	2.56E-06	y
YMR263W	*SAP30*	nucleus	histone deacetylation, Rpd3L complex	8.00E-03	2.56E-06	y
YNL097C	*PHO23*	nucleus	histone deacetylation, Rpd3L complex	8.00E-03	2.56E-06	y
YPL181W	*CTI6/RXT1*	nucleus	histone deacetylation, Rpd3L complex	8.00E-03	2.56E-06	y

YBR095C	*RXT2*	nucleus	histone deacetylation, Rpd3L complex	8.00E-03	2.56E-06	y
YAL013W	*DEP1/FUN54*	N/A	histone deacetylation, Rpd3L complex	4.00E-02	2.56E-06	y
YER072W	*VTC1*	ER	microautophagy, vacuole transport	8.00E-03	2.56E-06	y
YLR436C	*ECM30*	cytoplasm	cell wall organization and biogenesis, cytoplasm	6.40E-05	2.56E-06	y
YPR067W	*ISA2*	mitochondrion	biotin biosynthesis, mitochondrion	3.20E-04	2.56E-06	y
YIL055C	*YIL055C*	N/A	N/A	3.20E-04	2.56E-06	y
YNL239W	*LAP3*	cytoplasm/mitochondrion	cysteine-type peptidase activity, nucleic acid binding, mitochondrion	3.20E-04	2.56E-06	y
YCL005W	*LDB16*	lipid particles	mitochondrion	3.20E-04	2.56E-06	y
YKL116C	*PRR1*	cytoplasm	receptor signaling protein serine/threonine kinase activity	3.20E-04	6.40E-05	partial
YOL045W	*PSK2*	cytoplasm	PAS domain protein serine/threonine kinase	3.20E-04	6.40E-05	partial
YLR079W	*SIC1*	cytoplasm/nucleus	cdk inhibitor	1.60E-03	2.56E-06	y
YGL173C	*KEM1*	cytoplasm	5' - 3' exoribonuclease activity, telomere maintenance	6.40E-05	2.56E-06	y
YIL122W	*POG1*	nucleus	RNA Pol II transcription factor activity	3.20E-04	2.56E-06	y
YDR293C	*SSD1*	cytoplasm	RNA binding, cell wall organization	1.60E-03	2.56E-06	y
YGL081W	*YGL081W*	N/A	unknown protein, FHA domain	3.20E-04	2.56E-06	y
YPR028W	*YOP1*	ER	vesicle-mediated transport, cell membrane	6.40E-05	2.56E-06	y
YML095C	*RAD10*	cytoplasm/nucleus	DS break repair, nucleotide-excision repair factor 1 complex	4.00E-02	1.60E-03	partial
YGL163C	*RAD54*	cytoplasm/nucleus	chromatin remodeling, DS break repair, telomere maintenance	2.00E-01	2.00E-01	n
YOR305W	*YOR305W*	mitochondrion	unknown protein, mitochondrion localization	2.00E-01	2.00E-01	n
YMR007W	*YMR007W*	N/A	ORF, dubious	8.00E-03	1.60E-03	n
YBR078W	*ECM33*	N/A	GPI-anchored protein, cell membrane, mitochondrion	3.20E-04	3.20E-04	n
YLR337C	*VRP1*	punctate/actin	actin binding, actin organization	1.60E-03	1.60E-03	n
YMR206W	*YMR206W*	N/A	ORF, dubious	3.20E-04	3.20E-04	n

Table S1. Strains used in this study.

Strain #	Genotype		
YM3027	wild-type		
YM3028	*htz1*D::NatMX4	*HMR-C.a. URA3*	
YM2968	wild-type	*HMR-C.a. URA3*	*HMR*(right flank)NatMX4
YM2969	wild-type	*HMR-C.a. URA3*	*HMR*(right flank)NatMX4, *HMR*(left flank)HphMX4
YM2970	*ymr007wD::KanMX4*	*HMR-C.a. URA3*	*HMR*(right flank)NatMX4
YM2971	*ymr206wD::KanMX4*	*HMR-C.a. URA3*	*HMR*(right flank)NatMX4
YM2972	*yor305wD::KanMX4*	*HMR-C.a. URA3*	*HMR*(right flank)NatMX4
YM2973	*sin3D::KanMX4*	*HMR-C.a. URA3*	*HMR*(right flank)NatMX4
YM2974	*psk2D::KanMX4*	*HMR-C.a. URA3*	*HMR*(right flank)NatMX4
YM2975	*vtc1D::KanMX4*	*HMR-C.a. URA3*	*HMR*(right flank)NatMX4
YM2976	*prr1D::KanMX4*	*HMR-C.a. URA3*	*HMR*(right flank)NatMX4
YM2977	*elg1D::KanMX4*	*HMR-C.a. URA3*	*HMR*(right flank)NatMX4
YM2978	*sas5D::KanMX4*	*HMR-C.a. URA3*	*HMR*(right flank)NatMX4
YM2979	*sds3D::KanMX4*	*HMR-C.a. URA3*	*HMR*(right flank)NatMX4
YM2980	*sas2D::KanMX4*	*HMR-C.a. URA3*	*HMR*(right flank)NatMX4
YM2981	*rad54D::KanMX4*	*HMR-C.a. URA3*	*HMR*(right flank)NatMX4
YM2982	*pog1D::KanMX4*	*HMR-C.a. URA3*	*HMR*(right flank)NatMX4
YM2983	*slm4D::KanMX4*	*HMR-C.a. URA3*	*HMR*(right flank)NatMX4
YM2984	*isa2D::KanMX4*	*HMR-C.a. URA3*	*HMR*(right flank)NatMX4
YM2985	*cti6D::KanMX4*	*HMR-C.a. URA3*	*HMR*(right flank)NatMX4
YM2986	*nap1D::KanMX4*	*HMR-C.a. URA3*	*HMR*(right flank)NatMX4, *HMR*(left flank)HphMX4
YM2987	*swr1D::KanMX4*	*HMR-C.a. URA3*	*HMR*(right flank)NatMX4, *HMR*(left flank)HphMX4
YM2988	*htz1D::KanMX4*	*HMR-C.a. URA3*	*HMR*(right flank)NatMX4, *HMR*(left flank)HphMX4
YM2989	*asf1D::KanMX4*	*HMR-C.a. URA3*	*HMR*(right flank)NatMX4, *HMR*(left flank)HphMX4
YM2990	*sas4D::KanMX4*	*HMR-C.a. URA3*	*HMR*(right flank)NatMX4, *HMR*(left flank)HphMX4
YM2991	*cac2D::KanMX4*	*HMR-C.a. URA3*	*HMR*(right flank)NatMX4, *HMR*(left flank)HphMX4
YM2992	*sap30D::KanMX4*	*HMR-C.a. URA3*	*HMR*(right flank)NatMX4, *HMR*(left flank)HphMX4
YM2993	*ecm30D::KanMX4*	*HMR-C.a. URA3*	*HMR*(right flank)NatMX4, *HMR*(left flank)HphMX4
YM2994	*yop1D::KanMX4*	*HMR-C.a. URA3*	*HMR*(right flank)NatMX4, *HMR*(left flank)HphMX4
YM2995	*lap3D::KanMX4*	*HMR-C.a. URA3*	*HMR*(right flank)NatMX4, *HMR*(left flank)HphMX4
YM2996	*yil055cD::KanMX4*	*HMR-C.a. URA3*	*HMR*(right flank)NatMX4, *HMR*(left flank)HphMX4
YM2997	*yku80D::KanMX4*	*HMR-C.a. URA3*	*HMR*(right flank)NatMX4, *HMR*(left flank)HphMX4
YM2998	*rtt109D::KanMX4*	*HMR-C.a. URA3*	*HMR*(right flank)NatMX4, *HMR*(left flank)HphMX4
YM2999	*pho23D::KanMX4*	*HMR-C.a. URA3*	*HMR*(right flank)NatMX4, *HMR*(left flank)HphMX4
YM3000	*rif1D::KanMX4*	*HMR-C.a. URA3*	*HMR*(right flank)NatMX4, *HMR*(left flank)HphMX4
YM3001	*rxt2D::KanMX4*	*HMR-C.a. URA3*	*HMR*(right flank)NatMX4, *HMR*(left flank)HphMX4
YM3002	*srb2D::KanMX4*	*HMR-C.a. URA3*	*HMR*(right flank)NatMX4, *HMR*(left flank)HphMX4
YM3003	*dep1D::KanMX4*	*HMR-C.a. URA3*	*HMR*(right flank)NatMX4, *HMR*(left flank)HphMX4
YM3004	*ssd1D::KanMX4*	*HMR-C.a. URA3*	*HMR*(right flank)NatMX4, *HMR*(left flank)HphMX4
YM3005	*sic1D::KanMX4*	*HMR-C.a. URA3*	*HMR*(right flank)NatMX4, *HMR*(left flank)HphMX4
YM3006	*soh1D::KanMX4*	*HMR-C.a. URA3*	*HMR*(right flank)NatMX4, *HMR*(left flank)HphMX4
YM3007	*ybr077cD::KanMX4*	*HMR-C.a. URA3*	*HMR*(right flank)NatMX4, *HMR*(left flank)HphMX4
YM3008	*ygl081wD::KanMX4*	*HMR-C.a. URA3*	*HMR*(right flank)NatMX4, *HMR*(left flank)HphMX4
YM3009	*bdf2D::KanMX4*	*HMR-C.a. URA3*	*HMR*(right flank)NatMX4, *HMR*(left flank)HphMX4
YM3010	*ynl134cD::KanMX4*	*HMR-C.a. URA3*	*HMR*(right flank)NatMX4, *HMR*(left flank)HphMX4
YM3011	*dot6D::KanMX4*	*HMR-C.a. URA3*	*HMR*(right flank)NatMX4, *HMR*(left flank)HphMX4
YM3012	*kem1D::KanMX4*	*HMR-C.a. URA3*	*HMR*(right flank)NatMX4, *HMR*(left flank)HphMX4
YM3013	*rad10D::KanMX4*	*HMR-C.a. URA3*	*HMR*(right flank)NatMX4, *HMR*(left flank)HphMX4

YM3014	*srb5D::KanMX4*	*HMR-C.a. URA3*	*HMR*(right flank)NatMX4, *HMR*(left flank)HphMX4	
YM3015	*bdf1D::KanMX4*	*HMR-C.a. URA3*	*HMR*(right flank)NatMX4, *HMR*(left flank)HphMX4	
YM3016	*ldp16D::KanMX4*	*HMR-C.a. URA3*	*HMR*(right flank)NatMX4, *HMR*(left flank)HphMX4	
YM3029	*ymr007wD::KanMX4*	*HMR-C.a. URA3*	*HMR*(right flank)NatMX4	*sir3*D::hphMX4
YM3030	*ymr206wD::KanMX4*	*HMR-C.a. URA3*	*HMR*(right flank)NatMX4	*sir3*D::hphMX4
YM3031	*yor305D::KanMX4*	*HMR-C.a. URA3*	*HMR*(right flank)NatMX4	*sir3*D::hphMX4
YM3032	*sin3D::KanMX4*	*HMR-C.a. URA3*	*HMR*(right flank)NatMX4	*sir3*D::hphMX4
YM3033	*psk2D::KanMX4*	*HMR-C.a. URA3*	*HMR*(right flank)NatMX4	*sir3*D::hphMX4
YM3034	*vtc1D::KanMX4*	*HMR-C.a. URA3*	*HMR*(right flank)NatMX4	*sir3*D::hphMX4
YM3035	*prr1D::KanMX4*	*HMR-C.a. URA3*	*HMR*(right flank)NatMX4	*sir3*D::hphMX4
YM3036	*elg1D::KanMX4*	*HMR-C.a. URA3*	*HMR*(right flank)NatMX4	*sir3*D::hphMX4
YM3037	*sas5D::KanMX4*	*HMR-C.a. URA3*	*HMR*(right flank)NatMX4	*sir3*D::hphMX4
YM3038	*sds3D::KanMX4*	*HMR-C.a. URA3*	*HMR*(right flank)NatMX4	*sir3*D::hphMX4
YM3039	*sas2D::KanMX4*	*HMR-C.a. URA3*	*HMR*(right flank)NatMX4	*sir3*D::hphMX4
YM3041	*rad54D::KanMX4*	*HMR-C.a. URA3*	*HMR*(right flank)NatMX4	*sir3*D::hphMX4
YM3042	*pog1D::KanMX4*	*HMR-C.a. URA3*	*HMR*(right flank)NatMX4	*sir3*D::hphMX4
YM3043	*slm4D::KanMX4*	*HMR-C.a. URA3*	*HMR*(right flank)NatMX4	*sir3*D::hphMX4
YM3044	*isa2D::KanMX4*	*HMR-C.a. URA3*	*HMR*(right flank)NatMX4	*sir3*D::hphMX4
YM3045	*cti6D::KanMX4*	*HMR-C.a. URA3*	*HMR*(right flank)NatMX4	*sir3*D::hphMX4
YM3046		*HMR-C.a. URA3*	*HMR*(right flank)NatMX4	*sir3*D::*C.a.LYS2*
YM3047	*ldp16D::KanMX4*	*HMR-C.a. URA3*	*HMR*(right flank)NatMX4, *HMR*(left flank)HphMX4	*sir3*D::*C.a.LYS2*
YM3048	*nap1D::KanMX4*	*HMR-C.a. URA3*	*HMR*(right flank)NatMX4, *HMR*(left flank)HphMX4	*sir3*D::*C.a.LYS2*
YM3049	*swr1D::KanMX4*	*HMR-C.a. URA3*	*HMR*(right flank)NatMX4, *HMR*(left flank)HphMX4	*sir3*D::*C.a.LYS2*
YM3050	*htz1D::KanMX4*	*HMR-C.a. URA3*	*HMR*(right flank)NatMX4, *HMR*(left flank)HphMX4	*sir3*D::*C.a.LYS2*
YM3051	*asf1D::KanMX4*	*HMR-C.a. URA3*	*HMR*(right flank)NatMX4, *HMR*(left flank)HphMX4	*sir3*D::*C.a.LYS2*
YM3052	*sas4D::KanMX4*	*HMR-C.a. URA3*	*HMR*(right flank)NatMX4, *HMR*(left flank)HphMX4	*sir3*D::*C.a.LYS2*
YM3054	*sap30D::KanMX4*	*HMR-C.a. URA3*	*HMR*(right flank)NatMX4, *HMR*(left flank)HphMX4	*sir3*D::*C.a.LYS2*
YM3055	*vid21D::KanMX4*	*HMR-C.a. URA3*	*HMR*(right flank)NatMX4, *HMR*(left flank)HphMX4	*sir3*D::*C.a.LYS2*
YM3056	*ecm30D::KanMX4*	*HMR-C.a. URA3*	*HMR*(right flank)NatMX4, *HMR*(left flank)HphMX4	*sir3*D::*C.a.LYS2*
YM3057	*yop1D::KanMX4*	*HMR-C.a. URA3*	*HMR*(right flank)NatMX4, *HMR*(left flank)HphMX4	*sir3*D::*C.a.LYS2*
YM3058	*lap3D::KanMX4*	*HMR-C.a. URA3*	*HMR*(right flank)NatMX4, *HMR*(left flank)HphMX4	*sir3*D::*C.a.LYS2*
YM3059	*yil055cD::KanMX4*	*HMR-C.a. URA3*	*HMR*(right flank)NatMX4, *HMR*(left flank)HphMX4	*sir3*D::*C.a.LYS2*
YM3060	*yku80D::KanMX4*	*HMR-C.a. URA3*	*HMR*(right flank)NatMX4, *HMR*(left flank)HphMX4	*sir3*D::*C.a.LYS2*
YM3061	*rtt109D::KanMX4*	*HMR-C.a. URA3*	*HMR*(right flank)NatMX4, *HMR*(left flank)HphMX4	*sir3*D::*C.a.LYS2*
YM3062	*pho23D::KanMX4*	*HMR-C.a. URA3*	*HMR*(right flank)NatMX4, *HMR*(left flank)HphMX4	*sir3*D::*C.a.LYS2*
YM3063	*rif1D::KanMX4*	*HMR-C.a. URA3*	*HMR*(right flank)NatMX4, *HMR*(left flank)HphMX4	*sir3*D::*C.a.LYS2*
YM3064	*rxt2D::KanMX4*	*HMR-C.a. URA3*	*HMR*(right flank)NatMX4, *HMR*(left flank)HphMX4	*sir3*D::*C.a.LYS2*
YM3065	*srb2D::KanMX4*	*HMR-C.a. URA3*	*HMR*(right flank)NatMX4, *HMR*(left flank)HphMX4	*sir3*D::*C.a.LYS2*
YM3066	*dep1D::KanMX4*	*HMR-C.a. URA3*	*HMR*(right flank)NatMX4, *HMR*(left flank)HphMX4	*sir3*D::*C.a.LYS2*
YM3067	*ssd1D::KanMX4*	*HMR-C.a. URA3*	*HMR*(right flank)NatMX4, *HMR*(left flank)HphMX4	*sir3*D::*C.a.LYS2*
YM3068	*sic1D::KanMX4*	*HMR-C.a. URA3*	*HMR*(right flank)NatMX4, *HMR*(left flank)HphMX4	*sir3*D::*C.a.LYS2*
YM3069	*soh1D::KanMX4*	*HMR-C.a. URA3*	*HMR*(right flank)NatMX4, *HMR*(left flank)HphMX4	*sir3*D::*C.a.LYS2*
YM3070	*ybr077cD::KanMX4*	*HMR-C.a. URA3*	*HMR*(right flank)NatMX4, *HMR*(left flank)HphMX4	*sir3*D::*C.a.LYS2*
YM3071	*ygl081wD::KanMX4*	*HMR-C.a. URA3*	*HMR*(right flank)NatMX4, *HMR*(left flank)HphMX4	*sir3*D::*C.a.LYS2*
YM3072	*bdf2D::KanMX4*	*HMR-C.a. URA3*	*HMR*(right flank)NatMX4, *HMR*(left flank)HphMX4	*sir3*D::*C.a.LYS2*
YM3073	*ynl134cD::KanMX4*	*HMR-C.a. URA3*	*HMR*(right flank)NatMX4, *HMR*(left flank)HphMX4	*sir3*D::*C.a.LYS2*
YM3074	*dot6D::KanMX4*	*HMR-C.a. URA3*	*HMR*(right flank)NatMX4, *HMR*(left flank)HphMX4	*sir3*D::*C.a.LYS2*
YM3075	*kem1D::KanMX4*	*HMR-C.a. URA3*	*HMR*(right flank)NatMX4, *HMR*(left flank)HphMX4	*sir3*D::*C.a.LYS2*
YM3076	*rad10D::KanMX4*	*HMR-C.a. URA3*	*HMR*(right flank)NatMX4, *HMR*(left flank)HphMX4	*sir3*D::*C.a.LYS2*
YM3077	*ygl081wD::KanMX4*	*HMR-C.a. URA3*	*HMR*(right flank)NatMX4, *HMR*(left flank)HphMX4	*sir3*D::*C.a.LYS2*
YM3078	*srb5D::KanMX4*	*HMR-C.a. URA3*	*HMR*(right flank)NatMX4, *HMR*(left flank)HphMX4	*sir3*D::*C.a.LYS2*
YM3079	*bdf1D::KanMX4*	*HMR-C.a. URA3*	*HMR*(right flank)NatMX4, *HMR*(left flank)HphMX4	*sir3*D::*C.a.LYS2*
YM3080	*cac2D::KanMX4*	*HMR-C.a. URA3*	*HMR*(right flank)NatMX4, *HMR*(left flank)HphMX4	*sir3*D::*C.a.LYS2*

Chapter Two

Histone variant H2A.Z marks the 5' ends of both active and inactive genes in euchromatin

Histone variant H2A.Z marks the 5' ends of both active and inactive genes in euchromatin

Ryan M. Raisner[1,4], Paul D. Hartley[1,4], Marc D. Meneghini[1], Marie Z. Bao[1], Chih Long Liu[2], Stuart L. Schreiber[2], Oliver J. Rando[2], and Hiten D. Madhani[1,3]

[1]Dept. of Biochemistry and Biophysics

University of California

600 16th Street

San Francisco, CA 94143-2200

[2]Bauer Center for Genomics Research

Harvard University

7 Divinity Avenue

Cambridge, MA 02138

[3]Corresponding author

hiten@biochem.ucsf.edu

tel 415-514-0594

fax 415-502-4315

[4]Equal authors

SUMMARY

In *S. cerevisiae*, histone variant H2A.Z is deposited in euchromatin at the flanks of silent heterochromatin to prevent its ectopic spread. The degree to which H2A.Z is found and functions elsewhere is unknown. Here we show that H2A.Z nucleosomes are found at promoter regions of nearly all genes in euchromatin. They generally occur as two positioned nucleosomes that flank a nucleosome-free region (NFR) that contains the transcription start site. Astonishingly, enrichment at 5' ends is independent of transcriptional state as it is observed not only at actively transcribed genes, but also at inactive loci. Mutagenesis of a typical promoter revealed a 22 bp segment of DNA sufficient to program formation of a NFR flanked by two H2A.Z nucleosomes. This segment contains a binding site of the Myb-related protein Reb1 and an adjacent dT:dA tract. Efficient deposition of H2A.Z is further promoted by a specific pattern of histone H3 and H4 tail acetylation and the bromodomain protein Bdf1, a component of the Swr1 complex that deposits H2A.Z. These data define DNA- and histone-based mechanisms by which dividing cells define the 5' ends of genes and preserve their euchromatic state in the absence of transcription.

INTRODUCTION

The association of eukaryotic DNA with histone octamers to form nucleosomes has profound implications for all aspects of DNA metabolism. Epigenetic control mediated through chromatin is now recognized as a major form of genetic regulation that functions during both normal development and pathogenic processes such as tumorigenesis. Therefore, a critical challenge faced by dividing eukaryotic cells is the faithful maintenance of both active and inactive epigenetic states of specific genomic regions. Three known biochemical mechanisms exist to control the states of chromatin: histone posttranslational modifications (on both the unstructured N-terminal tails and core regions), ATP-dependent chromatin remodeling by Swi2/Snf2 family members, and histone variant substitution. The current goal of the field is to link these mechanisms to epigenetic regulation. Substantial progress has been made in understanding how silent heterochromatin is generated and maintained. In *S. cerevisiae*, cycles of histone tail deacetylation by Sir2 protein combined with binding of the Sir 2/3/4 complex to deacetylated tails appears to underlie the spread of heterochromatin (RUSCHE *et al.* 2003). In metazoan silencing systems, histone deacetylation is layered with methylation of lysines 9 or 27 of the H3 N-terminal tail, which serve as docking sites for chromodomain–containing members of the HP1 and Polycomb families, respectively (FISCHLE *et al.* 2003). In addition, recent work has shown that novel RNAi-based mechanisms promote the silent state in many systems (MATZKE and BIRCHLER 2005). Compared to heterochromatin, less is understood about how euchromatin is generated, maintained, and inherited. Indeed, euchromatin has widely been viewed as a default state.

More recently, however, several chromatin modifications have been identified that promote the euchromatic state by antagonizing silencing. These include the replacement of histone H2A by H2A.Z (MENEGHINI *et al.* 2003) and three histone modifications: acetylation on lysine 16 of the (NG *et al.* 2003a; SANTOS-ROSA *et al.* 2004; VAN LEEUWEN *et al.* 2002). H4 tail (KIMURA *et al.* 2002; SUKA *et al.* 2002), and methylation of lysines 4 and 79 of H3 In this paper, we focus on the deposition pattern of H2A.Z in euchromatin and its implications. In previous work, we demonstrated that in *S. cerevisiae,* the evolutionarily conserved histone variant H2A.Z functions in euchromatin to antagonize the spread of Sir-dependent silencing. Furthermore, we showed that at the right border of the *HMR***a** silent mating type cassette, H2A.Z functions in parallel with a well-characterized boundary element (MENEGHINI *et al.* 2003). Thus, H2A.Z is a component of euchromatin that functions to antagonize the opposite chromatin state. One key question, therefore, is whether H2A.Z is randomly distributed through euchromatin and if not, how its deposition to specific sites is determined. We and others have also identified a 13 subunit ATP-dependent chromatin remodeling complex, the Swr1 complex, that is required for the deposition of H2A.Z in vivo (KOBOR *et al.* 2004a; KROGAN *et al.* 2003b; MIZUGUCHI *et al.* 2004). Where the Swr1 complex acts and how its specificity is determined is not known. Interestingly, a subunit of this complex is Bdf1, a protein containing two tandem bromodomains known to bind acetylated histone tails (LADURNER *et al.* 2003; MATANGKASOMBUT and BURATOWSKI 2003). This suggests recognition of histone acetylation as one potential mechanism for the targeting of H2A.Z deposition to euchromatin. Bdf1 also associates with the yeast TFIID (MATANGKASOMBUT *et al.* 2000), a protein complex required for the transcription

of a subset of genes, and whose orthologs in other species directly recognize conserved core promoter sequences (CHALKLEY and VERRIJZER 1999).

Early chromatin immunoprecipitation (ChIP) experiments performed by Smith and coworkers suggested a relative enrichment of an epitope-tagged version of H2A.Z at the promoter regions of the highly inducible *GAL1-10* and *PHO5* genes in yeast (SANTISTEBAN *et al.* 2000). Moreover, these experiments demonstrated enrichment under non-inducing conditions for the linked genes and this enrichment decreased upon gene induction. However, it is difficult to make general conclusions from these studies for three reasons. First, since only four intergenic regions were examined, their correlation with higher H2A.Z levels could have been coincidental. Second, since no intergenic regions lacking a promoter were examined, the correlation with H2A.Z levels could have reflected preferential H2A.Z deposition in intergenic regions rather than in promoters per se. Third, since nucleosome density was not examined in the gene induction experiments, whether H2A.Z was selectively removed upon gene activation relative to H3, for example, was not clear. Thus, the following issues remain unresolved: 1) where is H2A.Z deposited in general? 2) what is the relationship between H2A.Z deposition to transcription? and 3) what are the signals that induce its deposition?

Using ChIP together with either quantitative PCR or hybridization to high-density oligonucleotide microarrays, we show here that H2A.Z is specifically enriched at 5' regions of genes throughout euchromatin. For the majority of genes, deposition occurs at two positioned nucleosomes that flank a nucleosome-free region (NFR) that contains the initiation site of transcription. Remarkably, this deposition is not correlated with transcription rate and even occurs at genes that are not transcribed. This striking finding

implies that cells have a mechanism for marking the 5' ends of genes independently of active transcription. We define two mechanisms that promote H2A.Z deposition. First, we define a bipartite DNA element that programs H2A.Z deposition: mutagenesis of a promoter revealed a 22 bp segment sufficient to induce formation of a nucleosome-free region flanked by two H2A.Z nucleosomes when placed into the middle of an inactive ORF. This segment contains a binding site for the Myb-related general regulatory factor Reb1 and an adjacent $d(T:A)_7$ tract, which are two sequence motifs commonly found in yeast promoters. Both elements were found to be required for H2A.Z deposition. Second, we show that histone tail acetylation and Bdf1 are required for efficient H2A.Z deposition. These data reveal a new aspect of eukaryotic gene structure and suggest parallels between mechanisms that promote the formation of euchromatin and heterochromatin.

RESULTS

H2A.Z is preferentially enriched at 5' regions in general

Previous studies have described a prominent role for H2A.Z at heterochromatin-proximal regions to antagonize the spread of silencing; however, we were curious to examine whether H2A.Z might play a broader role in the genome. Such additional roles could be elucidated through knowledge of the deposition profile of H2A.Z across chromosomes. We chose to examine the H2A.Z deposition profile in *S. cerevisiae* Chromosome III because it contains the *HMR*a and *HML*α silent mating type cassettes and is well-characterized with respect to the location of replication origins, cohesion sites and transcription initiation sites. This analysis was conducted with a strain carrying an allele of H2A.Z with an amino-terminal influenza hemeagglutinin epitope tag (*HA_3-HTZ1*) that was integrated at the endogenous locus as the sole genomic copy. This allele is functional in that it can complement the synthetic lethality of *htz1*Δ with *bre1*Δ (HWANG *et al.* 2003). ChIP and quantitative real-time PCR (QPCR) were used to determine H2A.Z enrichment at 300 bp segments whose 5' ends were spaced at 1000 bp intervals across Chromosome III. We observed a highly non-uniform and chromosome-wide distribution of H2A.Z (Fig. 1A; Table S1). Further analysis of our data indicated that the level of H2A.Z deposition at a given ChIP probe region was positively correlated with its proximity to the nearest 5' end of a gene (Fig. 1B). However, we observed no apparent correlation with proximity to 3' ends of genes that are not near 5' ends, the transcription rate of the nearest gene, cohesion sites, or origins of replication (unpublished observations and see below).

We next increased the resolution of our Chromosome III analysis to a single intergenic region flanked by two non-converging ORFs. The intergenic region upstream of *SNT1* was chosen because it is significantly smaller relative to the *SNT1* coding region. A 4.2 kb continuous region starting from 2 kb upstream of the *SNT1* initiation codon to 2.2 kb downstream was assayed for H2A.Z enrichment by ChIP and QPCR using primer sets that tiled the region. This assay revealed a striking intergenic enrichment for H2A.Z with a sharp decline in the coding region of *SNT1* and in the upstream gene *BPH1* (Fig. 1C).

We then identified a larger region of Chromosome III (the *LEU2-YCL012c* interval) containing a mixture of gene orientations: genes whose 5' ends share an intergenic region (5'-5'); genes whose 5' ends are adjacent to a 3' end (5' only); and genes whose 3' ends converge (3-3'). We assayed the H2A.Z deposition profile within this 11 kb region by ChIP and QPCR. This tiling analysis revealed that for every H2A.Z peak of enrichment, there was a corresponding 5' end (Fig. 1D). In most cases, the peak enrichment of H2A.Z was close to, or directly upstream of the initiation codon. The only shared 5' region in this dataset (the *DCC1-BUD3* intergenic region) had two distinct peaks of H2A.Z enrichment, one corresponding to the 5' end of each gene. The observed H2A.Z peaks in these promoter regions were not due to increased cross-linkability or nucleosome density of these regions because additional ChIP analysis of histone H3 across the same region revealed slightly lower, not higher, ChIP signals in intergenic regions (Fig. S1). Finally, the two regions with converging ORFs (3'-3') had no observable peak of H2A.Z, supporting the notion that H2A.Z is indeed selectively enriched at 5' regions of genes.

High resolution chromosome-wide mapping of endogenous H2A.Z nucleosomes

Our initial analyses of H2A.Z deposition relied on a ChIP protocol that involved shearing DNA to an average size of 500 bp, which meant that QPCR analyses of immunoprecipitated material resolved multiple nucleosomes, thereby obscuring finer details of H2A.Z localization. In addition, the tiling methods we used to assay H2A.Z deposition at an appropriate resolution are not feasible for rapidly examining much larger regions such as whole chromosomes. To overcome these two limitations, we used a ChIP and microarray hybridization protocol to analyze the distribution of endogenous, untagged H2A.Z at the resolution of single nucleosomes; the data were normalized for nucleosome density (see Experimental Procedures). The microarrays tiled the majority of Chromosome III and 223 additional regulatory regions at a resolution of 20 bp.. These experiments yielded a nucleosome-resolution map of H2A.Z enrichment patterns across nearly half a megabase of the *S. cerevisiae* genome (Table S2).

Analysis of the data recapitulated our initial conclusions about the specific deposition of H2A.Z at 5' ends of genes (Fig. 1) and extended these conclusions to a larger portion of the yeast genome. Fig. 2A shows the microarray data for the regions analyzed by QPCR in Fig. 1C and 1D. Consistent with the QPCR data, the region upstream of *SNT1* contains H2A.Z, and this H2A.Z signal has now been resolved into a striking distribution pattern in which two consecutive nucleosomes contain H2A.Z. Two H2A.Z nucleosomes are also found upstream of the *BPH1* gene, one upstream of the *FEN1* gene and two in the *RRP43-RBK1* intergenic region that is flanked by the 5' ends of the respective genes. In contrast, no H2A.Z peak was observed in the *FEN1-RRP43*

intergenic region that is flanked by the 3' ends of those two genes. Also shown in Fig. 2A is a portion of the *NFS1-YCL012C* region analyzed in Fig. 2B; *LEU2* is missing because this gene is deleted in the strain profiled using the microarray method. The QPCR analysis of this region was precisely recapitulated by the microarray data: H2A.Z was found specifically in intergenic regions that contain at least one 5' end of a gene. Indeed, analysis of the entirety of Chromosome III revealed H2A.Z upstream of most euchromatic genes and not at intergenic regions flanked by two converging 3' ends (Table S2). Genes on Chromosome III that lacked detectable H2A.Z in their promoter regions correspond to genes in the *HMLα* silent cassette, genes near the telomeres of Chromosome III, ORFs annotated as "dubious," and seven apparently bona fide euchromatic genes (*HIS4, POL4, ADY2, AGP1, RPS14A, PMP1,* and *YCR006C*). While it is not obvious why these genes lack H2A.Z in their promoter regions, we note that *YCR006C* contains a tRNA gene in its upstream regions. tRNA genes have been shown to contain boundary activity (DONZE *et al.* 1999) and have been shown to inhibit expression of adjacent PolII-transcribed genes (BOLTON and BOEKE 2003). Since genes lacking H2A.Z in their promoters represent a small minority, we conclude that H2A.Z generally marks the 5' ends of genes in euchromatin.

Recent work by Yuan and coworkers (2005) demonstrated that nucleosomes are generally uniformly distributed across yeast promoters and ORFs, but nearly all yeast genes contain a ~150 bp nucleosome free region (NFR) centered ~200 bp upstream of the initiation codon. cDNA hybridization studies demonstrated that these regions contain the initiation site for transcription of their associated genes (YUAN *et al.* 2005). The genes represented in the H2A.Z microarray data were aligned by the center of their NFRs to

generate a cluster hierarchy shown in Figure 2B. Remarkably, for about 2/3 of the genes analyzed, the NFR is flanked by two nucleosomes that contain H2A.Z. The remainder of these genes appear either to have H2A.Z present only at one nucleosome, or lack H2A.Z entirely for potential reasons explained above. (Table S3). Thus, not only does H2A.Z mark the 5' ends of genes, but two positioned H2A.Z nucleosomes typically flank the transcription initiation site. These data demonstrate that H2A.Z nucleosomes are placed in a highly stereotyped and organized manner at the 5' ends of genes.

Active transcription is not required for H2A.Z enrichment

The striking localization of H2A.Z at most gene promoters suggested that there could be a relationship between H2A.Z and gene transcription. To address this issue, we selected from the H2A.Z ChIP microarray data those genes that contain two H2A.Z nucleosomes flanking a NFR and compared the levels of H2A.Z enrichment at each of the two nucleosomes to two distinct measurements of transcriptional activity for the corresponding gene (Fig. 3). We used genome-scale data from either an analysis of initiation rates (Fraser, et al., 2004; Figures 4A and 4C) or RNA polymerase II occupancy (Kim, et al., 2004; Figures 3B and 3D). Comparison of H2A.Z enrichment at genes to either dataset showed no correlation between H2A.Z enrichment and transcriptional activity. In other words, the transcription rate of a gene does not predict the levels of H2A.Z at a given promoter.

To further assess whether H2A.Z requires active transcription for its selective enrichment at gene promoter regions, we examined several promoter regions under conditions known to produce their tight repression. We first chose to examine the

sporulation/meiosis-specific genes *DIT1, DIT2, HOP1*, and *SPO22* in a haploid strain grown in rich media. These genes are transcriptionally inactive in haploid cells and in non-meiotic diploid cells (CHU *et al.* 1998). Additionally, these four occur in two pairs in which their 5' ends flank an intergenic promoter region. Strikingly, we observed peaks of H2A.Z enrichment at both of the shared promoter regions (Fig. 4A and B). These patterns were not explained by underlying nucleosome density since H3 is relatively evenly distributed across these intervals (Fig. S2). To attempt to observe de novo deposition of H2A.Z at these loci, we constructed a galactose-inducible HA epitope-tagged allele of *HTZ1* with which we could selectively induce or repress the transcription of H2A.Z. As expected, under the repressive glucose condition, virtually no H2A.Z is detectable by ChIP (Fig. S3). However, after growth for several generations in galactose, peaks of H2A.Z enrichment were observed at the divergent promoters of both meiotic gene pairs (Fig. S3). Thus, H2A.Z can be deposited at inactive genes.

Another region we examined is the highly regulated mating-type specific gene *AGA2*. In yeast, **a**-specific genes (**a**sgs) such as *AGA2* have been well studied and are known to be active in *MAT***a** strains, but extremely tightly repressed by the α2-Mcm1 complex in *MAT*α and *MAT***a**/α strains (GALITSKI *et al.* 1999). We utilized isogenic strains harboring the chromosomal *HA$_3$-HTZ1* allele and differing only in the allele present at the mating type locus (*MAT***a** or *MAT*α). Using ChIP and QPCR, we observed a peak of H2A.Z signal at *AGA2* in *MAT***a** and its continued presence in *MAT*α strains (Fig. 4C). Although well above those seen in the ORF of the *BUD3* gene (Fig. 4C), H2A.Z levels were approximately two-fold lower at the repressed *AGA2* locus compared

to the active locus even though promoter histone H3 signals were similar in **a** versus α cells (Fig. 4C and Fig. S2).

Previous work showed that **a**sg promoters display relative hypoacetylation on the histone H4 tails in *MAT*α strains relative to *MAT***a** strains (DECKERT and STRUHL 2001)**.** We performed ChIP using antibodies raised against a tetra-acetylated peptide derived from the N-terminal tail of histone H4 (Ac_4H4), and confirmed this result—an approximately two-fold reduction of acetylation was observed in the *MAT*α strains (Fig. 4D). Interestingly, both the positioning and relative level of acetylation in **a** versus α cells closely parallels those of HA_3-*HTZ1* at *AGA2*, suggesting potential interplay between acetylation and H2A.Z deposition.

Finally, we identified two genes involved in mating in the microarray data that have been shown not to be expressed under vegetative conditions: *FIG2* and *PRM1*. Previous work has shown that expression of these genes only occurs in response to mating pheromone (ERDMAN *et al.* 1998; HEIMAN and WALTER 2000). Analysis of H2A.Z enrichment at these loci revealed peaks in their promoter regions (Fig. S4).

Effect of gene induction on H2A.Z levels: activation of *FIG1* by mating pheromone

Our analysis revealed no correlation between H2A.Z levels normalized for nucleosome density and transcription rates nor RNA polymerase II occupancies, suggesting no general relationship between transcription and H2A.Z levels. As described in the Introduction, previous studies of H2A.Z levels at *GAL1* and *PHO5* promoters revealed that it decreased upon gene induction, although whether this represented exchange of H2A.Z for H2A or general nucleosome depletion was not determined. In

contrast, we observed that while the inactive *AGA2* promoter contains H2A.Z, its levels are higher when the gene is active.

To extend these results, we examined H2A.Z and H3 levels at a gene that is highly inducible by mating pheromone, *FIG1* (ERDMAN *et al.* 1998). As shown in Fig. S5, *FIG1* expression is dependent on mating pheromone—treatment of cells with mating pheromone strongly induced mRNA accumulation over a one-hr. time course as determined by quantitative RT-PCR. ChIP analysis revealed that H2A.Z is depleted during gene induction. However, H3 was also depleted from the *FIG1* promoter during the time course such at the 5, 15 , and 30 min. time points, the ratio of H2A.Z to H3 was constant (Fig. S5). At the 60 min. time point, an apparent depletion of H2A.Z relative to H3 was observed; however, it seems likely that the promoter H3 signal at this time point was elevated as an artifact of signal from flanking nucleosomes that were not separated by sonication from the promoter nucleosomes prior to ChIP (Fig. S5). The H2A.Z signal would not be subject to this problem since H2A.Z nucleosomes are distributed in a punctate pattern whereas H3-containing nucleosomes are distributed homogenously. Thus, with the possible exception of this late time point, activation of *FIG1* results in nucleosome loss rather than the replacement of H2A.Z with H2A.

Histone tail acetylation is required for efficient recruitment of H2A.Z

We performed a reporter-based genome-wide screen of the *S. cerevisiae* knockout collection to identify genes that antagonize the spread of silencing from the *HMR***a** silent mating type cassette (R.M.R. and H.D.M., unpublished observations). This screen identified Eaf1, a nonessential component of the essential NuA4 HAT complex and the

bromodomain-containing proteins, Bdf1 and Bdf2. Bdf1 is a component of the Swr1 complex responsible for H2A.Z deposition, and both Bdf1 and Bdf2 bind to acetylated histone tails (LADURNER *et al.* 2003; MATANGKASOMBUT and BURATOWSKI 2003). To test whether histone acetylation is important for H2A.Z deposition, we generated strains bearing the HA_3-*HTZ1* allele containing deletions of the genes encoding the H4-specific histone acetyltransferase (HAT) Eaf1 or the H3- and H4-specific HAT Elp3. In addition, we created a strain lacking both HATs. ChIP analysis revealed a dependence upon histone tail acetylation for robust H2A.Z enrichment (Fig. 5A). At a majority of loci examined, deletion of *EAF1* resulted in a reproducible defect in H2A.Z levels. The defects varied from approximately 1.5- to 3-fold in magnitude. Likewise, deletion of *ELP3* also led to a defect at most loci, albeit more quantitatively modest than those of the *eaf1Δ* mutant. The severity of the defects in the *eaf1Δ elp3Δ* double mutant is not significantly greater than either of the single deletions (Fig. 5A), suggesting Eaf1 and Elp3 may act in the same pathway to mediate H2A.Z deposition.

To further test the role of histone acetylation in H2A.Z deposition, we utilized a series of histone H3 and H4 mutants in which specific target lysine residues have been mutated to arginine which prevents acetylation. We observed a consistent quantitative defect in H2A.Z enrichment values at most of the 10 loci examined (Fig. 5B, 5C). In general, the strongest defects were observed in cells harboring the H3-K9R mutant or the H4-K5R,K12R mutant. For the H4-K5R,K12R mutant, we performed ChIP using antibodies against H3 as well and found no differences in nucleosome density at the loci examined in Fig. 5C, indicating that the defect in H2A.Z deposition was not caused by general nucleosome loss (Fig. S6). Surprisingly, a deletion mutant in the H4 tail

displayed a less severe defect than the H4-K5R,K12R mutant (Fig. 5C). The H4-K8R,K16R mutant displayed no defect, indicating that not all mutants in acetylatable tail lysines produce a defect in H2A.Z deposition (Fig. 5C).

Bdf1 and Bdf2 act redundantly to promote H2A.Z deposition

Having established a role for histone tail acetylation for complete H2A.Z deposition, we hypothesized that acetylation could be acting to recruit targeting of the Swr1 complex via binding of its subunit Bdf1 to acetylated tails. This is an attractive model because in addition to being important for anti-silencing, Bdf1 is known to bind preferentially to acetylated forms of histone H4, and is enriched in intergenic regions throughout the genome (KURDISTANI *et al.* 2004). However, ChIP analysis using polyclonal Htz1 antibody raised against the C-terminal tail region showed that a *bdf1Δ* strain has little or no defect in H2A.Z enrichment at euchromatic loci (Fig 5E). We reasoned that this could be due to compensatory activity by the redundant gene *BDF2*, which when deleted yielded no detectable defect in H2A.Z enrichment (data not shown). Unfortunately, *bdf1*Δ *bdf2*Δ strains are inviable, precluding a test of this hypothesis using null alleles. Therefore, we elected to generate a "knockdown" allele of *BDF2* by replacing its 3' UTR region with a MX6 marker cassette. This maneuver has been found to consistently cause destabilization of the cognate mRNA (J. Weissman, pers. comm.). We refer to this allele as *bdf2-utr*Δ*,* and as is the case for the *bdf2*Δ, it also has no defect for H2A.Z enrichment (data not shown). As seen by tetrad dissection, the *bdf1Δ bdf2-utr*Δ double mutants grow more slowly than either single mutant, indicating a defect produced by *bdf2-utr*Δ (Fig. 5D). Examining these strains by ChIP, we found that

although *bdf1Δ* cells showed little or no defects in H2A.Z deposition, the *bdf1Δ bdf2-utrΔ* displayed a reproducible defect in H2A.Z deposition at a majority of loci examined (Fig. 5E), while no defect was observed in the ORF of the control locus *PRP8*. These experiments clearly demonstrate a dependence on Bdf1 and its redundant homolog Bdf2 for full H2A.Z deposition at the 5' regions of genes. However, since acetylation of promoter nucleosomes generally correlates with transcription (Liu et al., 2005), the requirement for Bdf1/2 and histone tail acetylation for efficient deposition of H2A.Z does not explain how it can be deposited at inactive genes in euchromatin.

Mutagenesis of the *SNT1* promoter reveals sequences necessary for H2A.Z deposition in vivo.

One hypothesis for how H2A.Z is deposited at inactive as well as active genes is that there exist specific DNA elements in promoters that program its deposition. Although there is no precedent for a DNA element that specifically induces variant histone deposition, we decided to pursue this model by systematically mutagenizing a typical promoter that contains two positioned H2A.Z nucleosomes (Fig. S7). For this analysis, we chose to analyze the *SNT1* promoter region described in Figure 1 because it was well separated from nearby promoters by the relatively large *BPH1* and *SNT1* ORFs.

To localize sequences required for H2A.Z deposition, we divided the *BPH1-SNT1* intergenic region into 75 bp segments and then precisely replaced each segment in the chromosome with a 75 bp fragment of the bacterial cloning vector pBluescript (Fig. S7). Mutants in either of two adjacent intervals (termed 5 and 6 in Fig. S7) resulted in a modest two-fold reduction in H2A.Z enrichment (Fig. S7). However, a mutant that

replaced both intervals resulted in a dramatic defect in H2A.Z enrichment (Fig. S7). Interestingly, these two intervals roughly correspond to the nucleosome-free region between the two H2A.Z nucleosomes that lie upstream of the *SNT1* gene. RT-QPCR analysis of *SNT1* expression revealed only a two-fold drop in *SNT1* mRNA levels (unpublished observations). These data suggested the presence of partially redundant signals for H2A.Z deposition in intervals 5 and 6.

To further define these signals, we constructed 14 additional substitution mutants in the NFR of the *SNT1* promoter (Fig. 6A). For these mutants, we replaced varying segments within intervals 5 and 6 with identical-sized segments from the ORF of *BUD3*, which lacks H2A.Z depositon (Fig. 1). We examined H2A.Z deposition using primers that span the two flanking positioned H2A.Z nucleosomes. Of the 14 mutants tested only two, *mu1* and *mu3*, abolished H2A.Z enrichment (Fig. 6A). The sequences replaced in *mu3* represent a subset of those in *mu1*, defining the minimal segment that must be mutated to produce a complete loss of H2A.Z deposition in the *SNT1* promoter. Substitution of smaller segments resulted in increased H2A.Z enrichment. For example, *mu4* has the identical 5' endpoint as *mu3* but substitutes 10 fewer bp on the 3' end and displays robust H2A.Z enrichment (Fig. 6A). These 10 bp are therefore critical for H2A.Z deposition in the context of *mu3*. Likewise, *mu10* substitutes 20 bp fewer than *mu3* on the 5' end and shows increased H2A.Z enrichment (Fig. 6A), indicating that there are sequences that promote H2A.Z deposition in the 20 bp that distinguish *mu3* from *mu10*. We note that for mutants that display an intermediate level of H2A.Z depostion, our analysis does not distinguish between a decrease in H2A.Z deposition versus a shift in the position of the H2A.Z nucleosomes. Nonetheless, our identification of mutants

that eliminate H2A.Z deposition in this region suggest that the segments identified play a role in deposition per se. Taken together, these data suggest the presence of two redundant signals for H2A.Z deposition, one that includes the 10 bp that distinguishes *mu3* from *mu4* and another that includes the 20 bp that distinguishes *mu3* from *mu10*.

A 22 bp segment from the *SNT1* promoter is sufficient to induce the formation of a NFR flanked by two H2A.Z nucleosomes

Our analysis of sequences necessary for H2A.Z deposition at the promoter of *SNT1* identified two discrete regions. We next tested whether these regions also sufficient to promote H2A.Z deposition at a novel site. To date, we have not succeeded in identifying a fragment containing the 20 bp 5' region that is sufficient to promote H2A.Z deposition. Therefore, we focus below on a signal that contains the 3' 10 bp segment hypothesized above to contain a H2A.Z deposition signal.

A magnified view of this 10 bp sequence and flanking sequences is shown in Fig. 6B. Two notable features of this sequence are a binding site for the general regulatory factor Reb1 and an adjacent tract of seven dT:dA base-pairs. Both sequence elements are disrupted in *mu3* compared to *mu4*. Moreover, previous studies had shown that a similar arrangement of sequences in the yeast *PFY1* promoter was important for the formation of a NFR in that promoter (ANGERMAYR *et al.* 2003). Therefore, we tested whether a DNA segment containing this region could generate an NFR flanked by H2A.Z nucleosomes when placed elsewhere in the genome.

We inserted the 22 bp segment containing the Reb1 site and $(dT:dA)_7$ tract in the middle of an inactive gene, *PRM1* (Fig. 7A). *PRM1* was chosen because it had been

shown previously to only be expressed in cells exposed to mating pheromone, and we sought to avoid the potentially complicating effects of transcription on H2A.Z deposition (HEIMAN and WALTER 2000). Examination of H2A.Z deposition using probes flanking the insertion site revealed robust H2A.Z enrichment in the strain containing the insertion (Fig. 7B). Replacement of the three G residues in the Reb1 consensus site abolished the effect of the insertion as did a deletion of the $(dT:dA)_7$ tract.

To determine whether an NFR was induced by the insertion, we performed nucleosome scanning analysis (SEKINGER *et al.* 2005) to determine the positions of nucleosomes containing H3 and H2A.Z in the parental strain and the strain containing the insertion. As described in the Experimental Procedures, crosslinked mononucleosomes were immunoprecipated with antibodies to either H3 or H2A.Z and then analyzed by QPCR analysis using primer pairs that amplified 100 bp segments every 20 bp across the *PRM1* ORF. As shown in Fig. 7C, five nucleosomes containing histone H3 were found in the *PRM1* ORF in the parental strain. The arrow in Fig. 6C indicates the site of insertion, which was in the center of the +4 nucleosome. The 22 bp insert had two effects on the nucleosome pattern (Fig. 7D). First it caused a delocalization of nucleosome pattern in the first part of the *PRM1* ORF. Second it results in a formation of an NFR. This can be deduced by examining the peak-to-peak distance of nucleosomes flanking the insertion site, which is 320 bp in the strain containing the insertion versus 180 bp between the center points of the +3 and +4 nucleosomes in the parental strain. Assuming that 147 bp of DNA is wrapped by the yeast histone octamer, one calculates that the insertion caused an expansion of the linker region between these two nucleosomes from approximately 33 bp to 173 bp.

We next determined the positions of H2A.Z nucleosomes in the parental and insertion strains. As shown in Fig. 7E, little H2A.Z enrichment was observed in ORF of the *PRM1* gene in the parental strain, as expected. Strikingly, insertion of the 22 bp segment from the *SNT1* gene resulted in the appearance of two positioned variant H2A.Z nucleosomes. Moreover, the peaks were separated by 320 bp, confirming the formation of an NFR in the insertion strain.

DISCUSSION

Our results show that nucleosomes containing the conserved histone variant H2A.Z occur in euchromatin in a highly organized rather than a random pattern. In particular, the experiments decisively demonstrate that H2A.Z is selectively present at the vast majority of gene promoter regions. Most commonly, it occurs as two positioned nucleosomes that flank a NFR that includes the transcription initiation site. The most striking finding is that H2A.Z enrichment is uncorrelated with transcription rates and is observed at promoters of genes that are not detectably transcribed. The implications of this observation are potentially far-reaching, as it indicates that cells can identify the 5' ends of genes in the absence of ongoing transcription. We describe two mechanisms that begin to provide insight into how this remarkable pattern of histone variant deposition occurs. Analysis of the *SNT1* promoter resulted in the identification of a 22 bp bipartite DNA element sufficient to promote H2A.Z deposition when placed in a novel context. This signal contains two necessary elements that are generally conserved in yeast promoters: a binding site for the Myb-related general regulatory factor Reb1 and an $(dT:dA)_7$ tract. In addition, we demonstrated that H2A.Z deposition is linked to histone acetylation and Bdf1, a double bromodomain protein that binds acetylated histone tails. Below we discuss the results in further detail and suggest models for how the marking of 5' ends by H2A.Z could occur and the ramifications for how genes are defined in eukaryotic cells.

H2A.Z nucleosomes mark the 5' ends of both active and inactive genes in euchromatin

Our results provide the first single nucleosome-resolution global picture of the deposition pattern of a conserved histone variant. Alignment of the microarray data based on the identified nucleosome-free regions (NFR) of yeast promoters that includes the transcription initiation site (YUAN *et al.* 2005) revealed that most euchromatic genes contain two positioned H2A.Z nucleosomes which flank the NFR. Our analysis to date cannot distinguish whether these each nucleosomes contain two copies of H2A.Z, or one copy of H2A.Z and one copy of H2A. However, it has been suggested based on structural analysis that heteromeric H2A.Z/H2A nucleosomes may be unable to form due to steric clash (SUTO *et al.* 2000). Because one of the two H2A.Z nucleosomes is typically downstream of the initiation site of transcription and one is not, it is unlikely that passage of RNA polymerase alone plays a role in either depositing or removing H2A.Z nucleosomes in general. Indeed, a small group of genes contains only the downstream H2A.Z nucleosome (Fig. 2B). It is not yet obvious why these genes differ in their deposition pattern. Consistent with our previous data that indicated the exclusion of H2A.Z nucleosomes from the *HMR***a** silent mating type cassette, the microarray analysis (which was performed in a mating type **a** strain) reveals an exclusion of H2A.Z from the *HML*α silent cassette and from subtelomeric regions (see Tables S2 and S3).

Most strikingly, we find that the levels of deposition of H2A.Z in promoters are clearly not correlated with either the transcription rate or RNA polymerase II occupancy of the linked coding sequences (Fig. 4). This is in contrast to modificiations such as trimethylation of lysine 4 of histone H3 in yeast, which does correlates with transcription

rate and typically occurs on the first nucleosomes downstream of the transcription initiation site (BERNSTEIN *et al.* 2002; KROGAN *et al.* 2003a; NG *et al.* 2003b)**.** Indeed, our analysis of genes that are not transcribed and/or tightly repressed demonstrated enrichment of H2A.Z in their promoters. These include two meiotic gene pairs examined in haploid cells in rich media, the **a**-specific gene *AGA2* assayed in α cells, and two genes only expressed in pheromone treated cells, *FIG2* and *PRM1,* that were assessed in the absence of pheromone. Although we cannot rule out the possibility that H2A.Z deposition occurs at these genes in response to rare transcription events that produce mRNAs that fail to detectably accumulate, a simpler interpretation of our data is that cells have a transcription independent mechanism to specify H2A.Z deposition at the 5' ends of genes.

Although H2A.Z can be deposited at inactive genes, our data suggests that transcription can modulate H2A.Z levels in at least two ways. First, at *AGA2*, we observed higher H2A.Z levels when the gene was active than when it was inactive. Second, at *FIG1*, we observed that activation resulted in concomitant depletion of H2A.Z and H3, consistent with the removal of variant octamers. Since the relative levels of H2A.Z and transcription are uncorrelated when considering large numbers of genes (Fig. 3), it seems likely that transcription modulates the relative amounts of H2A.Z variant nucleosomes differently at different genes. Further work will be needed to define the relationships between transcription and H2A.Z promoter marking. Nonetheless, our results demonstrate that for cells to identify the 5' ends of genes and deposit H2A.Z, genes need not be transcribed.

Histone tail acetylation and Bdf1 promote deposition of H2A.Z

Our genetic experiments led us to investigate the potential connection between histone tail acetylation and H2A.Z deposition. ChIP analyses demonstrated that for various defects in histone tail acetylation, whether produced by mutation of acetylated lysines or deletion of genes encoding histone acetyltransferases, there is a moderate decrease in H2A.Z at most sites assayed. The quantitative rather than qualitative defect in H2A.Z deposition in these mutant backgrounds may reflect either a partial dependence on histone tail acetylation for deposition or that histone acetylation was only partially eliminated in our experiments. Distinguishing between these two possibilities is not trivial since the H3 and H4 N-terminal tails are together essential for viability (LING *et al.* 1996). Moreover, cells lacking the catalytic subunit of the NuA4 HAT and cells lacking both the Gcn5 and Sas3 HATs are inviable (CLARKE *et al.* 1999; HOWE *et al.* 2001). We also note that the in vivo deposition assays used here do not measure the rate of H2A.Z deposition. Therefore, the modest defects observed in acetylation mutants at steady-state may reflect a more profound defect in the rate of deposition, especially if one considers that as few as one exchange event at a nucleosome per cell cycle might be sufficient to produce wild-type levels of H2A.Z.

We find that the bromodomain proteins Bdf1 and Bdf2 act redundantly to promote H2A.Z deposition. Bdf1 is a subunit of both the Swr1 complex that deposits H2A.Z in vivo and is also associated with TFIID. Because Bdf1 contains two bromodomains and selectively binds acetylated versions of histone H4, we suggest that Bdf1 recognition of acetylated histone tails promotes recruitment of the Swr1 complex and deposition of H2A.Z. In vitro studies of the purified Swr1 complex and acetylated

nucleosomal substrates will be required to confirm this model. It is notable that the H4-K8R, K16R mutation did not affect H2A.Z deposition: recent work has shown that deacetylation of H4-K16 is actually necessary for the association of Bdf1 with chromatin in vivo (KURDISTANI *et al.* 2004). Consistent with these observations, recent studies of histone acetylation patterns at the mononucleosome level demonstrated that the two nucleosomes flanking the NFR have a unique acetylation pattern (LIU *et al.* 2005). In particular, these nucleosomes are both highly deacetylated on H4-K8 and 16, and this deacetylation domain occurs independently of transcription level, thereby precisely paralleling the H2A.Z localization pattern presented here. Moreover, the nucleosome downstream of the NFR is acetylated on H3-K9,14 and H4-K5,12. It is unlikely to be coincidental that lysine-to-arginine mutation of the residues that are deacetylated on the NFR-flanking nucleosomes does not affect H2A.Z deposition, while mutation of acetylated residues inhibits H2A.Z deposition (Table 1). Together with the data showing that Bdf1 binding to chromatin is inhibited by H4-K16 acetylation, these results are consistent with a direct role for Bdf1 in recognizing the acetylation patterns of the NFR-flanking nucleosomes to promote H2A.Z deposition. However, since acetylation of nucleosome downstream of the NFR correlates with transcription rates (Liu et al., 2005), efficient deposition of H2A.Z at highly deacetylated inactive promoters must involve mechanisms that would not in principle depend on ongoing transcription.

Identification of a bipartite DNA signal sufficient to induce H2A.Z deposition

We have defined one such mechanism, namely the existence of DNA signals that program H2A.Z deposition. Our analysis of the *SNT1* promoter revealed two segments

of DNA that appear to function redundantly since mutations in two segments with the NFR were necessary to eliminate H2A.Z deposition. We showed that the 3' signal, which contains a site for the Myb-related general regulatory factor Reb1 and an adjacent $(dT:dA)_7$ tract, was sufficient to induce the formation of an NFR and the replacement of H2A with H2A.Z in the two flanking nucleosomes when placed into the middle of the coding sequence of inactive *PRM1* gene. Both the Reb1 site and $(dT:dA)_7$ motif were found to be necessary for H2A.Z deposition.

Reb1 was originally identified as an abundant nuclear protein involved in rDNA transcriptional termination but was subsequently shown to associate with a large number of yeast promoter regions (JU *et al.* 1990). Recent studies of the conservation of the Reb1 DNA binding motif have shown that it is the single most conserved motif found in yeast promoters and is even more conserved across species than the TATA box (ELEMENTO and TAVAZOIE 2005). Several studies have shown that tethering of Reb1 or related Myb-family general regulatory factors (Rap1, Abf1, or Tbf1) to DNA can prevent the spread of silent chromatin but the mechanism remains unknown (FOUREL *et al.* 2002; YU *et al.* 2003). Given our results, it could be that this property of these factors involves the induction of a NFR and/or the deposition of H2A.Z nucleosomes.

The second motif that we found to be important for H2A.Z deposition is a tract of dT:dA base pairs which have been noted to be common in yeast promoters, particularly in NFRs (Yuan et al., 2005). Studies of global nucleosome density have also shown that the abundance of motifs containing dT:dA tracts correlate with nucleosome depletion from promoters (BERNSTEIN *et al.* 2004; LEE *et al.* 2004). These studies concluded that promoters show transcription-independent reductions in nucleosome density compared

coding sequences but this conclusion has been questioned on technical grounds(POKHOLOK *et al.* 2005). Our study is relevant to this issue as it shows the functional importance of a dT:dA tract flanked by a site for Reb1 in the formation of NFR..Our data may also be relevant to the recent proposal that dT:dA tracts promote the formation of NFRs because of their intrinsic nuclesome excluding properties (SEKINGER *et al.* 2005). Although further work is necessary to understand how it functions, it seems unlikely that a sequence as short as 22 bp could act to program the formation of an ~170 bp NFR purely because of its intrinsic properties.

Although both Reb1 sites and dA:dT tracts are common features of yeast promoters, we do not yet know whether this is the sole type of DNA element that programs H2A.Z deposition at promoters. As mentioned above, other Myb-related factors might also be expected to play a role. A previous study of a Reb1 site and an adjacent dA:dT tract in the NFR in the promoter of the yeast *PFY1* gene (ANGERMAYR *et al.* 2003). This work showed that mutation of the Reb1 site eliminated the NFR; the role of the adjacent dA:dT tract was not assessed. Thus, it may be that Reb1 generally induces the formation of NFRs in promoters. This raises the question of whether Reb1 promotes H2A.Z deposition and NFR formation through independent or coupled mechanisms. Our preliminary studies show that deletion of *HTZ1* or *SWR1* does not prevent the formation of the NFR in the strain containing the 22 bp insertion into *PRM1* (unpublished observations). Thus, the 22 bp element either promotes NFR formation and H2A.Z independently (e.g. via recruitment of different factors) or the formation of the NFR itself induces H2A.Z deposition.

Potential similarities between H2A.Z deposition in euchromatin to Sir complex deposition in heterochromatin

Our results indicate two features of chromatin contribute to the deposition of H2A.Z: a DNA signal and histone tail acetylation. It seems worth noting that heterochromatin formation in yeast also involves specific DNA signals and histone acetylation. For example, at the silent mating type cassettes *HMR***a** and *HML*α, silencer elements that nucleate silent chromatin formation function through binding sites for ORC, Rap1, and Abf1, which in turn recruit the Sir histone deacetylase complex. As with the Reb1-$(dT:dA)_n$ element described here, silencers harbor binding sites for sequence-specific DNA binding proteins that in other contexts appear to promote transcription. It is thought provoking that in a close relative of *S. cerevisiae*, the yeast *K. lactis*, Reb1 itself functions directly in *HM* silencing (SJOSTRAND *et al.* 2002). One observation that appears to distinguish H2A.Z deposition in euchromatin from the formation of heterochromatin, however, is that we have not observed spreading of H2A.Z beyond the two nucleosomes that flank NFRs.

Such thinking also raises the question of whether euchromatin, like heterochromatin might be subject to epigenetic inheritance (which we define here as inheritance of expression state which is templated in cis by the expression state of a region in the previous cell generation). In this regard, the existence of two rather than one H2A.Z nucleosomes that flank the NFR of a typical gene may be significant: conceivably, the inheritance of these two nucleosomes could be nonrandom such that each daughter strand of DNA after replication receives one of the two H2A.Z nucleosomes which, in turn templates that exchange of H2A.Z into the other to restore

the parental arrangement. Although these notions of epigenetic inheritance of euchromatic states are speculative at this point, we note that mutations in *ARP4*, which encodes an actin-related protein found in several chromatin modifying enzyme complexes, have been reported to yield the apparent epigenetic inheritance of expression state of a gene in euchromatin (JIANG and STILLMAN 1996).

Genome-wide functions of H2A.Z

Our previous studies showed that H2A.Z protects genes from the encroachment of silent heterochromatin. The genome-wide occurrence of H2A.Z at promoter nucleosomes raises the question of whether this is the sole function of H2A.Z or whether it has other roles in gene expression. We have recently determined that H2A.Z indeed functions genome-wide to antagonize silencing but that this function is redundant with histone H3 lysine 4 methylation (S. Venkatasubrahmanyam, W.W. Hwang, and H.D.M,, unpublished observations). Likewise, several studies have demonstrated that H2A.Z plays a role in gene activation, particularly when other chromatin modifications are inactived by mutation (ADAM *et al.* 2001; LAROCHELLE and GAUDREAU 2003; MILGROM *et al.* 2005; SANTISTEBAN *et al.* 2000). However, the precise mechanisms by which H2A.Z functions in anti-silencing and transcription are unclear. The presence of H2A.Z nucleosomes flanking the transcription start site of gene provides a unique protein surface at the 5' ends of genes. We speculate that H2A.Z may provide a docking site for proteins involved in various steps of gene expression while at the same time inhibiting the action of silencing proteins. Although further work will be required to identify these interactions, the data presented here suggest that they are likely to apply to the vast

majority of genes in euchromatin. Moreover, because H2A.Z is required for development in Drosophila and mice (FAAST *et al.* 2001; VAN DAAL and ELGIN 1992), understanding its role in genome organization and function in yeast is likely to inform studies of developmental gene regulation in more complex systems.

EXPERIMENTAL PROCEDURES

Yeast Strains

Strains used in these studies are described in Table S5.

Site-directed mutagenesis in *S. cerevisiae*.

Chromosomal mutations were created as described (STORICI *et al.* 2003).

Mapping DNA sequences necessary for H2A.Z deposition.

All strains generated for mapping sequences necessary for H2A.Z deposition at *SNT1* used a targeted site directed mutagenesis strategy described above. The initial mapping was accomplished by substitution of 75bp promoter intervals with a 75bp sequence of the pBluescript multiple cloning site (the region corresponding to 657-731 of the pBluescript KS+ plasmid sequence provided by Stratagene; the sequence is shown in Table S2. The sequence substituted for endogenous sequence to generate the 5,6 mutant (see Figure S5) corresponds to region 1540-1689 of pBluescript KS+.

Finer mapping of sequences necessary for H2A.Z deposition at *SNT1* involved the substitution of varying lengths of promoter DNA with an equal length of sequence from a portion of the *BUD3* ORF that essentially has no associated H2A.Z (Fig. 1D, coordinate 98544. In all cases, the sequence inserted came from a 150bp region (SGD coordinates 98544-98693 of Chromosome III). Sequences from *BUD3* rather than pBluescript were used to ensure that the results were not dependent on the particular sequence used to replace *SNT1* sequences. Table S7 shows the sequences inserted for each of the mutants shown in Figure 6.

Galactose induction of HA-Htz1 Expression

Cultures were grown at 30°C. Strains bearing an HA_3 epitope-tagged allele of *HTZ1* driven by the *GAL1* promoter at the endogenous *HTZ1* locus were grown to saturation in YPAD, then diluted to an A_{600} of 0.1, and outgrown in YEP containing 2% glucose to an A_{600} of 0.6. At that point, 50 mL of the cultures were cross-linked and harvested as described for ChIP-QPCR. The remaining cells were washed twice in water and added to YEP containing 2% galactose and 2% raffinose to an approximate A_{600} of 0.001 and grown for 2 days. These cultures were then back diluted to fresh YEP containing 2% galactose and 2% raffinose to an A_{600} OD of 0.1 and grown to an A_{600} of 0.6, cross-linked and harvested. Prior to cross-linking of all cultures, 3 absorbance units were harvested from each and analyzed by immunoblotting with antibodies against H2A.Z.

Induction of *FIG1* by mating pheromone

A wild-type *MAT***a** strain was grown in YPAD at 30°C overnight, diluted to an A_{600} of 0.1 and grown to an A_{600} of 0.6. An amount of culture representing 30 absorbance units was crosslinked and harvested for ChIP, and 3 absorbance units were harvested for total RNA isolation and RT-QPCR analysis of transcript levels using gene-specific primers for *FIG1* and *ACT1*. The remaining culture was split 4 ways and α−factor was added to a concentration of 10 μM to each and grown to the appropriate time point (5 min., 15 min., 30 min. or 1 hr.), whereupon 30 and 3 absorbance units of cells respectively were harvested as described above for ChIP and RT-QPCR analysis.

Mononucleosome preparation for microarray and nucleosome scanning experiments.

Mononucleosomes were preparared as described (Liu et al., 2005).

Chromatin Immunoprecipitation.

A variety of ChIP procedures were employed based on the desired analysis of the recovered DNA.

Chromatin immunoprecipitation for QPCR.

Yeast culture. Yeast strains were grown to saturation overnight in YPAD, followed by dilution to an A_{600} of 0.15 and growth to an A_{600} of 0.6-1.2 at 30°C in YPAD. Cells were crosslinked with 1% formaldehyde for 15 min. at room temperature, followed by quenching with 125mM glycine for 5 min. at room temperature. The cultures were then centrifuged to discard the media, and the cell pellets were washed twice with ice-cold TBS.

All ChIP steps were done at 4°C unless otherwise indicated. For each culture, the cell pellet was resuspended in 500 μl of Lysis Buffer (50 mM HEPES-KOH pH 7.5, 140 mM NaCl, 1 mM EDTA, 1% Triton X-100, 0.1% sodium deoxycholate containing protease inhibitors). The cells were lysed by glass bead homogenization with a bead mill set at maximum speed for 5 cycles of 1 min. each with 2 min. rest periods on ice. The lysates were centrifuged to obtain precipitated material that contains chromatin, which was resuspended in 500ul fresh Lysis Buffer. Chromatin was sheared by sonication with a Sonics Vibra-Cell sonicator (12 cycles of 12 seconds each at 50-75% power with 2 min.

rests on ice in between cycles). The lysate was then centrifuged to pellet precipitates, followed by recovery of the supernatant, which contains solubilized chromatin. This supernatant was brought up to 1.6 ml with Lysis Buffer and then split into 3 aliquots of 500 ul each in order to carry out immunoprecipitations in triplicate. For each aliquot, 10% (50 ul) of the supernatant was set aside as input material, which was diluted into a TE/SDS/proteinase K buffer (final concentrations: 10mM TE, 1% SDS, 200ug/ml proteinase K).

The appropriate antibodies were added to the 500 ul aliquots for at least 2 hrs. of immunoprecipitation with gentle rocking, followed by recovery of immunological complexes with either Protein A or G sepharose beads. The beads were then subjected to a wash process at room temperature; each wash was done for 5 min. with gentle rocking. First, beads were washed twice with Lysis Buffer, followed by two washes with High Salt Lysis Buffer (Lysis Buffer with 0.5M NaCl) and two washes with Wash Buffer (10 mM Tris-Cl pH 8.0, 0.25 M LiCl, 0.5% NP-40, 0.5% sodium deoxycholate). A final wash was done once with 10 mM Tris-Cl pH 8.0/1mM EDTA, and the bound antibody material was eluted by a 15 min. incubation at 65° in Elution Buffer (50 mM Tris-Cl pH 8.0, 1 mM EDTA, 1% SDS). The beads were pelleted at maximum speed for 15 min., and the supernatant was recovered. The beads were washed once with a TE/SDS solution containing proteinase K, and this wash was combined with the initial eluate. The final composition of this elutate was 10mM Tris-Cl pH 8.0, 1% SDS, 200ug/ml proteinase K. This elutate was incubated along with the input material at 65° overnight to reverse formaldehyde crosslinks. DNA was recovered with Qiagen PCR purification kits following the provided protocol; the elution buffer was TE pH 8.0 containing 10ug/ml

RNase A. The recovered DNA was incubated at 37° for 1 hr. to degrade any remaining RNA.

Chromatin immunoprecipitation for microarrays.

This procedure was used to generate the data shown in Figure 2, and was performed as described (Liu et al., 2005).

Chromatin immunoprecipitation for nucleosome scanning.

This procedure was used to generate the data shown in Figures 7C-7F. After micrococcal nuclease digestion (see above), 200 ul of a 4X stock of Lysis Buffer was added to each 600ul aliquot. Precipitated material was pelleted at maximum speed, and the supernatant was recovered. For each 450 ml of starting culture, six aliquots were available for immunoprecipitation; three aliquots were used for α-H3 or α-H2A.Z immunoprecipitation at 4° for at least 6 hrs. with gentle rocking. Protein A Sepharose beads were used to recover immunological complexes. The wash and elution procedures were the same as those described for ChIP-QPCR above. After an overnight 65°C incubation to reverse formaldehyde crosslinks, DNA was recovered with Qiagen MinElute PCR columns using the recommended procedure. The elution buffer was TE pH 8.0 containing 10 ug/ml RNase A.

High density microarray tiling analysis of H2A.Z deposition profile.

The yeast strain used in these microarray experiments was BY4741. Hybridization and analysis was performed as described (Liu et al., 2005).

Quantitation of DNA by Quantitative PCR.

Quantitative PCR with Opticon themocyclers (MJ Research/BioRad) was used to quantitate by Sybr green dye incorporation the starting amount of DNA in each PCR reaction. Relative starting amounts were calculated based on a serially diluted set of standards.

Assaying chromatin immunoprecipitation by quantitative PCR.

For each PCR amplicon, the amount of DNA recovered by immunoprecipitation was quantified and normalized to a quantification of input DNA recovered from the same cell extract. This normalization expresses the amount of DNA associated with the protein of interest in terms of an IP:input ratio. To take into account differences in efficiency during immunoprecipitation, this IP:input ratio was normalized to an IP:input ratio of a different locus (either an amplicon within *BUD3* or *PRP8*). In most cases, the data shown are representative of three independent immunoprecipitations of one culture, and error bars show the standard error of the mean.

Nucleosome scanning by quantitative PCR.

A 960 bp region of the *PRM1* ORF that contains the site of insertion for the sufficiency experiments was tiled with 48 PCR sets that amplified 100-105 bp segments of DNA. The amplicons overlapped one another across the region by 20 bp, which enables scanning the region at a resolution of 20bp. Table S7 shows the sequences of the primers used in this study.

The raw quantification data obtained from the nucleosome scanning is expressed in terms of mononucleosome:genomic ratios; in essence, the amount of DNA amplified from a mixture of mononucleosome-sized DNA is normalized to the amount of DNA amplified from pure genomic DNA. The genomic DNA was prepared by first recovering pure genomic DNA using a Qiagen Genomic-tip 100/G and lightly digesting a portion with micrococcal nuclease such that the average DNA size is about 1 kb. This light digestion takes into account hot spots for micrococcal nuclease within the template.

While the mononucleosome:genomic ratios shown in Figures 7E and 7F have not been further transformed, the ratios shown in Figures 7C and 7D have been normalized to the amplicon that represents the median value.

SUPPLEMENTARY MATERIAL.

Seven figures, seven tables, and legends are available online.

ACKNOWLEDGEMENTS

We are grateful to Sharon Roth Dent for histone point mutants. This work was supported by grants from the NIH-NIGMS (H.D.M., S.L.S., O.J.R.), the Packard Foundation (H.D.M.), the Bauer Center (S.L.S., O.J.R.), and the Burroughs-Wellcome Fund (M.D.M.). We thank Wallace Marshall for critical reading of the manuscript and Sandy Johnson and Joe DeRisi for support and advice. Author contributions are as follows: R.M.R. performed the experiments shown in Figures 1C, 1D, 4, 5, S1, S2, S3, S5, and S6. P.D.H. performed the experiments shown in Figures 6, 7 and S7. M.Z.B. and M.D.M. performed the experiments shown in Figures 1A and 1B. C.L.L. and O.J.R. performed the experiments shown in Figures 2, 3, and S4. R.M.R., P.D.H., O.J.R., and H.D.M. wrote the paper.

FIGURE LEGENDS

Figure 1. H2A.Z enrichment in euchromatin.

A. Schematic of *HA_3-HTZ1* ChIP enrichment across Chromosome III. Bars represents IP/WCE value as determined by QPCR for a single 300 bp segment. Each 5' primer is separated by 1000 bp.

B. Log scale graph comparing H2A.Z enrichment values to distance to the nearest initiation codon. The correlation coefficient is 0.2662

C and D. Diagram of *BPH1-SNT1* interval (C) and the *LEU2-YCL012c* interval (D). Both regions were assayed by ChIP and QPCR *HA_3-HTZ1* deposition. Enrichment values are average IP/WCE ratios from triplicate samples with standard error of the mean (SEM) error bars. Genes encoded on the Watson strand in red, and the Crick strand in green with arrows denoting the direction of transcription. Vertical dashed lines are drawn through each gene's initiation codon. X-axis values are the chromosomal coordinates of the 5' primers of each pair used.

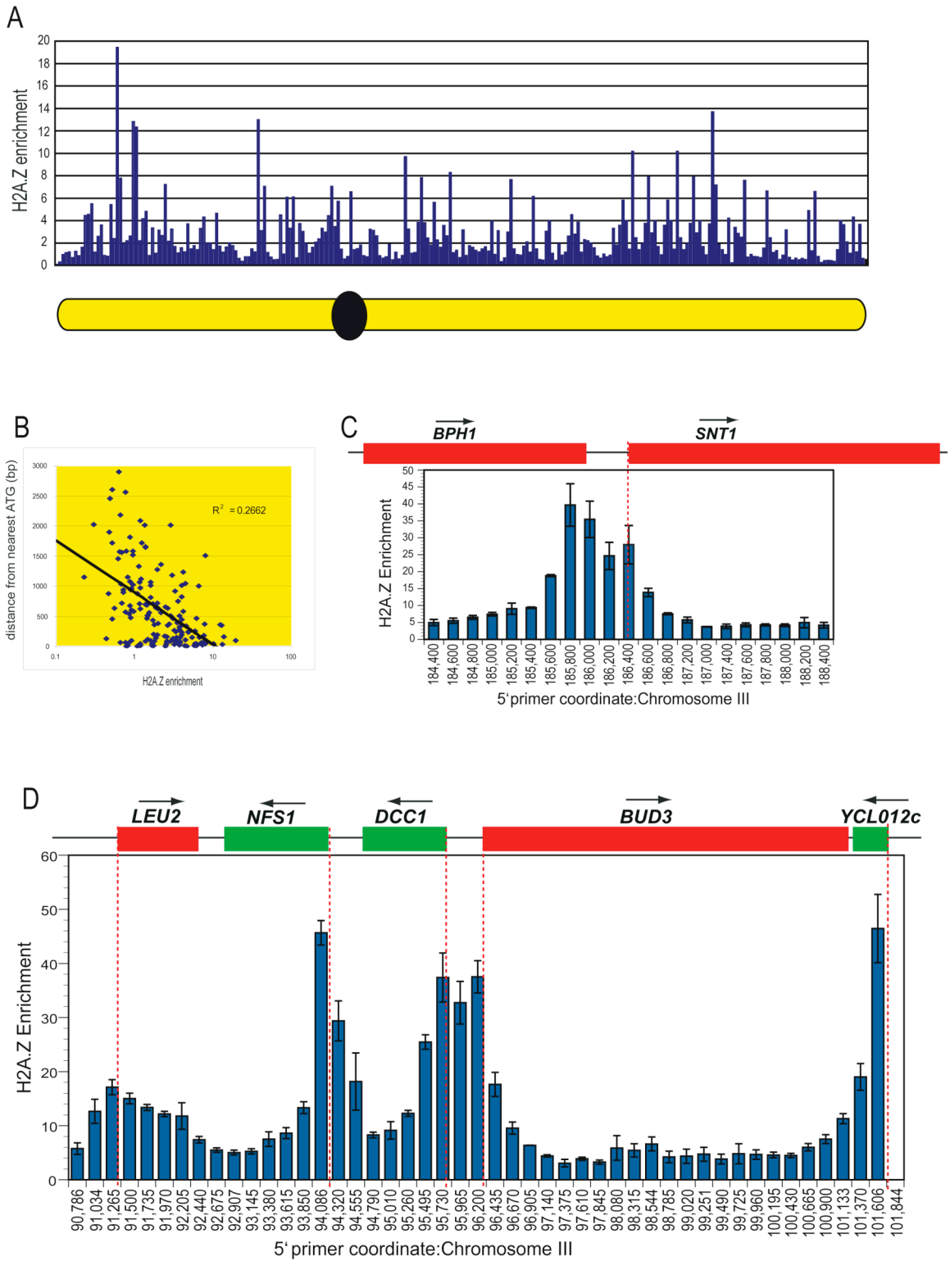
A
H2A.Z enrichment
B
distance from nearest ATG (bp)
R² = 0.2662
H2A.Z enrichment
C
BPH1
SNT1
H2A.Z Enrichment
5' primer coordinate:Chromosome III
D
LEU2
NFS1
DCC1
BUD3
YCL012c
H2A.Z Enrichment
5' primer coordinate:Chromosome III

Figure 2. High resolution mapping of H2A.Z nucleosomes.

Shown is a color depiction of ratio of the ChIP signal for mononucleosomal DNA immunoprecipitated using anti-Htz1 antibodies divided by those for DNA extracted from mononucleosomes for regions covered by a high-resolution oligonucleotide tiling microarray.

(A) H2A.Z enrichment in representative euchromatic regions analyzed in Fig. 2A. Shown are the data for five replicate microarray hybridizations. Yellow represents a positive relative enrichment for H2A.Z over the median enrichment versus blue for negative enrichment.

(B) Clustered array dataset centered on nucleosome free regions (NFRs) of gene promoters. Shown are data from probes from up to 1 kb upstream and 1 kb downstream of the position of the NFR estimated from previous studies (Yuan et al., 2005) . Each row represents a single promoter region and columns correspond to data from microarray oligonucleotides at a given position with respect to the NFR.

Figure 2

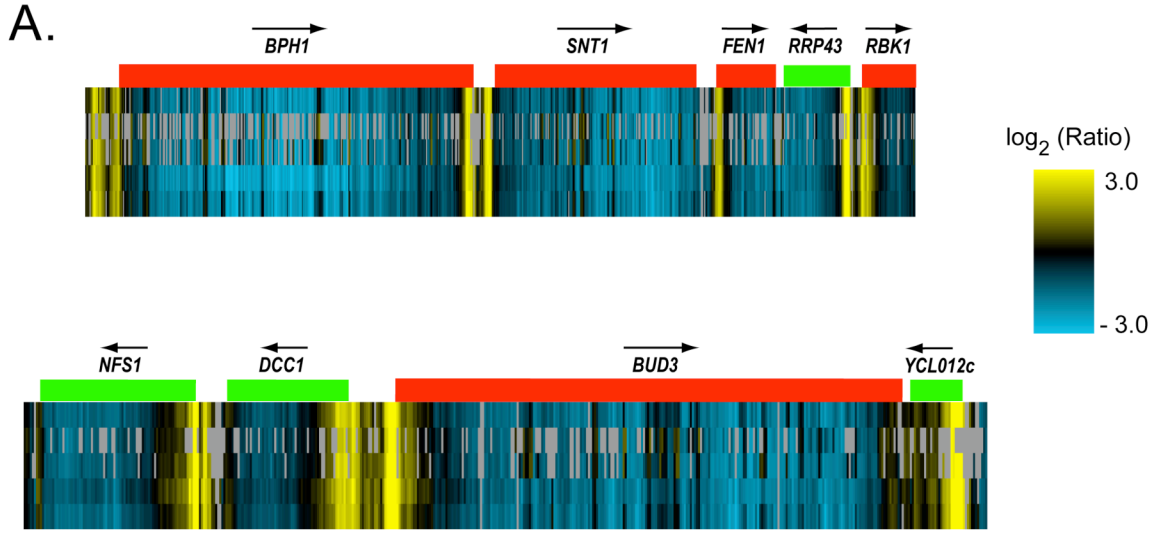
A.
BPH1
SNT1
FEN1
RRP43
RBK1
log2 (Ratio)
3.0
- 3.0
NFS1
DCC1
BUD3
YCL012c

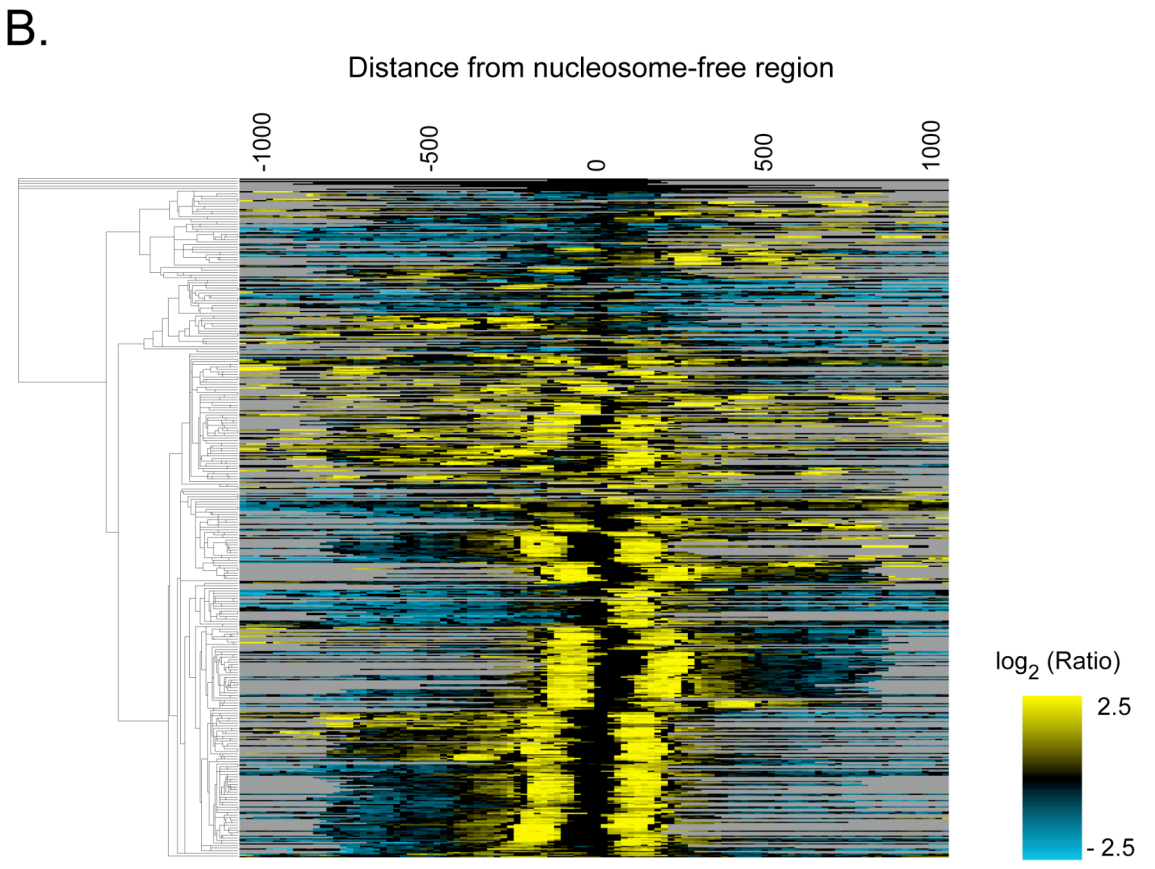
B.
Distance from nucleosome-free region
-1000
-500
0
500
1000
log2 (Ratio)
2.5
- 2.5

Figure 3. Comparison of H2A.Z enrichment normalized for nucleosome density with transcription rate and RNA polymerase II occupancy.

Shown are plots of promoter H2A.Z enrichments shown in Fig. 2 versus calculated transcription rates and RNA polymerase II occupancy as determined by ChIP. (A) and (B) show plots for H2A.Z nucleosomes 3' of the whereas (C) and (D) show plots for the nucleosomes 5' to the NFR. R^2 values are shown.

Figure 3

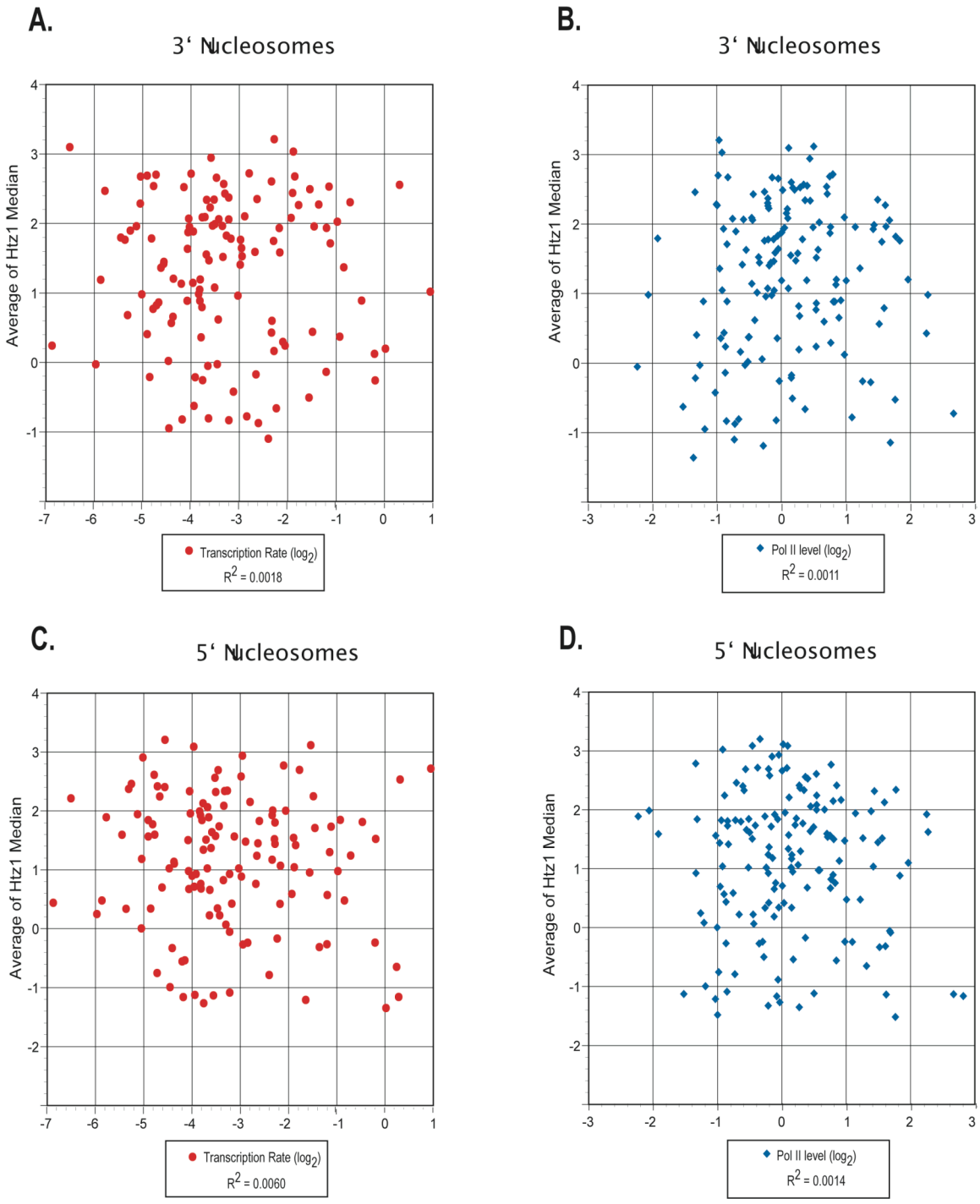
A.
3‘ Nucleosomes
Average of Htz1 Median
Transcription Rate (log2)
R2 = 0.0018
B.
3‘ Nucleosomes
Average of Htz1 Median
Pol II level (log2)
R2 = 0.0011
C.
5‘ Nucleosomes
Average of Htz1 Median
Transcription Rate (log2)
R2 = 0.0060
D.
5‘ Nucleosomes
Average of Htz1 Median
Pol II level (log2)
R2 = 0.0014

Figure 4. H2A.Z enrichment at meiosis-specific and **a**-specific genes.

All enrichment values are triplicate averages of *HA$_3$-HTZ1* or Ac$_4$H4 ChIP DNA amounts normalized to the *BUD3* ORF region with SEM error bars. Sidebars show *BUD3* and *SGF29* (positive control) loci. (A and B) *HA$_3$-HTZ1* enrichment at the *DIT1/DIT2* (A) and *HOP1/SPO22* (B) promoter and ORF regions. QPCR fragments are for consecutive 200 bp segments; dashed lines are drawn through gene initiation codons to their approximate relative position. (C) *HA$_3$-HTZ1* and (D) Ac$_4$H4 normalized enrichment at *AGA2* for *MAT***a** and *MAT*α strains. QPCR probes correspond to consecutive 100 bp segments with the position of the 5' primer relative to the initiation codon of *AGA2* denoted.

Figure 4

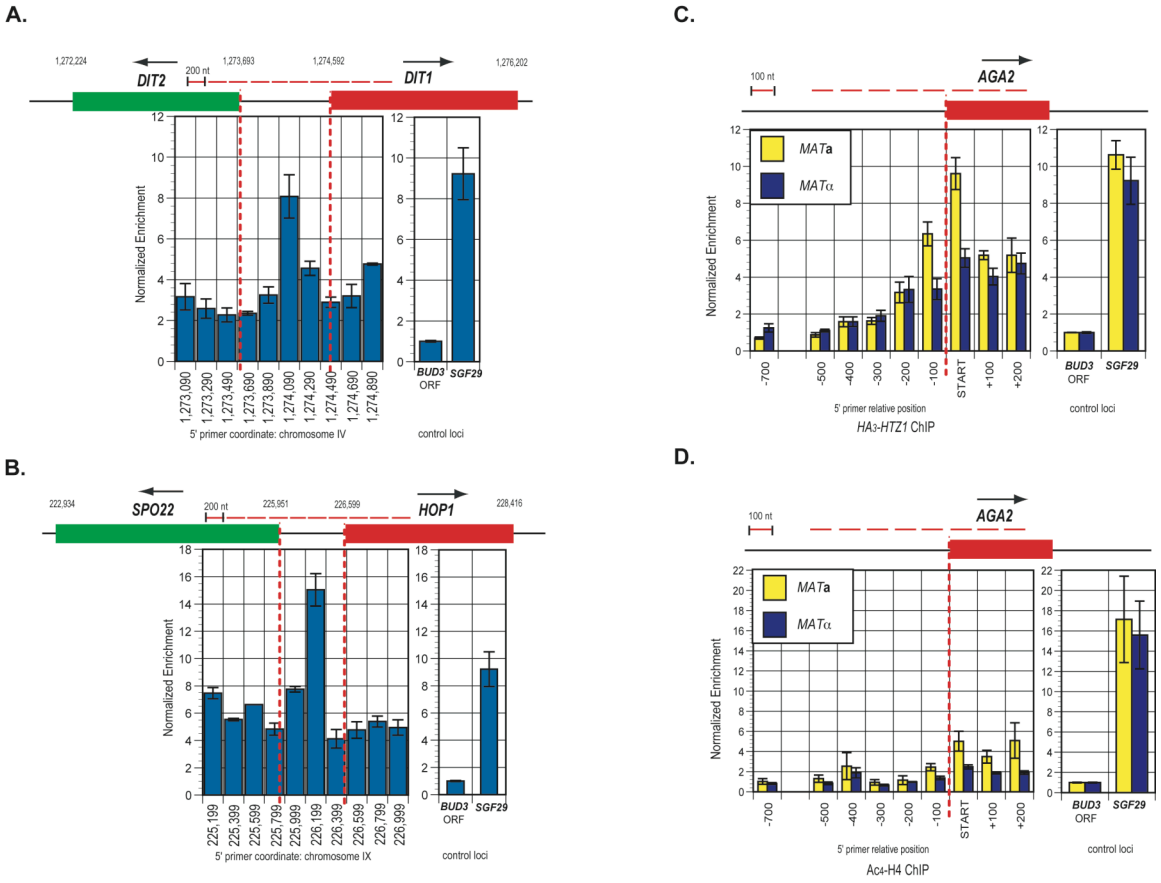
A.
1,272,224
200 nt
1,273,693
1,274,592
1,276,202
DIT2
DIT1
Normalized Enrichment
1,273,090
1,273,290
1,273,490
1,273,690
1,273,890
1,274,090
1,274,290
1,274,490
1,274,690
1,274,890
5' primer coordinate: chromosome IV
BUD3
SGF29
ORF
control loci
B.
222,934
200 nt
225,951
226,599
228,416
SPO22
HOP1
Normalized Enrichment
225,199
225,399
225,599
225,799
225,999
226,199
226,399
226,599
226,799
226,999
5' primer coordinate: chromosome IX
BUD3
SGF29
ORF
control loci
C.
100 nt
AGA2
MATa
MATα
Normalized Enrichment
-700
-500
-400
-300
-200
-100
START
+100
+200
5' primer relative position
HA3-HTZ1 ChIP
BUD3
SGF29
ORF
control loci
D.
100 nt
AGA2
MATa
MATα
Normalized Enrichment
-700
-500
-400
-300
-200
-100
START
+100
+200
5' primer relative position
Ac4-H4 ChIP
BUD3
SGF29
ORF
control loci

Figure 5. ChIP analysis of H2A.Z enrichment at selected euchromatic promoters in wild type, histone acetylation-defective mutants, and in *bdf1*Δ mutants

A.-C. Triplicate average *HA$_3$-HTZ1* enrichment ratios of HAT mutants (A), histone H4 mutants (B), and histone H3 mutants (C) compared to those of wild-type strains plotted on a log scale with SEM error bars.

D. Tetrad analysis of meiotic products of *BDF1*/*bdf1*Δ *BDF2*/*bdf2-utr*Δ heterozygous diploids. Genotypes of first column of spores are shown. Their phenotypes are representative.

E. Quadruplicate normalized average H2A.Z enrichment values for mutant compared to wild-type with SEM error bars.

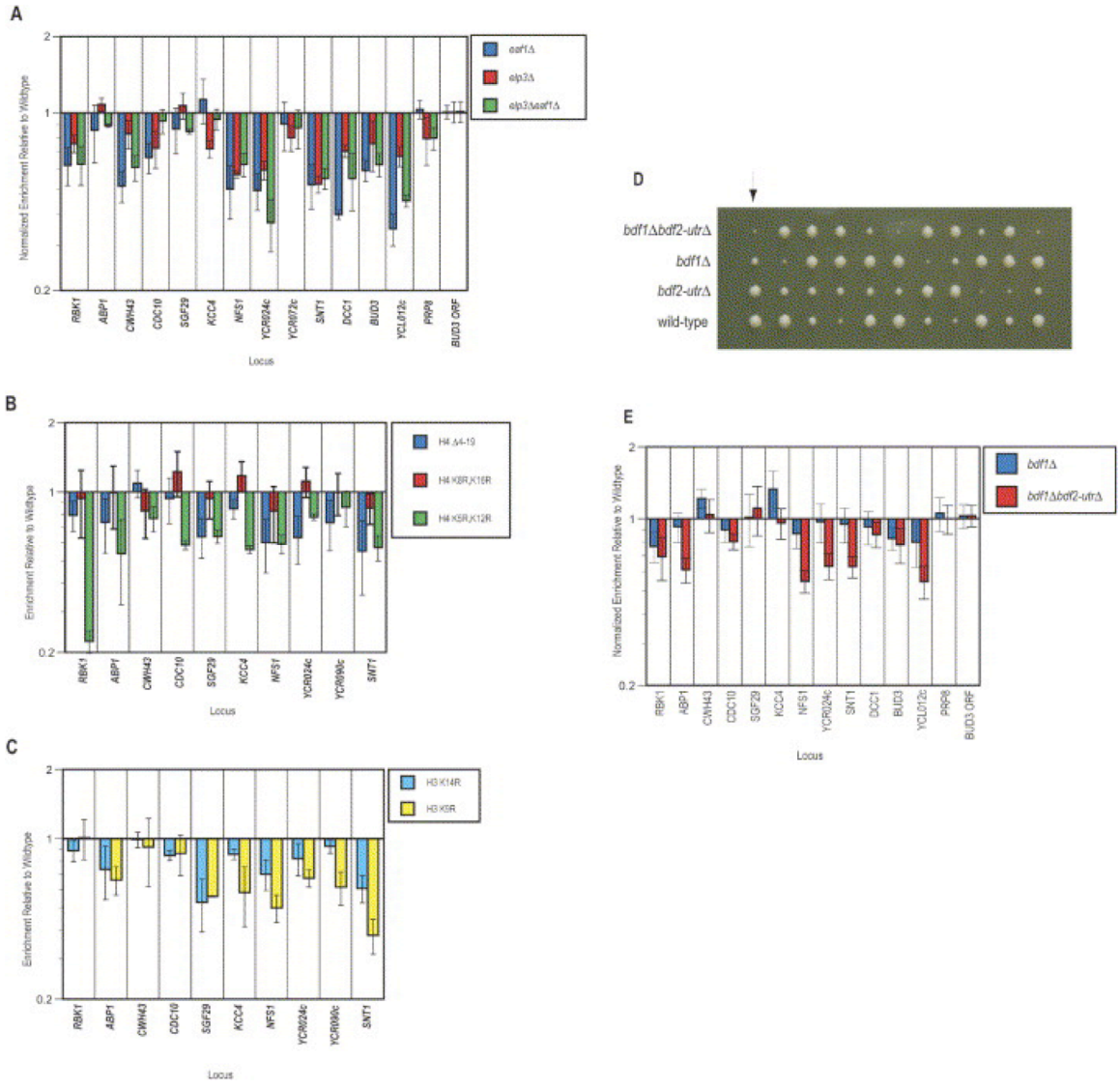
A
Normalized Enrichment Relative to Wildtype
2
1
0.2
eaf1Δ
elp3Δ
elp3Δeaf1Δ
RBK1
ABP1
CWH43
CDC10
SGF29
KCC4
NFS1
YCR024c
YCR073c
SNT1
DCC1
BUD3
YCL012c
PRP8
BUD3 ORF
Locus
B
Enrichment Relative to Wildtype
H4Δ4-19
H4KBRK16R
H4KBRK12R
RBK1
ABP1
CWH43
CDC10
SGF29
KCC4
NFS1
YCR024c
YCR098c
SNT1
Locus
C
Enrichment Relative to Wildtype
H3K14R
H3K9R
RBK1
ABP1
CWH43
CDC10
SGF29
KCC4
NFS1
YCR024c
YCR098c
SNT1
Locus
D
bdf1Δbdf2-utrΔ
bdf1Δ
bdf2-utrΔ
wild-type
E
Normalized Enrichment Relative to Wildtype
bdf1Δ
bdf1Δbdf2-utrΔ
RBK1
ABP1
CWH43
CDC10
SGF29
KCC4
NFS1
YCR024c
SNT1
DCC1
BUD3
YCL012c
PRP8
BUD3 ORF
Locus

Figure 6. High-resolution substitution mutagenesis of the *BPH1-SNT1* intergenic region defines sequences necessary for H2A.Z deposition in vivo.

A. Summary of substitution mutants. Shown is the *SNT1-BPH1* interval and microarray data from Fig. 2 showing the position of the two H2A.Z nucleosomes that lie in the *SNT1* promoter region. The regions defined as intervals 5 and 6 in Figure S7 were subjected to further mutagenesis. Shown are the sequences that were replaced with heterologous sequences from the *BUD3* ORF. Mutants are designated *mu1-mu14*. To the right are shown the normalized H2A.Z enrichments as determined by ChIP. Experiments were performed in triplicate. Mean values and their standard errors are displayed.

B. Detail of 3' signal identified by substitution mutagenesis of interval 5. Shown is wild-type sequence corresponding to the right end of interval 5 (underlined in A). Above this sequence is shown the consensus DNA binding site for the general regulatory factor Reb1; residues shown in large font are invariant (LIAW and BRANDL 1994). The adjacent dT:dA tract is indicated in blue. Shown below are the right endpoints of the *mu3* and *mu4* mutants from A and their H2A.Z deposition levels. Substituted sequences are indicated by dashes.

A

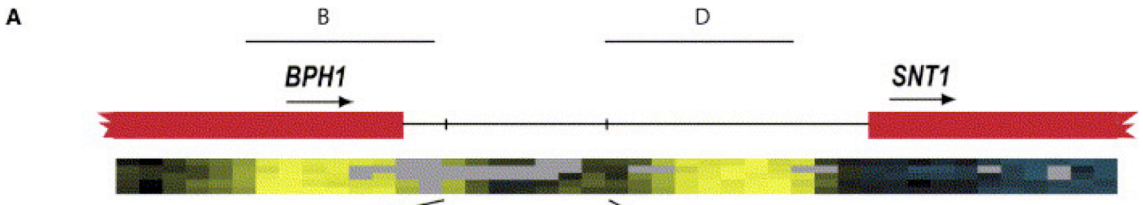

AGTTTATATCTTTACTTTTGAAACTGATTTCTCATCCCATCTAGTATTGTAATTGCGTACGTATCCAATATCATTACCAACGCCGGGTATTTTTTCTAGTA

AGTTTATATCTTTACTTTTGAAACTGATTTCTCATCCCATCTAGTATTGTAATTGCGTACGTATCCAATATCATTACCAACGCCGGGTATTTTTT

AGTTTATATCTTTACTTTTGAAACTGATTTCTCATCCCATCTAGTATTGTAATTGCGTACGTATCCAATATCATTACCAACGCC

TTTACTTTTGAAACTGATTTCTCATCCCATCTAGTATTGTAATTGCGTACGTATCCAATATCATTACCAACGCCGGGTATTTTTT

TTTACTTTTGAAACTGATTTCTCATCCCATCTAGTATTGTAATTGCGTACGTATCCAATATCATTACCAACGCC

TTTACTTTTGAAACTGATTTCTCATCCCATCTAGTATTGTAATTGCGTACGTATCCAATATCATT

TTTACTTTTGAAACTGATTTCTCATCCCATCTAGTATTGTAATTGCGTACGTATC

TTTACTTTTGAAACTGATTTCTCATCCCATCTAGTATTGTAATTG

AAACTGATTTCTCATCCCATCTAGTATTGTAATTGCGTACGTATCCAATATCATTACCAACGCCGGGTATTTTTT

AAACTGATTTCTCATCCCATCTAGTATTGTAATTG

CTCATCCCATCTAGTATTGTAATTGCGTACGTATCCAATATCATTACCAACGCCGGGTATTTTTT

CTCATCCCATCTAGTATTGTAATTG

CTAGTATTGTAATTG

CTAGTATTGT

AATTG

Strain	H2A.Z Deposition B	D
mu1	0.96 ± 0.08	1.62 ± 0.15
mu2	4.76 ± 0.83	5.72 ± 0.76
mu3	0.89 ± 0.08	1.32 ± 0.10
mu4	7.46 ± 0.43	12.38 ± 0.63
mu5	6.97 ± 0.21	17.16 ± 1.12
mu6	5.50 ± 0.47	11.63 ± 1.25
mu7	5.27 ± 0.29	15.69 ± 3.43
mu8	2.05 ± 0.05	3.92 ± 0.18
mu9	7.64 ± 1.32	6.78 ± 0.64
mu10	3.98 ± 0.28	9.89 ± 1.31
mu11	4.85 ± 0.05	11.65 ± 2.57
mu12	7.64 ± 0.43	11.17 ± 0.71
mu13	5.96 ± 0.36	9.65 ± 0.94
mu14	6.13 ± 0.51	12.50 ± 1.21
WT	13.25 ± 1.05	9.75 ± 0.73
htz1Δ	1.06 ± 0.14	1.49 ± 0.02

B

Strain	Reb1 cGGGTAA	H2A.Z Deposition B	D
WT	CAACGCCGGGTATTTTTTCTAGTA	13.25 ± 1.05	9.75 ± 0.73
mu4	----------GGGTATTTTTTCTAGTA	7.46 ± 0.43	12.38 ± 0.63
mu3	----------TCTAGTA	0.89 ± 0.08	1.32 ± 0.10

Figure 7. A 22 bp bipartite DNA sequence from the *SNT1* promoter is sufficient to direct the deposition of two H2A.Z nucleosomes and the formation of a nucleosome-free region

A. Experimental Design. Shown is the sequence from the *SNT1* promoter and its site of insertion in the *PRM1* ORF. Also shown are mutants constructed and PCR probes used in B.

B. Demonstration that 22 bp element from *SNT1* promoter is sufficient to promote H2A.Z deposition: standard ChIP analysis. Shown are the normalized H2A.Z enrichment values for the indicated probes for a wild-type strain and three isogenic strains containing either the 22bp insertion shown in A, a GGG→TAA mutant in the Reb1 site, or a mutant that precisely deletes the T tract. Experiments were performed in triplicate. Mean values and standard errors are displayed.

C. Nucleosome scanning analysis of histone H3 positions in the *PRM1* ORF in wild-type cells. Shown is the analysis of mononucleosomes immunoprecipitated using an anti-H3 antibodies. The immunoprecipitated material was analyzed by quantitative PCR using PCR probes that amplified 100 bp fragments whose 5' ends are spaced every 20 bp across the *PRM1* ORF. Plotted is a four-window moving average for two replicate experiments (thin red and green lines) and their averages (thick black line). The moving average is plotted such that the first datapoint is relative to position 30, which is the center of the window. Indicated below are the deduced positions of nucleosomes. Also marked is the site of the 22 bp insertion from the *SNT1* promoter, which was placed into

the middle of the +4 nucleosome. The peak-to-peak distance between the two nucleosomes flanking the site of insertion is indicated.

D. Nucleosome scanning analysis of histone H3 positions in the *PRM1* ORF in cells containing the 22 bp insertion. A strain containing the insertion was analyzed as in C. The peak-to-peak distance between the two nucleosomes flanking the site of insertion is indicated.

E. Nucleosome scanning analysis of histone H2A.Z positions in the *PRM1* ORF in wild-type cells. Mononucleosomal material from the indicated strains was immunoprecipitated with anti-H2A.Z antibodies and analyzed as in C.

F. Nucleosome scanning analysis of histone H2A.Z positions in the *PRM1* ORF in cells containing the 22bp insertion. Mononucleosomal material from the indicated strains was immunoprecipitated with anti-H2A.Z antibodies and analyzed as in C. The peak-to-peak distance between the two nucleosomes flanking the site of insertion is indicated.

FIGURE 7

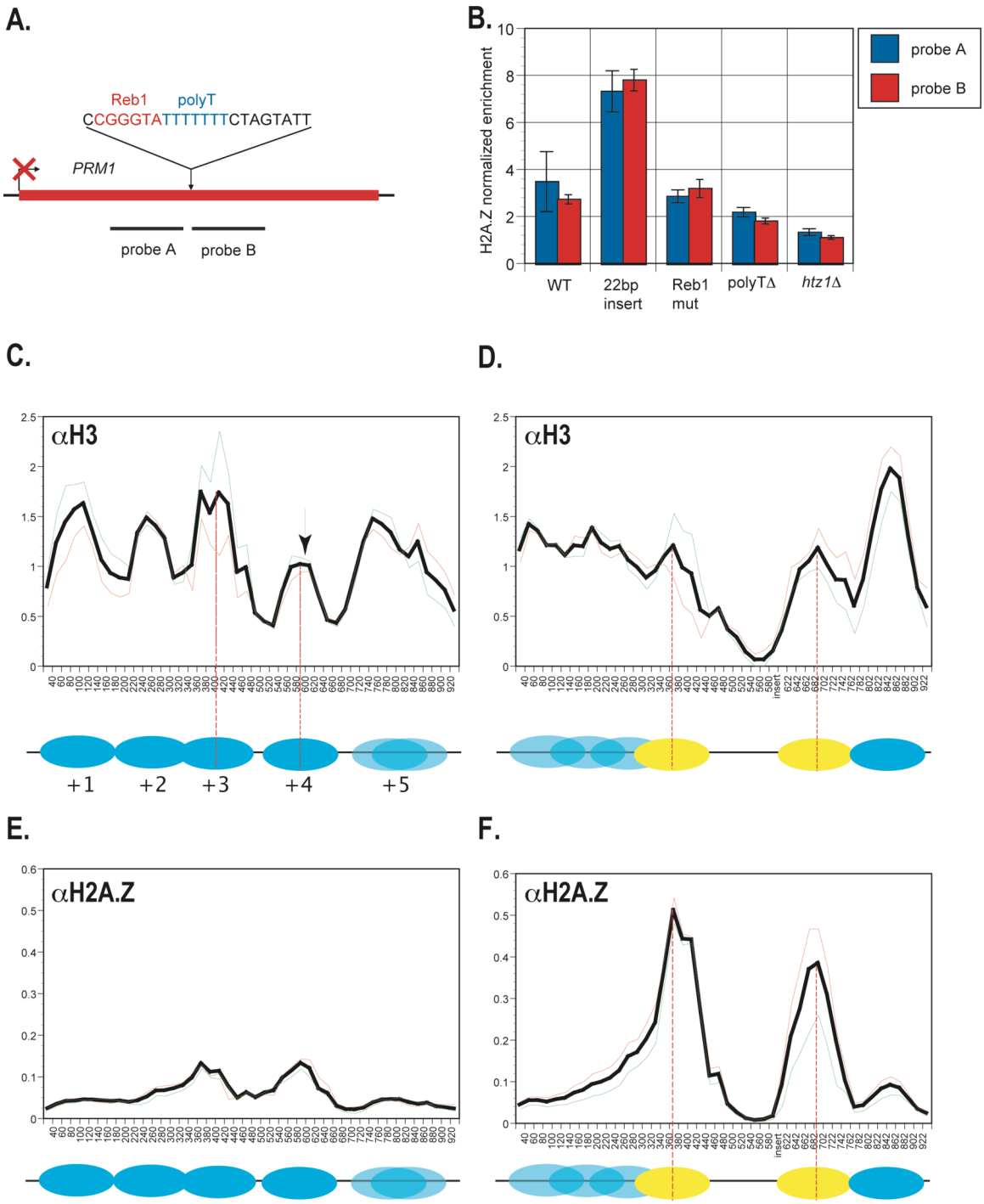
A.
Reb1
polyT
CCGGGTATTTTTTTCTAGTATT
PRM1
probe A
probe B
B.
H2A.Z normalized enrichment
probe A
probe B
WT
22bp insert
Reb1 mut
polyTΔ
htz1Δ
C.
αH3
+1
+2
+3
+4
+5
D.
αH3
E.
αH2A.Z
F.
αH2A.Z

Table 1.

Comparison of Histone Tail Acetylation Patterns at NFR-Flanking Nucleosomes and Residues Required for H2A.Z Deposition

Modification	Present at NFR-Flanking Nucleosomes?	Required for H2A.Z Deposition?
Ac-H3-K9	Yes	Yes
Ac-H3-K14	Yes	Yes
Ac-H4-K5	Yes	Yes*
Ac-H4-K8	No	No
Ac-H4-K12	Yes	Yes*
Ac-H4-K16	No	No

* Based on H4-K5,12 double mutant.

Figure S1. **Comparison of H2A.Z and H3 Enrichment in the *LEU2-YCL012c* interval**

Diagram of the *LEU2-YCL012c* interval showing unmodified anti-H3 (blue) and anti-Htz1 (red) ChIP amounts. Enrichment values are average IP/WCE ratios from triplicate samples with standard error of the mean (SEM) error bars. Genes encoded on the Watson strand in red, and the Crick strand in green with arrows denoting the direction of transcription. Vertical dashed lines are drawn through each gene's initiation codon. X-axis values are the chromosomal coordinates of the 5' primers of each pair used.

Figure S1

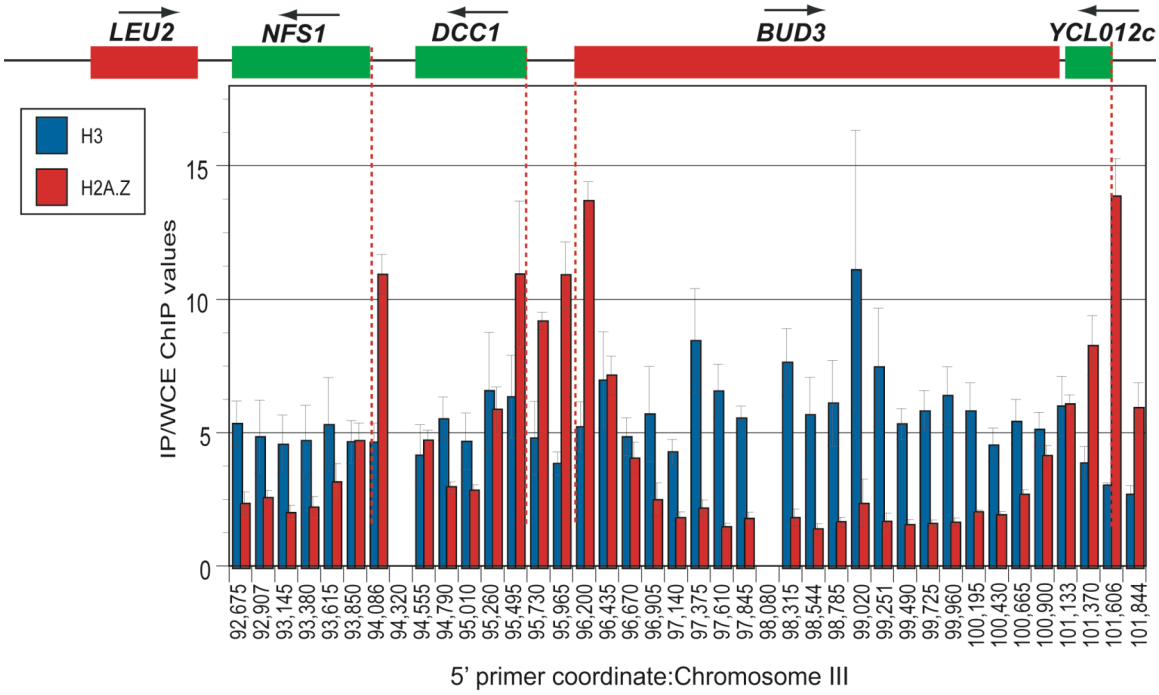
LEU2
NFS1
DCC1
BUD3
YCL012c
H3
H2A.Z
IP/WCE ChIP values
0
5
10
15
92,675
92,907
93,145
93,380
93,615
93,850
94,086
94,320
94,555
94,790
95,010
95,260
95,495
95,730
95,965
96,200
96,435
96,670
96,905
97,140
97,375
97,610
97,845
98,080
98,315
98,544
98,785
99,020
99,251
99,490
99,725
99,960
100,195
100,430
100,665
100,900
101,133
101,370
101,606
101,844
5’ primer coordinate:Chromosome III

Figure S2. ChIP Analysis of H3 Enrichment at Meiosis-Specific and a-Specific Genes

All enrichment values are triplicate averages of unmodified anti-H3 ChIP DNA amounts normalized to the *BUD3* ORF region for the meiosis loci, or the *PRP8* ORF for *AGA2*, with SEM error bars. (A and B) H3 enrichment at the *DIT1/DIT2* (A) and *HOP1/SPO22* (B) promoter and ORF regions. QPCR fragments are for consecutive 200 bp segments; dashed lines are drawn through gene initiation codons to their approximate relative position. (C) H3 normalized enrichment at *AGA2* for *MAT***a** and *MAT*α strains. QPCR fragments are for consecutive 100 bp segments with the position of the 5' primer relative to the initiation codon of *AGA2* denoted.

Figure S2

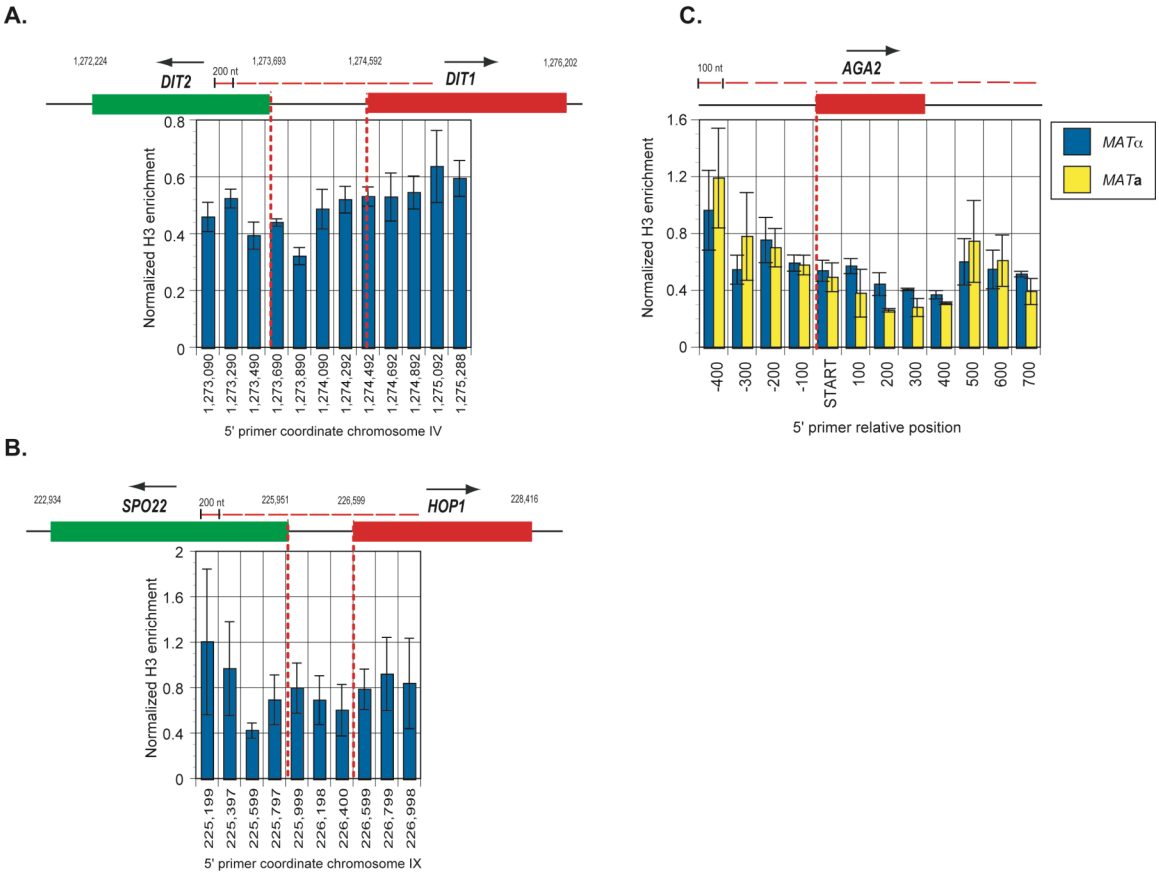
A.
1,272,224
DIT2
200 nt
1,273,693
1,274,592
DIT1
1,276,202
Normalized H3 enrichment
0
0.2
0.4
0.6
0.8
1,273,090
1,273,290
1,273,490
1,273,690
1,273,890
1,274,090
1,274,292
1,274,492
1,274,692
1,274,892
1,275,092
1,275,288
5' primer coordinate chromosome IV
B.
222,934
SPO22
200 nt
225,951
226,599
HOP1
228,416
Normalized H3 enrichment
0
0.4
0.8
1.2
1.6
2
225,199
225,397
225,599
225,797
225,999
226,198
226,400
226,599
226,799
226,998
5' primer coordinate chromosome IX
C.
100 nt
AGA2
Normalized H3 enrichment
0
0.4
0.8
1.2
1.6
MATα
MATa
-400
-300
-200
-100
START
100
200
300
400
500
600
700
5' primer relative position

Figure S3. ChIP Analysis of Galactose-Inducible *HA3-HTZ1* Enrichment at Meiosis-Specific Genes

All values are triplicate averages of HA3-Htz1 ChIP DNA amounts (IP/WCE) with SEM error bars. Sidebars show IP/WCE ratios for *BUD3* ORF and *BUD3* promoter. (A and B) HA3-Htz1 enrichment at the *DIT1/DIT2* (A) and *HOP1/SPO22* (B) promoter and ORF regions. QPCR fragments are for consecutive 200 bp segments; dashed lines are drawn through gene initiation codons to their approximate relative position. (C) Immunoblot for HA3-Htz1 protein levels for inducing (galactose) and repressing condition (glucose), showing tubulin loading control.

Figure S3

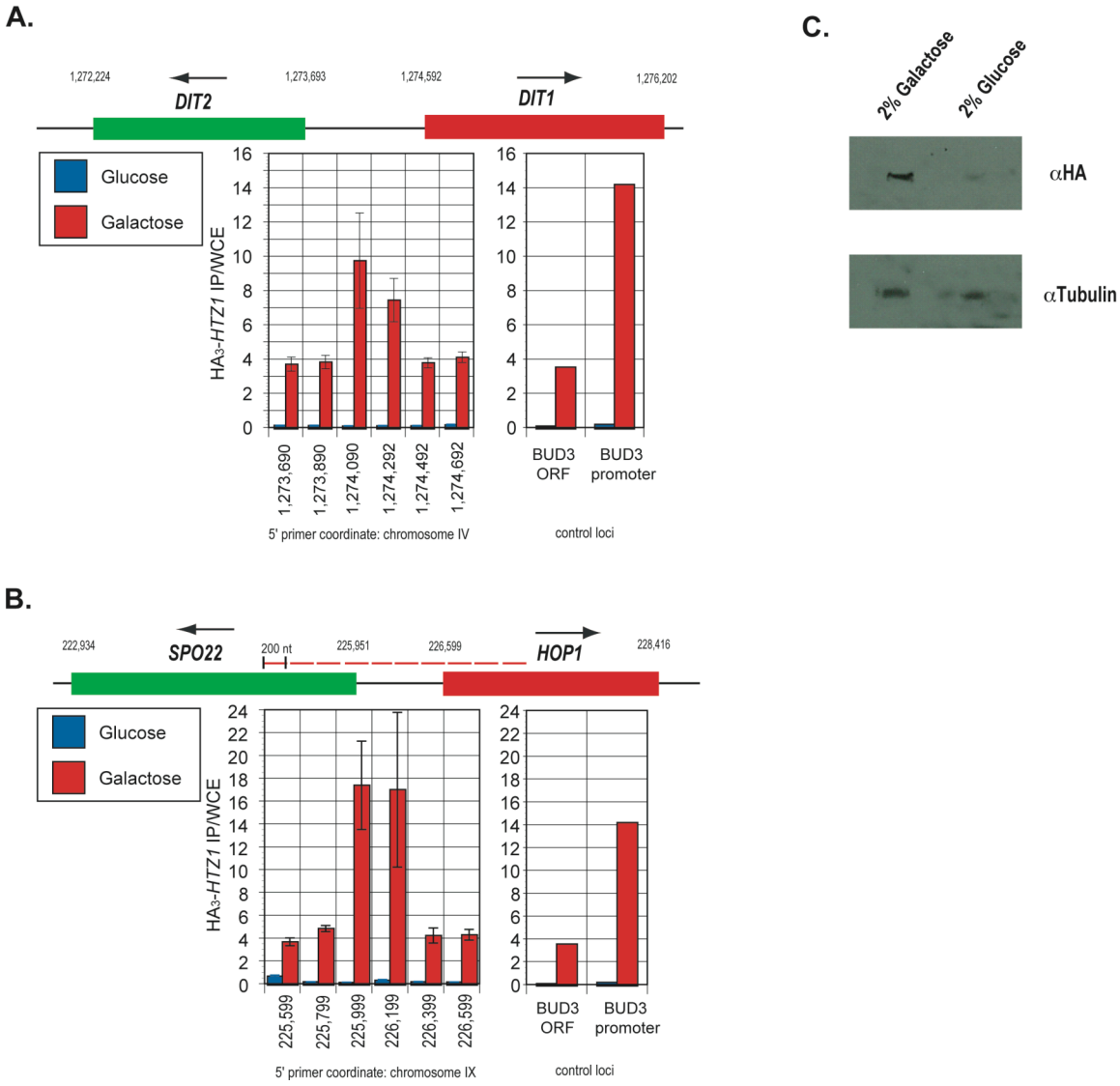
A.
1,272,224
1,273,693
1,274,592
1,276,202
DIT2
DIT1
Glucose
Galactose
HA3-HTZ1 IP/WCE
16
14
12
10
8
6
4
2
0
1,273,690
1,273,890
1,274,090
1,274,292
1,274,492
1,274,692
BUD3 ORF
BUD3 promoter
5' primer coordinate: chromosome IV
control loci
B.
222,934
SPO22
200 nt
225,951
226,599
HOP1
228,416
Glucose
Galactose
HA3-HTZ1 IP/WCE
24
22
20
18
16
14
12
10
8
6
4
2
0
225,599
225,799
225,999
226,199
226,399
226,599
BUD3 ORF
BUD3 promoter
5' primer coordinate: chromosome IX
control loci
C.
2% Galactose
2% Glucose
αHA
αTubulin

Figure S4. Microarray Data for *FIG2* and *PRM1* Regions

Figure S4

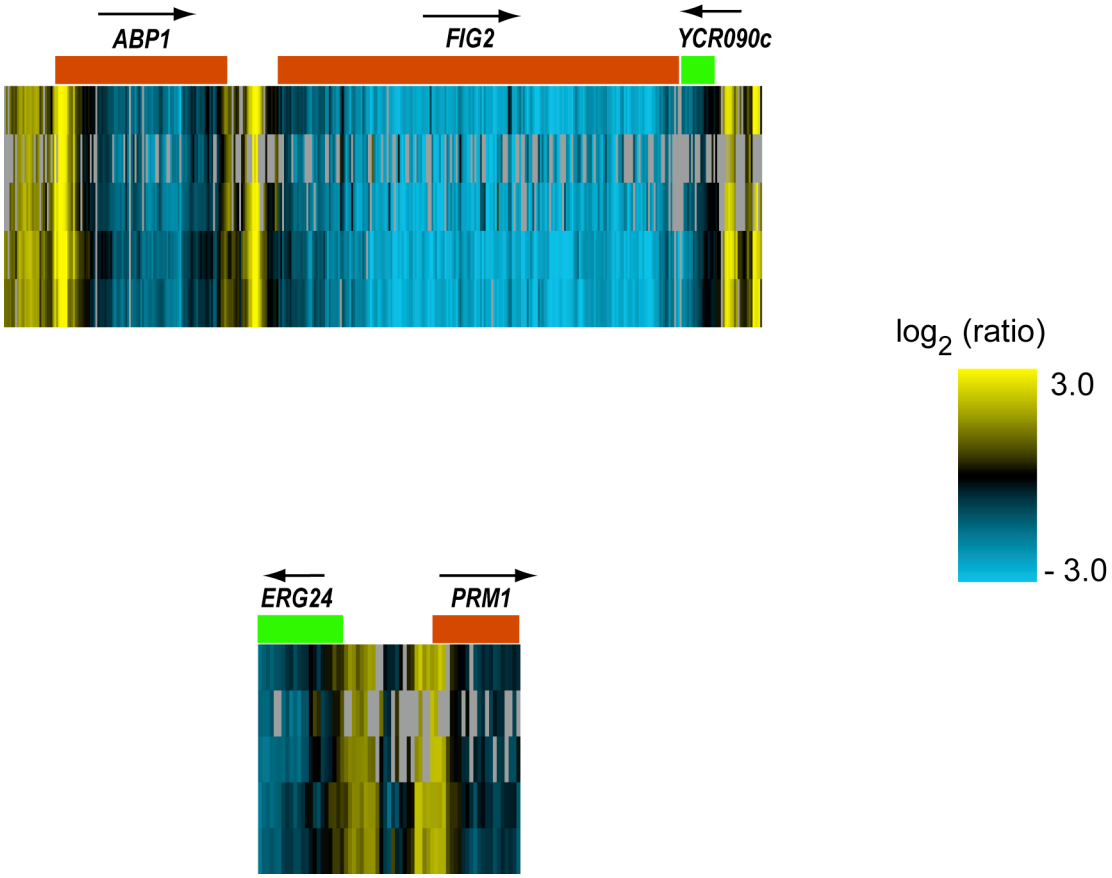

Figure S5. ChIP Analysis of H2A.Z Enrichment at *FIG1* in Response to Pheromone Induction

All ChIP values are triplicate averages of H2A.Z or unmodified histone H3 ChIP DNA enrichments, normalized to *PRP8* with SEM error bars. (A and B) ChIP values for time-course of *FIG1* induction by α factor for 0' (dark blue), 5' (red), 15' (green), 30' (yellow), and 60' (light blue) for Htz1 (A) and H3 (B) across the *FIG1* promoter and ORF region. (C) Ratio of normalized Htz1 and H3 ChIP values across the *FIG1* promoter and ORF region. QPCR fragments are for consecutive 200 bp segments; *FIG1* and its upstream gene *ATP3* are shown with their approximate relative positions. (D) Quantitative RT-PCR values for *FIG1* expression normalized to *ACT1* during time-course.

Figure S5

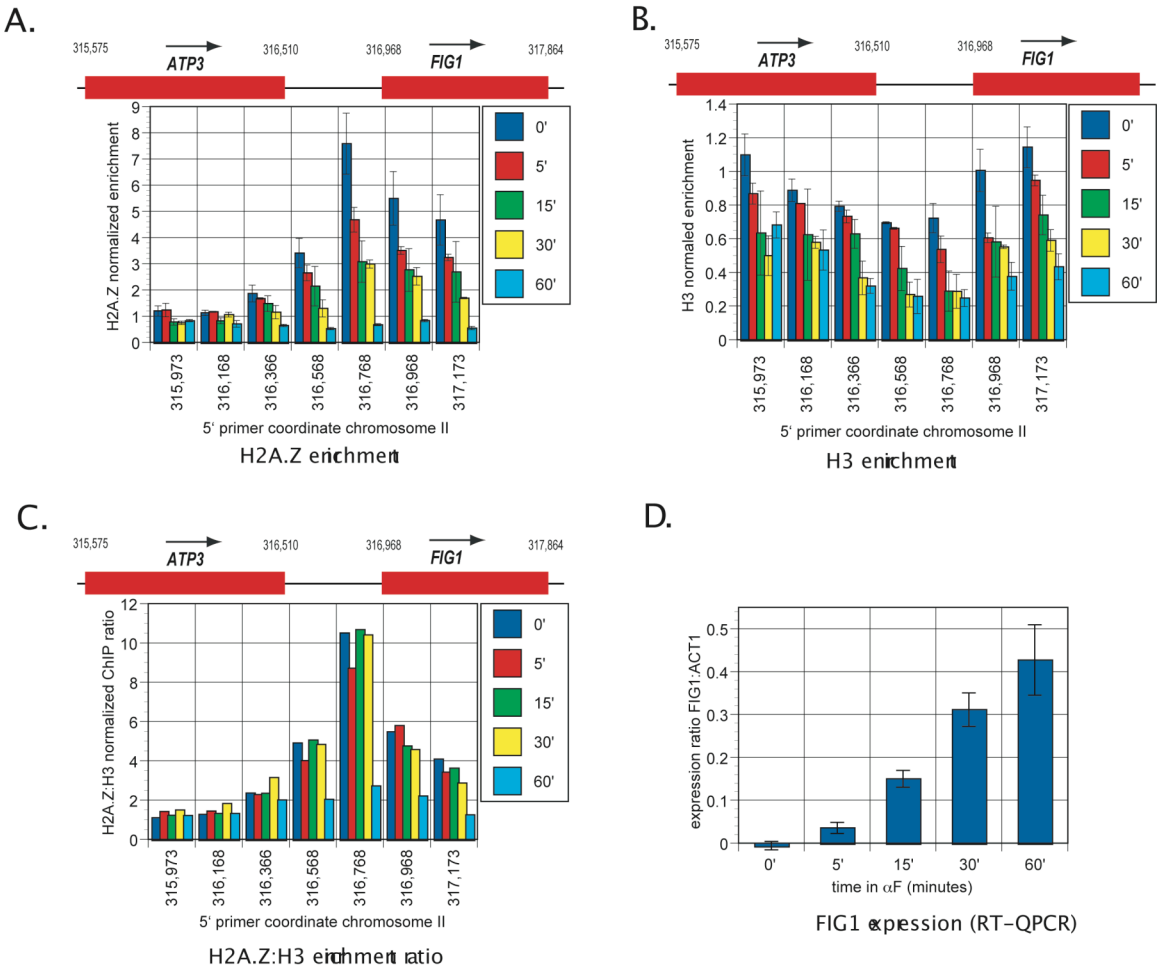
A.
315,575
ATP3
316,510
316,968
FIG1
317,864
H2A.Z normalized enrichment
0'
5'
15'
30'
60'
315,973
316,168
316,366
316,568
316,768
316,968
317,173
5' primer coordinate chromosome II
H2A.Z enrichment
B.
H3 normaled enrichment
H3 enrichment
C.
H2A.Z:H3 normalized ChIP ratio
H2A.Z:H3 enrichment ratio
D.
expression ratio FIG1:ACT1
time in αF (minutes)
FIG1 expression (RT-QPCR)

Figure S6. ChIP Analysis of H3 Enrichment at Selected Euchromatic Promoters in Wild-Type and Histone H4-K5R, K12R Mutant

Triplicate average unmodified anti-H3 enrichment ratios for wild-type (blue bars) and histone H4-K5R, K12R mutant (red bars) strains, normalized to the *BUD3* ORF region, with SEM error bars.

Figure S6

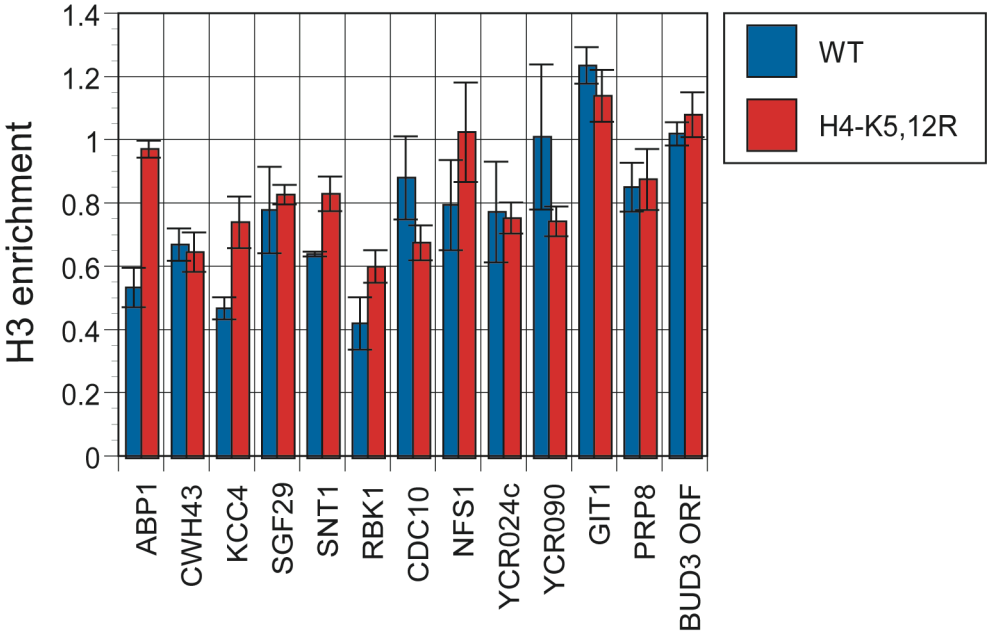
H3 enrichment
1.4
1.2
1
0.8
0.6
0.4
0.2
0
ABP1
CWH43
KCC4
SGF29
SNT1
RBK1
CDC10
NFS1
YCR024c
YCR090
GIT1
PRP8
BUD3 ORF
WT
H4-K5,12R

Figure S7. Low-Resolution Substitution Mutagenesis of the *BPH1-SNT1* Intergenic Region

Shown is the *BPH1-SNT1* intergenic region and positions of seven 75 bp intervals that were subjected to substitution mutagenesis. Microarray data indicating the positions of the two H2A.Z nucleosomes and the intervening nucleosome-free region are shown. Mutants were constructed by replacing 75 bp segments with a fragment of pBluescript. Displayed below are the normalized H2A.Z deposition levels for each mutant determined using standard ChIP/QPCR and probes A-D. Experiments were performed in triplicate. Mean values and their SEM are displayed.

FIGURE S7

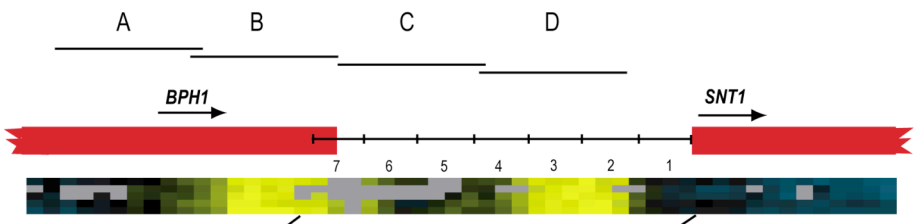

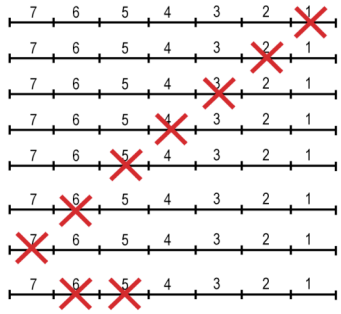

H2A.Z deposition (normalized) mean +/- SEM

	Probe Name			
Mutant	A	B	C	D
1	2.99 +/- 1.02	10.1 +/- 3.1	5.65 +/- 0.31	8.52 +/- 2.45
2	5.14 +/- 1.12	12.82 +/- 2.36	11.25 +/- 0.74	11.73 +/- 3
3	5.59 +/- 1.46	12.24 +/- 1.61	8.7 +/- 1.55	11.06 +/- 2.68
4	4.87 +/- 0.54	13.76 +/- 0.62	ND	4.45 +/- 0.64
5	2.5 +/- 0.43	5.44 +/- 0.89	6.3 +/- 0.65	5.01 +/- 0.28
6	2.14 +/- 0.33	4.64 +/- 0.23	6.19 +/- 1.42	6.72 +/- 0.7
7	3.7 +/- 0.38	10.04 +/- 0.71	8.96 +/- 0.79	7.84 +/- 0.47
5, 6	1.45 +/- 0.21	2.01 +/- 0.37	ND	1.29 +/- 0.22
wt	5.22 +/- 0.09	11.66 +/- 0.42	11.03 +/- 1.17	9.17 +/- 0.88

Chapter Three

Patterning chromatin: form and function for H2A.Z variant nucleosomes

Patterning chromatin: form and function for H2A.Z variant nucleosomes

Ryan M. Raisner and Hiten D. Madhani

Dept. of Biochemistry and Biophysics

University of California

600 16th St.

San Francisco, CA 94143-2240

fax: 415-502-4315

ryan.raisner@ucsf.edu

hiten@biochem.ucsf.edu

Summary

While many histone variants are specific to higher eukaryotes, the H2A variant H2A.Z has been conserved during eukaryotic evolution. Genetic studies have demonstrated roles for H2A.Z in antagonizing gene silencing, chromosome stability, and gene activation. Biochemical work has identified a conserved chromatin remodeling complex responsible for H2A.Z deposition. Recent studies have shown that two H2A.Z nucleosomes flank a nucleosome-free region containing the transcription initiation site in promoters of both active and inactive genes in *Saccharomyces cerevisiae.* This chromatin pattern is generated through the action of a DNA deposition signal and a specific pattern of histone tail acetylation.

The two major classes of chromatin are euchromatin and heterochromatin, terms that were originally coined to describe the morphology of chromosomes in *Drosophila*. Despite significant progress in identifying the proteins and modifications involved in the formation of heterochromatin, the mechanism by which these factors lead to the properties of heterochromatin is not known. Even less is known about how euchromatin is specified. One mechanism that promotes the euchromatic state is the substitution of H2A for the variant H2A.Z. This review focuses on this molecule, for which there have been rapid advances in our understanding of its localization, deposition mechanisms, and functions.

H2A.Z is conserved across eukaryotes

Of the core histone subunits, variants of H2A are particularly common. There are five major H2A-type histones (THATCHER and GOROVSKY 1994). Canonical H2A is the most abundant form; its expression and deposition are coupled to replication. H2A.X is involved in the response to DNA damage. MacroH2A is involved in constitutive heterochromatin and transcriptional silencing (COSTANZI and PEHRSON 1998). Another variant, H2ABbd, named for its relative depletion from Barr bodies in mammals, remains relatively uncharacterized (GAUTIER *et al.* 2004). H2A.Z (sometimes referred to as H2A.Z/F) is the most conserved variant—it is found in organisms as diverse as the early branching eukaryote *Plasmodium falciparum* [J. DeRisi, personal communication] to humans. Table 1 lists H2A variants found in commonly studied species along with their respective names. In some cases, two H2A types exist as a single, bifunctional molecule; for example, the *S. cerevisiae* H2A also functions as H2A.X (REDON *et al.* 2003).

H2A.Z homologs are more similar across species than canonical H2A. Characterized H2A.Z-type variants include H2A.Z in mammals, *C. elegans*, and fungi (CARR *et al.* 1994; JACKSON and GOROVSKY 2000), H2Av in *Drosophila* (which is a bifunctional H2A.Z/H2A.X variant) (LEACH *et al.* 2000), H2Ahv1 in *Tetrahymena* (ALLIS *et al.* 1986), H2A.F in birds (HARVEY *et al.* 1983), and H2A.Z/F in sea urchins (ERNST *et al.* 1987). The strong conservation of H2A.Z between species likely reflects common and important functions.

Insights from the atomic resolution structure of the H2A.Z variant nucleosome

The core region of the H2A.Z variant differs significantly from that of the H2A core. Three conserved residues that differ between H2A and H2A.Z are of particular note. The crystal structure of a *Xenopus laevis* H2A.Z nucleosome solved by Suto et al. (SUTO *et al.* 2000) identified a difference in the $(H3\text{-}H4)_2$ tetramer docking domain between the H2A subunits (residues 81-119 in H2A). Specifically, the substitution of Gln 104 in H2A to glycine (Gly 106 in H2A.Z) results in the loss of 3 hydrogen bonds, which is predicted to cause a subtle destabilization of the H2A.Z-H3 interaction. Additionally, the His 112 residue on the surface of the H2A.Z histone octamer is observed to bind to a metal ion, and this interaction may be stabilized by the nearby His 114 residue. This ion may provide a unique surface for protein interaction. Finally, H2A.Z-H2B dimers display an extended acidic patch on the surface of the histone octamer that may be important for making contacts with adjacent H4 tails or non-histone protein factors.

Physical properties of H2A.Z nucleosomes

In vitro studies have characterized various biochemical properties of nucleosomes containing H2A.Z. Reconstituted nucleosomes bearing H2A.1 or H2A.Z from humans display differences in electrophoretic mobility, and in sedimentation values under varying salt conditions (ABBOTT *et al.* 2001). FRET-based assays with *Xenopus laevis* core histones and mouse H2A.Z revealed that H2A.Z-H2B dimers dissociate slower in salt conditions than canonical H2A-H2B (PARK *et al.* 2004), in contrast to earlier studies that used different methods. However, it was also reported that H2A.Z nucleosomes display a lower melting temperature than canonical nucleosomes (FLAUS *et al.* 2004). In purified yeast chromatin, H2A.Z can be released from nucleosomes by treatment with a lower concentration of sodium chloride salt than concentrations required to release either H2A or H3 (ZHANG *et al.* 2005). It seems likely that many of the different conclusions among these studies are due to differences in the sources of chromatin and the methodology used to define the stability of H2A.Z-H2B dimers. Further work seems necessary to clarify the physical properties of H2A.Z nucleosomes and their potential relevance to the biological functions of H2A.Z.

The deposition pattern of H2A.Z nucleosomes

Early studies of an H2A.Z type variant in the ciliate *Tetrahymena* species, called hv1 showed that it preferentially associates with the transcriptionally active macronucleus versus the silent micronucleus (STARGELL *et al.* 1993). This distribution was proposed to be consistent with a role in transcriptional activation.

Genome-scale studies of budding yeast *Saccharomyces cerevisiae* have demonstrated H2A.Z deposition at the vast majority of gene promoters in euchromatin, but a depletion from silenced regions such as subtelomeric domains (GUILLEMETTE *et al.* 2005; RAISNER *et al.* 2005a; ZHANG *et al.* 2005). Most strikingly, H2A.Z generally occupies single nucleosomes upstream and downstream of a nucleosome-free region (NFR) that encompasses the transcription initiation site of most genes (Figure 1). Remarkably, a short 22 bp sequence from a promoter was shown to be sufficient to promote both the formation of an NFR and the deposition of H2A.Z in the two flanking nucleosomes (RAISNER *et al.* 2005a). This sequence consists of a binding site for the Myb-related DNA binding protein Reb1 and an adjacent dT:dA tract, and both motifs are required for H2A.Z deposition. Both these sequence elements are commonly found in yeast promoters; indeed the Reb1 site is the most conserved element of yeast promoters, exceeding that of the TATA box. Thus, there exists a DNA signal for H2A.Z deposition.

In *Drosophila melanogaster* the H2A.Z homolog, H2Av, is not confined to euchromatin: immunofluorescence studies demonstrated that H2Av is localized to heterochromatic chromocenters as well as throughout the arms of polytene chromosomes (LEACH *et al.* 2000). H2Av distribution was further compared with that of RNA polymerase II, and, while the two patterns partially overlapped, H2Av was also found at loci where no detectable Pol II was present, which suggests the presence of H2Av at inactive genes. Chromatin immunoprecipitation (ChIP) experiments showed that H2Av is present at various loci such as from constitutively active genes, both the uninduced and induced forms of genes, as well as transcriptionally inactive loci. H2Av also functions as

an H2A.X (MADIGAN *et al.* 2002); therefore, some if its observed localization pattern may be due to its other identity.

A recent study of H2A.Z localization in chicken erythrocytes showed an association of H2A.Z with the 5' ends of several genes assayed by ChIP (BRUCE *et al.* 2005). Remarkably, in the β-globin locus, H2A.Z is highly enriched in the well-characterized 5' insulator that flanks a heterochromatic region. This finding is consistent with studies in yeast that show that H2A.Z antagonizes heterochromatin spread (see below). If H2A.Z nucleosomes generally closely flank heterochromatic regions, could cytological data showing concentrations of H2A.Z in heterochromatin actually reflect its enrichment in flanking nucleosomes?

Different mammalian cell types show distinct cytological patterns of H2A.Z localization. In mouse embryos, H2A.Z displays diffuse staining but is concentrated at pericentric chromatin. However, it is selectively depleted from constitutive heterochromatin such as the inactive X chromosome. H2A.Z is not present prior to differentiation of totipotent cells early in development, suggesting it is not required for early transcriptional programs (RANGASAMY *et al.* 2003). In cultured monkey COS-7 cells, H2A.Z is in fact depleted from centromeric heterochromatin and is found associated with chromosomes arms (RANGASAMY *et al.* 2004). Some concentration in heterochromatic "knobs" on chromosome arms was also observed.

A conserved chromatin remodeling complex that deposits H2A.Z

In *S. cerevisiae*, H2A.Z is deposited in chromatin by the 13 subunit Swr1-C remodeling complex (KOBOR *et al.* 2004b; KROGAN *et al.* 2003b; MIZUGUCHI *et al.*

2004). The catalytic subunit, Swr1, is homologous to the SWI/SNF family of ATP-dependent chromatin remodeling enzymes. The Bdf1 subunit contains tandem bromodomains that have been shown to specifically bind the acetylated tails of histones H3 and H4. Both Bdf1 and histone tail acetylation are important for H2A.Z targeting and deposition in promoter regions. Swr1-C has four subunits--Swc4, Yaf9, Arp4, and actin--that are shared with the NuA4 histone acetyltransferase complex. Swr1-C also shares components with the Ino80-C remodeling complex, namely, Arp1, actin, Rvb1 and Rvb2. There are also six subunits unique to Swr1-C.

The *Drosophila* homolog of Swr1-C, the Tip60 complex, deposits H2Av (KUSCH *et al.* 2004). Each subunit of the Tip60 complex has a homologous subunit in the human SRCAP complex (CAI *et al.* 2005). As with SRCAP, each subunit has a homolog in *S. cerevisiae* (Table 2). The Tip60 and SRCAP complexes appear to be the sum of the *S. cerevisiae* Swr1-C and NuA4 complexes. This organization is consistent with the established role for histone H4 tail acetylation in H2A.Z deposition in *S. cerevisiae*. Indeed, the Tip60 complex acetylates nucleosomes and this acetylation is important for replacement of phosphorylated H2Av with unphosphorylated H2Av at the sites of DNA lesions. Given the complete conservation of all the subunits of Swr1-C in the Tip60 and SRCAP complexes, it is likely that the fundamental molecular mechanisms of targeting and replacing H2A.Z are also conserved.

Functions for H2A.Z: anti-silencing, transcription, and centromere function

Several studies over the last five years have examined specific roles for H2A.Z in transcription in *S. cerevisiae.* Early work by Smith and colleagues showed that cells

harboring a null mutation in the gene encoding H2A.Z (*HTZ1*) display defects in the induction of the *PHO5* and *GAL1* genes when combined with null mutations in genes encoding the chromatin remodeling enzyme Snf2/Swi2 or Sin1, an HMG-like protein (SANTISTEBAN *et al.* 2000). No transcriptional defect was observed for several other genes. Subsequent studies of H2A/H2A.Z chimeric genes showed that *GAL1* and *GAL10* gene activation was specifically dependent upon the C-terminal domain of H2A.Z (ADAM *et al.* 2001), consistent with earlier analysis of chimeric H2Av/H2A genes in *Drosophila*. Pull-down experiments using crude extracts demonstrated an association between the H2A.Z C-terminal domain and RNA polymerase II (Rpb1). A defect in the binding of Rpb1 *in vivo* to the *GAL1* promoter was observed when an *htz1Δ* strain was shifted to galactose. It has been shown recently that at the *GAL1* gene promoter, the positioned nucleosome immediately downstream of the transcription initiation site shifts by approximately 20 bp in an *htz1Δ* strain (GUILLEMETTE *et al.* 2005), perhaps contributing to the defective Rpb1 binding. In addition to the dependence of *GAL1* and *GAL10* on H2A.Z for full activation, it has also been shown that the cell cycle genes *CLN2* and *CLB5* have H2A.Z at their promoters, and require H2A.Z for fast and complete transcriptional activation of these genes which results in a delayed progression through S-phase and reduced cell cycle synchrony [Dhillon N, *et al*., unpublished]. For the vast majority of genes however, microarray studies have demonstrated only a modest defect in general transcriptional induction in *htz1*Δ cells (MENEGHINI *et al.* 2003). Thus, while H2A.Z appears to play a role in transcriptional induction, it appears to be largely redundant with other factors.

In contrast, microarray and ChIP studies in *S. cerevisiae* suggest that the major function for H2A.Z in gene expression is to antagonize gene silencing. Genes whose expression is dependent on H2A.Z cluster near silencing regions. Cells lacking H2A.Z exhibit the ectopic spread of the Sir2/3/4 silencing complex beyond its normal boundaries (MENEGHINI *et al.* 2003). Its localization in promoter regions of genes in euchromatin and its exclusion from heterochromatin places it at an appropriate site to protect genes from silencing. The fact that genes need not be transcribed for H2A.Z deposition to occur is consistent with this function for H2A.Z.

In metazoans, null mutations in H2A.Z yield lethal phenotypes across a range of species including *Drosophila* and mouse (FAAST *et al.* 2001; VAN DAAL and ELGIN 1992). Mutants in *Drosophila* H2Av show a defect in heterochromatin formation (SWAMINATHAN *et al.* 2005). Moreover, H2Av was recruited to the location of a silenced transgene array, suggesting a direct role of this hybrid variant in silencing. In *Xenopus laevis*, either RNAi of H2A.Z or expression of dominant alleles result in developmental defects (RIDGWAY 2004). Whether these defects are due to defects in transcriptional regulation is unclear.

In *S. pombe*, *S. cerevisiae*, and cultured mammalian cells, knockout or depletion of H2A.Z results in increased rates of chromosome loss (CARR *et al.* 1994; RANGASAMY *et al.* 2004). Although this phenotype could in principle be due to indirect effects of H2A.Z loss on the expression of factors important for chromosome segregation, it more likely reflects a direct role for H2A.Z in centromere function. Indeed, it has been reported that the mouse H2A.Z protein interacts with the kinetochore component INCENP (RANGASAMY *et al.* 2003).

Euchromatin and heterochromatin: yin and yang

In *S. cerevisiae* two features of chromatin contribute to the deposition of H2A.Z in euchromatin: a DNA signal and histone tail acetylation (RAISNER *et al.* 2005a; ZHANG *et al.* 2005). Heterochromatin formation in yeast is also nucleated by specific DNA signals, but is propagated by histone tail deacetylation rather than histone tail acetylation (RUSCHE *et al.* 2003). One apparent difference is that H2A.Z does not appear to spread to coat regions of the chromosome in yeast, but is generally restricted to promoter regions. Nonetheless, these recent results suggest that euchromatin and heterochromatin may be two sides of the same coin. An intriguing property of heterochromatin is its ability to template its own propagation. Whether the same is true of euchromatin is an interesting question for future investigation.

Figure 1. High resolution mapping of H2A.Z nucleosomes in *S. cerevisiae*.

Clustered view of tiled microarray array data centered on nucleosome-free regions. Each row represents a single promoter region, and each column corresponds to data from a particular microarray spot. H2A.Z levels are normalized for nucleosome density. See [17] for further details.

Figure 1

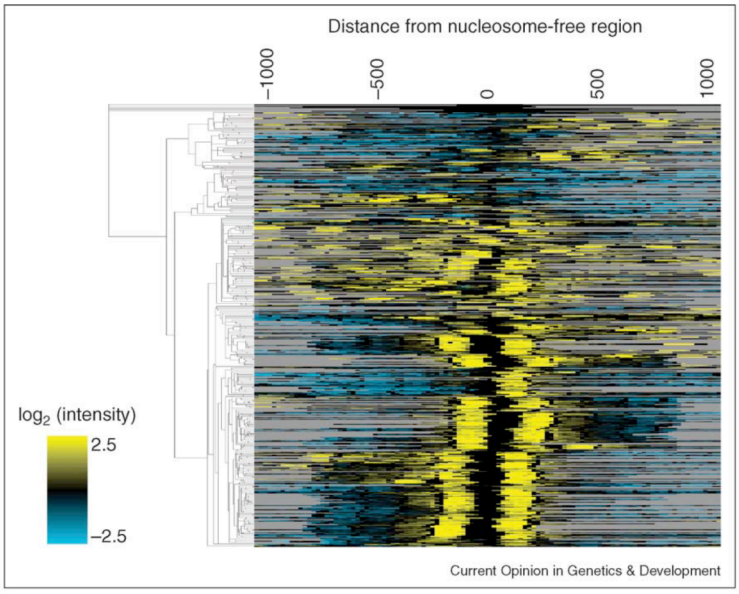

High-resolution mapping of H2A.Z nucleosomes in S. cerevisiae. Clustered view of tiled microarray array data centered on nucleosome-free regions. Each row represents a single promoter region, and each column corresponds to data from a particular microarray spot. H2A.Z levels are normalized for nucleosome density. See Raisner et al. [17[11]] for further details.

Table 1.

A list of the commonly used names for H2A variants across species. A (-) indicates that either no protein exists or has yet been reported.

	Protists	Fungi	Metazoans					
H2A Class	**Ciliate**	**Yeast**	**Nematode**	**Fly**	**Fish**	**Amphibian**	**Bird**	**Mammal**
Canonical	H2A	H2A	H2A	H2A	H2A	H2A	H2A	H2A
H2A.Z	H2Ahv1	H2A.Z	H2AZ	H2Av	H2A.Z	H2A.Z	H2A.F	H2AZ
H2A.X	-	H2A	-	H2Av	-	H2A.X	H2A.X	H2A.X
macroH2A	-	-	-	-	macroH2A	mH2A	mH2A	macroH2A
H2ABbd	-	-	-	-	-	-	-	H2ABbd

Table 2.

List of the H2A.Z chromatin remodeling complexes for budding yeast, fly, and human. Note for yeast, the NuA4 subunits that share homology those of the Tip60 and SRCAP complexes, but do not co-purify with Swr1-C. * Indicates that the Domino/p400 subunits are actually a fusion of Swr1 and Eaf1 from yeast.

Table 2

Yeast Swr1-C	Yeast NuA4	Fly Tip60	Human SRCAP	Comment
Rvb1		dPontin	Pontin	
Rvb2		dReptin	Reptin	
Arp4		BAP55	Baf53a	Actin-Related
Eaf7		dMrgB	MrgBP	
Swc4 (Eaf2, God1)		dDMA	DMAP1	
Bdf1		dBrd8	Brd8/TRCp12	Bromodomain Protein
Act1		Act87E	Actin	Actin
Yaf9		dGas41	Gas41	
Swr1*		Domino	p400	SWI/SNF ATPase
Swc2 (Vps72)		dYL-1	YL-1	
H2A/H2A.Z		H2Av	H2A.Z/H2A.X	
H2B		H2B	H2B	
Swc3 (Alr1)				
Swc5 (Aor1)				
Swc6 (Vps71)				
Swc7 (Aws1)				
	Eaf1*	Domino	p400	
	Eaf3	dMrg15	Mrg15	Chromodomain Protein
	Epl1	E(Pc)	Epc1	
	Esa1	dTip60	Tip60	Histone Acetylation
	Tra1	dTra1	TRRAP	
	Yng2	dIng3~	Ing3	ING Family
	Eaf6	dEaf6	FLJ11730	

Acknowledgements:

This work was supported by grants from the NIH-NIGMS and the Packard Foundation.

We thank Rachel Tompa and Paul Hartley for critical reading of the manuscript.

Bibliography

ABBOTT, D. W., V. S. IVANOVA, X. WANG, W. M. BONNER and J. AUSIO, 2001 Characterization of the stability and folding of H2A.Z chromatin particles: implications for transcriptional activation. J Biol Chem **276:** 41945-41949.

ADAM, M., F. ROBERT, M. LAROCHELLE and L. GAUDREAU, 2001 H2A.Z is required for global chromatin integrity and for recruitment of RNA polymerase II under specific conditions. Mol Cell Biol **21:** 6270-6279.

ALLIS, C. D., R. RICHMAN, M. A. GOROVSKY, Y. S. ZIEGLER, B. TOUCHSTONE *et al.*, 1986 hv1 is an evolutionarily conserved H2A variant that is preferentially associated with active genes. J Biol Chem **261:** 1941-1948.

ANGERMAYR, M., U. OECHSNER and W. BANDLOW, 2003 Reb1p-dependent DNA bending effects nucleosome positioning and constitutive transcription at the yeast profilin promoter. J Biol Chem **278:** 17918-17926.

BELL, A. C., and G. FELSENFELD, 2000 Methylation of a CTCF-dependent boundary controls imprinted expression of the Igf2 gene. Nature **405:** 482-485.

BELL, A. C., A. G. WEST and G. FELSENFELD, 2001 Insulators and boundaries: versatile regulatory elements in the eukaryotic. Science **291:** 447-450.

BEN-AROYA, S., A. KOREN, B. LIEFSHITZ, R. STEINLAUF and M. KUPIEC, 2003 ELG1, a yeast gene required for genome stability, forms a complex related to replication factor C. Proc Natl Acad Sci U S A **100:** 9906-9911.

BERNSTEIN, B. E., E. L. HUMPHREY, R. L. ERLICH, R. SCHNEIDER, P. BOUMAN *et al.*, 2002 Methylation of histone H3 Lys 4 in coding regions of active genes. Proc Natl Acad Sci U S A **99:** 8695-8700.

BERNSTEIN, B. E., C. L. LIU, E. L. HUMPHREY, E. O. PERLSTEIN and S. L. SCHREIBER, 2004 Global nucleosome occupancy in yeast. Genome Biol **5:** R62.

BOLTON, E. C., and J. D. BOEKE, 2003 Transcriptional interactions between yeast tRNA genes, flanking genes and Ty elements: a genomic point of view. Genome Res **13:** 254-263.

BRACHMANN, C. B., J. M. SHERMAN, S. E. DEVINE, E. E. CAMERON, L. PILLUS *et al.*, 1995 The SIR2 gene family, conserved from bacteria to humans, functions in silencing, cell cycle progression, and chromosome stability. Genes Dev **9:** 2888-2902.

BRUCE, K., F. A. MYERS, E. MANTOUVALOU, P. LEFEVRE, I. GREAVES *et al.*, 2005 The replacement histone H2A.Z in a hyperacetylated form is a feature of active genes in the chicken. Nucleic Acids Res **33:** 5633-5639.

CAI, Y., J. JIN, L. FLORENS, S. K. SWANSON, T. KUSCH *et al.*, 2005 The mammalian YL1 protein is a shared subunit of the TRRAP/TIP60 histone acetyltransferase and SRCAP complexes. J Biol Chem **280:** 13665-13670.

CARR, A. M., S. M. DORRINGTON, J. HINDLEY, G. A. PHEAR, S. J. AVES *et al.*, 1994 Analysis of a histone H2A variant from fission yeast: evidence for a role in chromosome stability. Mol Gen Genet **245:** 628-635.

CHALKLEY, G. E., and C. P. VERRIJZER, 1999 DNA binding site selection by RNA polymerase II TAFs: a TAF(II)250-TAF(II)150 complex recognizes the initiator. Embo J **18:** 4835-4845.

CHU, S., J. DERISI, M. EISEN, J. MULHOLLAND, D. BOTSTEIN *et al.*, 1998 The transcriptional program of sporulation in budding yeast. Science **282:** 699-705.

CLARKE, A. S., J. E. LOWELL, S. J. JACOBSON and L. PILLUS, 1999 Esa1p is an essential histone acetyltransferase required for cell cycle progression. Mol Cell Biol **19:** 2515-2526.

COLLINS, S. R., K. M. MILLER, N. L. MAAS, A. ROGUEV, J. FILLINGHAM *et al.*, 2007 Functional dissection of protein complexes involved in yeast chromosome biology using a genetic interaction map. Nature **446:** 806-810.

COSTANZI, C., and J. R. PEHRSON, 1998 Histone macroH2A1 is concentrated in the inactive X chromosome of female mammals. Nature **393:** 599-601.

DECKERT, J., and K. STRUHL, 2001 Histone acetylation at promoters is differentially affected by specific activators and repressors. Mol Cell Biol **21:** 2726-2735.

DONZE, D., C. R. ADAMS, J. RINE and R. T. KAMAKAKA, 1999 The boundaries of the silenced HMR domain in Saccharomyces cerevisiae. Genes Dev **13:** 698-708.

DRISCOLL, R., A. HUDSON and S. P. JACKSON, 2007 Yeast Rtt109 promotes genome stability by acetylating histone H3 on lysine 56. Science **315:** 649-652.

ELEMENTO, O., and S. TAVAZOIE, 2005 Fast and systematic genome-wide discovery of conserved regulatory elements using a non-alignment based approach. Genome Biol **6:** R18.

ERDMAN, S., L. LIN, M. MALCZYNSKI and M. SNYDER, 1998 Pheromone-regulated genes required for yeast mating differentiation. J Cell Biol **140:** 461-483.

ERNST, S. G., H. MILLER, C. A. BRENNER, C. NOCENTE-MCGRATH, S. FRANCIS *et al.*, 1987 Characterization of a cDNA clone coding for a sea urchin histone H2A variant related to the H2A.F/Z histone protein in vertebrates. Nucleic Acids Res **15:** 4629-4644.

FAAST, R., V. THONGLAIROAM, T. C. SCHULZ, J. BEALL, J. R. WELLS *et al.*, 2001 Histone variant H2A.Z is required for early mammalian development. Curr Biol **11:** 1183-1187.

FISCHLE, W., Y. WANG, S. A. JACOBS, Y. KIM, C. D. ALLIS *et al.*, 2003 Molecular basis for the discrimination of repressive methyl-lysine marks in histone H3 by Polycomb and HP1 chromodomains. Genes Dev **17:** 1870-1881.

FLAUS, A., C. RENCUREL, H. FERREIRA, N. WIECHENS and T. OWEN-HUGHES, 2004 Sin mutations alter inherent nucleosome mobility. Embo J **23:** 343-353.

FOUREL, G., T. MIYAKE, P. A. DEFOSSEZ, R. LI and E. GILSON, 2002 General Regulatory Factors (GRFs) as Genome Partitioners. J Biol Chem **277:** 41736-41743.

FRITZE, C. E., K. VERSCHUEREN, R. STRICH and R. EASTON ESPOSITO, 1997 Direct evidence for SIR2 modulation of chromatin structure in yeast rDNA. Embo J **16:** 6495-6509.

GALITSKI, T., A. J. SALDANHA, C. A. STYLES, E. S. LANDER and G. R. FINK, 1999 Ploidy regulation of gene expression. Science **285:** p251-254.

GAUTIER, T., D. W. ABBOTT, A. MOLLA, A. VERDEL, J. AUSIO *et al.*, 2004 Histone variant H2ABbd confers lower stability to the nucleosome. EMBO Rep **5:** 715-720.

GOLDSTEIN, A. L., and J. H. MCCUSKER, 1999 Three new dominant drug resistance cassettes for gene disruption in Saccharomyces cerevisiae. Yeast **15:** 1541-1553.

GOTTLIEB, S., and R. E. ESPOSITO, 1989 A new role for a yeast transcriptional silencer gene, SIR2, in regulation of recombination in ribosomal DNA. Cell **56:** 771-776.

GUILLEMETTE, B., A. R. BATAILLE, N. GEVRY, M. ADAM, M. BLANCHETTE *et al.*, 2005 Variant Histone H2A.Z Is Globally Localized to the Promoters of Inactive Yeast Genes and Regulates Nucleosome Positioning. PLoS Biol **3:** e384.

HAN, J., H. ZHOU, B. HORAZDOVSKY, K. ZHANG, R. M. XU *et al.*, 2007 Rtt109 acetylates histone H3 lysine 56 and functions in DNA replication. Science **315:** 653-655.

HARVEY, R. P., J. A. WHITING, L. S. COLES, P. A. KRIEG and J. R. WELLS, 1983 H2A.F: an extremely variant histone H2A sequence expressed in the chicken embryo. Proc Natl Acad Sci U S A **80:** 2819-2823.

HEIMAN, M. G., and P. WALTER, 2000 Prm1p, a pheromone-regulated multispanning membrane protein, facilitates plasma membrane fusion during yeast mating. J Cell Biol **151:** 719-730.

HOWE, L., D. AUSTON, P. GRANT, S. JOHN, R. G. COOK *et al.*, 2001 Histone H3 specific acetyltransferases are essential for cell cycle progression. Genes Dev **15:** 3144-3154.

HWANG, W. W., S. VENKATASUBRAHMANYAM, A. G. IANCULESCU, A. TONG, C. BOONE *et al.*, 2003 A conserved RING finger protein required for histone H2B monoubiquitination and cell size control. Mol Cell **11:** 261-266.

IMAI, S., C. M. ARMSTRONG, M. KAEBERLEIN and L. GUARENTE, 2000 Transcriptional silencing and longevity protein Sir2 is an NAD-dependent histone deacetylase. Nature **403:** 795-800.

JACKSON, J. D., and M. A. GOROVSKY, 2000 Histone H2A.Z has a conserved function that is distinct from that of the major H2A sequence variants. Nucleic Acids Res **28:** 3811-3816.

JAMBUNATHAN, N., A. W. MARTINEZ, E. C. ROBERT, N. B. AGOCHUKWU, M. E. IBOS *et al.*, 2005 Multiple bromodomain genes are involved in restricting the spread of heterochromatic silencing at the Saccharomyces cerevisiae HMR-tRNA boundary. Genetics **171:** 913-922.

JIANG, Y. W., and D. J. STILLMAN, 1996 Epigenetic effects on yeast transcription caused by mutations in an actin-related protein present in the nucleus. Genes Dev **10:** 604-619.

JU, Q. D., B. E. MORROW and J. R. WARNER, 1990 REB1, a yeast DNA-binding protein with many targets, is essential for growth and bears some resemblance to the oncogene myb. Mol Cell Biol **10:** 5226-5234.

KAEBERLEIN, M., M. MCVEY and L. GUARENTE, 1999 The SIR2/3/4 complex and SIR2 alone promote longevity in Saccharomyces cerevisiae by two different mechanisms. Genes Dev **13:** 2570-2580.

KIMURA, A., T. UMEHARA and M. HORIKOSHI, 2002 Chromosomal gradient of histone acetylation established by Sas2p and Sir2p functions as a shield against gene silencing. Nat Genet.

KOBOR, M. S., S. VENKATASUBRAHMANYAM, M. D. MENEGHINI, J. W. GIN, J. JENNINGS *et al.*, 2004a A protein complex containing the conserved Swi2/Snf2-related ATPase Swr1p deposits histone variant H2A.Z into euchromatin. PLoS Biology **2:** 587-599.

KOBOR, M. S., S. VENKATASUBRAHMANYAM, M. D. MENEGHINI, J. W. GIN, J. L. JENNINGS *et al.*, 2004b A protein complex containing the conserved Swi2/Snf2-

related ATPase Swr1p deposits histone variant H2A.Z into euchromatin. PLoS Biol **2:** E131.

KROGAN, N. J., J. DOVER, A. WOOD, J. SCHNEIDER, J. HEIDT *et al.*, 2003a The Paf1 complex is required for histone H3 methylation by COMPASS and Dot1p: linking transcriptional elongation to histone methylation. Mol Cell **11:** 721-729.

KROGAN, N. J., M. C. KEOGH, N. DATTA, C. SAWA, O. W. RYAN *et al.*, 2003b A Snf2 family ATPase complex required for recruitment of the histone H2A variant Htz1. Mol Cell **12:** 1565-1576.

KURDISTANI, S. K., S. TAVAZOIE and M. GRUNSTEIN, 2004 Mapping global histone acetylation patterns to gene expression. Cell **117:** 721-733.

KUSCH, T., L. FLORENS, W. H. MACDONALD, S. K. SWANSON, R. L. GLASER *et al.*, 2004 Acetylation by Tip60 is required for selective histone variant exchange at DNA lesions. Science **306:** 2084-2087.

LADURNER, A. G., C. INOUYE, R. JAIN and R. TJIAN, 2003 Bromodomains mediate an acetyl-histone encoded antisilencing function at heterochromatin boundaries. Mol Cell **11:** 365-376.

LANDRY, J., A. SUTTON, S. T. TAFROV, R. C. HELLER, J. STEBBINS *et al.*, 2000 The silencing protein SIR2 and its homologs are NAD-dependent protein deacetylases. Proc Natl Acad Sci U S A **97:** 5807-5811.

LANGLEY, E., M. PEARSON, M. FARETTA, U. M. BAUER, R. A. FRYE *et al.*, 2002 Human SIR2 deacetylates p53 and antagonizes PML/p53-induced cellular senescence. Embo J **21:** 2383-2396.

LAROCHELLE, M., and L. GAUDREAU, 2003 H2A.Z has a function reminiscent of an activator required for preferential binding to intergenic DNA. Embo J **22:** 4512-4522.

LEACH, T. J., M. MAZZEO, H. L. CHOTKOWSKI, J. P. MADIGAN, M. G. WOTRING *et al.*, 2000 Histone H2A.Z is widely but nonrandomly distributed in chromosomes of Drosophila melanogaster. J Biol Chem **275:** 23267-23272.

LEE, C. K., Y. SHIBATA, B. RAO, B. D. STRAHL and J. D. LIEB, 2004 Evidence for nucleosome depletion at active regulatory regions genome-wide. Nat Genet **36:** 900-905.

LI, H., I. J. BYEON, Y. JU and M. D. TSAI, 2004 Structure of human Ki67 FHA domain and its binding to a phosphoprotein fragment from hNIFK reveal unique recognition sites and new views to the structural basis of FHA domain functions. J Mol Biol **335:** 371-381.

LIAW, P. C., and C. J. BRANDL, 1994 Defining the sequence specificity of the Saccharomyces cerevisiae DNA binding protein REB1p by selecting binding sites from random-sequence oligonucleotides. Yeast **10:** 771-787.

LIN, S. J., P. A. DEFOSSEZ and L. GUARENTE, 2000 Requirement of NAD and SIR2 for life-span extension by calorie restriction in Saccharomyces cerevisiae. Science **289:** 2126-2128.

LING, X., T. A. HARKNESS, M. C. SCHULTZ, G. FISHER-ADAMS and M. GRUNSTEIN, 1996 Yeast histone H3 and H4 amino termini are important for nucleosome assembly in vivo and in vitro: redundant and position-independent functions in assembly but not in gene regulation. Genes Dev **10:** 686-699.

LITT, M. D., M. SIMPSON, F. RECILLAS-TARGA, M. N. PRIOLEAU and G. FELSENFELD, 2001 Transitions in histone acetylation reveal boundaries of three separately regulated neighboring loci. Embo J **20:** 2224-2235.

LIU, C. L., T. KAPLAN, M. KIM, S. BURATOWSKI, S. L. SCHREIBER *et al.*, 2005 Single-Nucleosome Mapping of Histone Modifications in S. cerevisiae. PLoS Biol **3:** e328.

MAAS, N. L., K. M. MILLER, L. G. DEFAZIO and D. P. TOCZYSKI, 2006 Cell cycle and checkpoint regulation of histone H3 K56 acetylation by Hst3 and Hst4. Mol Cell **23:** 109-119.

MADIGAN, J. P., H. L. CHOTKOWSKI and R. L. GLASER, 2002 DNA double-strand break-induced phosphorylation of Drosophila histone variant H2Av helps prevent radiation-induced apoptosis. Nucleic Acids Res **30:** 3698-3705.

MAILLET, L., F. GADEN, V. BREVET, G. FOUREL, S. G. MARTIN *et al.*, 2001 Ku-deficient yeast strains exhibit alternative states of silencing competence. EMBO Rep **2:** 203-210.

MATANGKASOMBUT, O., R. M. BURATOWSKI, N. W. SWILLING and S. BURATOWSKI, 2000 Bromodomain factor 1 corresponds to a missing piece of yeast TFIID. Genes Dev **14:** 951-962.

MATANGKASOMBUT, O., and S. BURATOWSKI, 2003 Different sensitivities of bromodomain factors 1 and 2 to histone H4 acetylation. Mol Cell **11:** 353-363.

MATZKE, M. A., and J. A. BIRCHLER, 2005 RNAi-mediated pathways in the nucleus. Nat Rev Genet **6:** 24-35.

MENEGHINI, M. D., M. WU and H. D. MADHANI, 2003 Conserved histone variant H2A.Z protects euchromatin from the ectopic spread of silent heterochromatin. Cell **112:** 725-736.

MILGROM, E., R. W. WEST JR, C. GAO and W. C. SHEN, 2005 TFIID and SAGA functions probed by genome-wide synthetic genetic array (SGA) analysis using a Saccharomyces cerevisiae taf9-ts allele. Genetics.

MIZUGUCHI, G., X. SHEN, J. LANDRY, W. H. WU, S. SEN *et al.*, 2004 ATP-driven exchange of histone H2AZ variant catalyzed by SWR1 chromatin remodeling complex. Science **303:** 343-348.

NG, H. H., D. N. CICCONE, K. B. MORSHEAD, M. A. OETTINGER and K. STRUHL, 2003a Lysine-79 of histone H3 is hypomethylated at silenced loci in yeast and mammalian cells: a potential mechanism for position-effect variegation. Proc Natl Acad Sci U S A **100:** 1820-1825.

NG, H. H., F. ROBERT, R. A. YOUNG and K. STRUHL, 2003b Targeted recruitment of Set1 histone methylase by elongating Pol II provides a localized mark and memory of recent transcriptional activity. Mol Cell **11:** 709-719.

PARK, Y. J., P. N. DYER, D. J. TREMETHICK and K. LUGER, 2004 A new fluorescence resonance energy transfer approach demonstrates that the histone variant H2AZ stabilizes the histone octamer within the nucleosome. J Biol Chem **279:** 24274-24282.

POKHOLOK, D. K., C. T. HARBISON, S. LEVINE, M. COLE, N. M. HANNETT *et al.*, 2005 Genome-wide map of nucleosome acetylation and methylation in yeast. Cell **122:** 517-527.

PRAKASH, L., 1977 Defective thymine dimer excision in radiation-sensitive mutants rad10 and rad16 of Saccharomyces cerevisiae. Mol Gen Genet **152:** 125-128.

RAISNER, R. M., P. D. HARTLEY, M. D. MENEGHINI, M. Z. BAO, C. L. LIU *et al.*, 2005a Histone Variant H2A.Z Marks the 5' Ends of Both Active and Inactive Genes in Euchromatin. Cell **123:** 233-248.

RAISNER, R. M., P. D. HARTLEY, M. D. MENEGHINI, M. Z. BAO, C. L. LIU *et al.*, 2005b Histone variant H2A.Z marks the 5' ends of both active and inactive genes in euchromatin. Cell **123:** 233-248.

RANGASAMY, D., L. BERVEN, P. RIDGWAY and D. J. TREMETHICK, 2003 Pericentric heterochromatin becomes enriched with H2A.Z during early mammalian development. EMBO J **22:** 1599-1607.

RANGASAMY, D., I. GREAVES and D. J. TREMETHICK, 2004 RNA interference demonstrates a novel role for H2A.Z in chromosome segregation. Nat Struct Mol Biol **11:** 650-655.

REDON, C., D. R. PILCH, E. P. ROGAKOU, A. H. ORR, N. F. LOWNDES *et al.*, 2003 Yeast histone 2A serine 129 is essential for the efficient repair of checkpoint-blind DNA damage. EMBO Rep **4:** 678-684.

RIDGWAY, P., BROWN, KD, RANGASAMY, D, SVENSSON, U, TREMETHICK, DJ, 2004 Unique Residues on the H2A.Z Containing Nucleosome Surface Are Important for *Xenopus laevis* Development. the Journal of Biological Chemistry **279:** 43815-43820.

RINE, J., and I. HERSKOWITZ, 1987 Four genes responsible for a position effect on expression from HML and HMR in Saccharomyces cerevisiae. Genetics **116:** 9-22.

RUSCHE, L. N., A. L. KIRCHMAIER and J. RINE, 2003 The Establishment, Inheritance, and Function of Silenced Chromatin in Saccharomyces cerevisiae. Annu Rev Biochem.

RUTTER, J., B. L. PROBST and S. L. MCKNIGHT, 2002 Coordinate regulation of sugar flux and translation by PAS kinase. Cell **111:** 17-28.

SANTISTEBAN, M. S., T. KALASHNIKOVA and M. M. SMITH, 2000 Histone H2A.Z regulats transcription and is partially redundant with nucleosome remodeling complexes. Cell **103:** 411-422.

SANTOS-ROSA, H., A. J. BANNISTER, P. M. DEHE, V. GELI and T. KOUZARIDES, 2004 Methylation of H3 lysine 4 at euchromatin promotes Sir3p association with heterochromatin. J Biol Chem **279:** 47506-47512.

SEKINGER, E. A., Z. MOQTADERI and K. STRUHL, 2005 Intrinsic histone-DNA interactions and low nucleosome density are important for preferential accessibility of promoter regions in yeast. Mol Cell **18:** 735-748.

SJOSTRAND, J. O., A. KEGEL and S. U. ASTROM, 2002 Functional diversity of silencers in budding yeasts. Eukaryot Cell **1:** 548-557.

SMITH, B. C., and J. M. DENU, 2007 Mechanism-based inhibition of sir2 deacetylases by thioacetyl-lysine Peptide. Biochemistry **46:** 14478-14486.

SMITH, J. S., and J. D. BOEKE, 1997 An unusual form of transcriptional silencing in yeast ribosomal DNA. Genes Dev **11:** 241-254.

STARGELL, L. A., J. BOWEN, C. A. DADD, P. C. DEDON, M. DAVIS *et al.*, 1993 Temporal and spatial association of histone H2A variant hv1 with transcriptionally competent chromatin during nuclear development in Tetrahymena thermophila. Genes Dev **7:** 2641-2651.

STORICI, F., C. L. DURHAM, D. A. GORDENIN and M. A. RESNICK, 2003 Chromosomal site-specific double-strand breaks are efficiently targeted for repair by oligonucleotides in yeast. Proc Natl Acad Sci U S A **100:** 14994-14999.

STRAHL-BOLSINGER, S., A. HECHT, K. LUO and M. GRUNSTEIN, 1997 SIR2 and SIR4 interactions differ in core and extended telomeric heterochromatin in yeast. Genes Dev **11:** 83-93.

SUKA, N., K. LUO and M. GRUNSTEIN, 2002 Sir2p and Sas2p opposingly regulate acetylation of yeast histone H4 lysine16 and spreading of heterochromatin. Nat Genet **32:** 378-383.

SUTO, R. K., M. J. CLARKSON, D. J. TREMETHICK and K. LUGER, 2000 Crystal structure of a nucleosome core particle containing the variant histone H2A.Z. Nat Struct Biol **7:** 1121-1124.

SWAMINATHAN, J., E. M. BAXTER and V. G. CORCES, 2005 The role of histone H2Av variant replacement and histone H4 acetylation in the establishment of Drosophila heterochromatin. Genes Dev **19:** 65-76.

TANNY, J. C., G. J. DOWD, J. HUANG, H. HILZ and D. MOAZED, 1999 An enzymatic activity in the yeast Sir2 protein that is essential for gene silencing. Cell **99:** 735-745.

THATCHER, T. H., and M. A. GOROVSKY, 1994 Phylogenetic analysis of the core histones H2A, H2B, H3, and H4. Nucleic Acids Res **22:** 174-179.

TOMPA, R., and H. D. MADHANI, 2007 Histone H3 lysine 36 methylation antagonizes silencing in Saccharomyces cerevisiae independently of the Rpd3S histone deacetylase complex. Genetics **175:** 585-593.

TONG, A. H., M. EVANGELISTA, A. B. PARSONS, H. XU, G. D. BADER *et al.*, 2001 Systematic genetic analysis with ordered arrays of yeast deletion mutants. Science **294:** 2364-2368.

VAN DAAL, A., and S. C. ELGIN, 1992 A histone variant, H2AvD, is essential in Drosophila melanogaster. Mol Biol Cell **3:** 593-602.

VAN LEEUWEN, F., P. R. GAFKEN and D. E. GOTTSCHLING, 2002 Dot1p modulates silencing in yeast by methylation of the nucleosome core. Cell **109:** 745-756.

VENKATASUBRAHMANYAM, S., W. W. HWANG, M. D. MENEGHINI, A. H. TONG and H. D. MADHANI, 2007 Genome-wide, as opposed to local, antisilencing is mediated redundantly by the euchromatic factors Set1 and H2A.Z. Proc Natl Acad Sci U S A **104:** 16609-16614.

WANG, X., J. J. CONNELLY, C. L. WANG and R. STERNGLANZ, 2004 Importance of the Sir3 N terminus and its acetylation for yeast transcriptional silencing. Genetics **168:** 547-551.

XU, F., Q. ZHANG, K. ZHANG, W. XIE and M. GRUNSTEIN, 2007 Sir2 deacetylates histone H3 lysine 56 to regulate telomeric heterochromatin structure in yeast. Mol Cell **27:** 890-900.

XU, H. E., and S. A. JOHNSTON, 1994 Yeast bleomycin hydrolase is a DNA-binding cysteine protease. Identification, purification, biochemical characterization. J Biol Chem **269:** 21177-21183.

YU, Q., R. QIU, T. B. FOLAND, D. GRIESEN, C. S. GALLOWAY *et al.*, 2003 Rap1p and other transcriptional regulators can function in defining distinct domains of gene expression. Nucleic Acids Res **31:** 1224-1233.

YUAN, G. C., Y. J. LIU, M. F. DION, M. D. SLACK, L. F. WU *et al.*, 2005 Genome-scale identification of nucleosome positions in S. cerevisiae. Science **309:** 626-630.

ZHANG, H., D. N. ROBERTS and B. R. CAIRNS, 2005 Genome-Wide Dynamics of Htz1, a Histone H2A Variant that Poises Repressed/Basal Promoters for Activation through Histone Loss. Cell **123:** 219-231.

Publishing Agreement

It is the policy of the University to encourage the distribution of all theses and dissertations. Copies of all UCSF theses and dissertations will be routed to the library via the Graduate Division. The library will make all theses and dissertations accessible to the public and will preserve these to the best of their abilities, in perpetuity.

Please sign the following statement:

I hereby grant permission to the Graduate Division of the University of California, San Francisco to release copies of my thesis or dissertation to the Campus Library to provide access and preservation, in whole or in part, in perpetuity

Author Signature Date